# Smart Step: Wearable Mobility Assistance using Machine Learning and Haptic Feedback

Astrini Sie

A dissertation
submitted in partial fulfillment of the
requirements for the degree of

Doctor of Philosophy

University of Washington

2020

Reading Committee:

Blake Hannaford, Chair

Eric Rombokas, Chair

Samuel A. Burden

Brittney C. Muir

Program Authorized to Offer Degree:
Electrical and Computer Engineering

University of Washington

**Abstract**

Smart Step: Wearable Mobility Assistance
using Machine Learning and Haptic Feedback

Astrini Sie

Co-Chairs of the Supervisory Committee:
Dr. Blake Hannaford
Electrical and Computer Engineering

Dr. Eric Rombokas
Electrical and Computer Engineering

Reinventing the sensory world for prosthesis users remains a challenge. I leverage recent advances in machine learning and miniaturized sensors to build a smart wearable that tackles a cognitively demanding and ill-researched mobility task: stair descent. The human sensory system enables error correction of foot placement during stair descent; however, amputation removes access to much of this information. People with lower limb amputations often compensate for the absence of ankle range of motion and plantar sensation by employing the "overhanging toe" strategy during stair descent. Such users will pivot the foot over the stair edge in a smooth rolling motion, which requires the prosthetic foot to be placed optimally on the stair edge.

*Smart Step* replaces the role of the human sensory system in foot placement, particularly stair descent. *Smart Step* consists of the sensing element (insole with force sensors and wearable Inertial Measurement Units strapped on the body) and the cueing element (haptic band worn on the thigh or the wrist). The sensors will feed data into a machine learning algorithm, predicting foot placement, and subsequently provide instructional haptic cues for the user. The cues enable users to achieve optimal foot placement with each step, thus the device adopts the cognitive load and enables a smooth and controlled gait during stair descent. By using low cost materials and noninvasive techniques to fit in any shoe, *Smart Step* may be useful not only for prosthesis users, but also for anyone with gait impairments.

# ACKNOWLEDGMENTS

I would like to express my sincere gratitude to my academic advisers, Blake Hannaford and Eric Rombokas. Thank you Blake for inspiring me to see the beauty and lending your realistic perspectives of the journey towards a PhD, for helping me shape my research identity. Eric, I am grateful for you for listening to and trusting me with all the unusual ideas and things that I wanted to do, for all the hours discussing about the wonders of the brain and the neural behaviors.

I would like to especially thank my research assistants, Maxim Karrenbach, Charlie Fisher, Elisabeth Case, Callysta Caraballo, Nathaniel Wieck, and Shawn Fisher, without whom a lot of these findings would not be found. Thank you for trusting me with your time, effort, and intellectual curiosity. I hope that by doing this research, you are inspired to explore the beauty of science and technology, and to be a great researcher yourself.

I would also like to thank my industry advisers and colleagues during my internships. Thank you for giving me the opportunities to learn. I will be forever grateful for all the experience, the skills, and the connections during and beyond my internships. Thank you for inspiring me to delve deeper into the world of wearables and smart technologies.

I would like to acknowledge all the collaborators, mentors, teachers, colleagues, and friends who have helped me with their time, advice, knowledge, hands, thoughts, and supports. There are so many of you who have positively impacted me over the past 6 years and beyond. I cannot name every single one of you but please know that you are very much appreciated.

I would like to acknowledge David Boe. Thank you for your patience, for brainstorming all the ideas with me, for always giving me a sanity check, and for being there when things are hard.

Lastly, I can never repay the love, kindness, and patience from my parents. Thank you for raising me to be who I am today, for your unconditional love, and for encouraging me to pursue more.

Without all of you, this work would not have been possible, but most importantly, I would not be who I am today.

# DEDICATION

To the future generations to come...

I hope that I can inspire you to keep pursuing more,

to create technologies that make humans live more beautifully.

# TABLE OF CONTENTS

Page

List of Figures . . . . . v

List of Tables . . . . . viii

Chapter 1: **Introduction** . . . . . 1
1.1 Motivation . . . . . 1
1.2 Research aims . . . . . 3
1.3 Scope and future implementations . . . . . 5
1.4 Organization . . . . . 6

Chapter 2: **Prior Art** . . . . . 7
2.1 State of the art lower limb prostheses . . . . . 7
2.1.1 Restoring motion: active powered and microcontroller-ankle prostheses 7
2.1.2 Restoring sensation: sensory feedback in prostheses . . . . . 8
2.1.3 Cognitive load imposed by sensory feedback . . . . . 9
2.1.4 Conclusion . . . . . 10
2.2 Haptic feedback systems . . . . . 10
2.2.1 Haptic feedback in human bodies . . . . . 10
2.2.2 Haptic guidance for timing-focused tasks . . . . . 12
2.2.3 Cueing for mobile tasks - visual, auditory, and haptics . . . . . 12
2.2.4 Foot placement cueing . . . . . 13
2.2.5 Conclusion . . . . . 14
2.3 Gait modeling, analysis, and estimation . . . . . 14
2.3.1 Gait measurement techniques . . . . . 15
2.3.2 Gait analysis . . . . . 16
2.3.3 State of the art for gait analysis . . . . . 17
2.3.4 Conclusion . . . . . 21

Chapter 3: **Provision of Direct Haptic Feedback on the Thigh as Sensory Restoration of Prosthetic Foot** . . . 22
3.1 Device design . . . 22
3.1.1 Sensor insole . . . 23
3.1.2 Actuator thigh band . . . 23
3.1.3 On-board embedded processor . . . 24
3.1.4 Haptics actuation scheme . . . 24
3.2 Experimental protocol . . . 25
3.2.1 Experiment 1 - benchtop verification . . . 25
3.2.2 Experiment 2 - hidden step experiment . . . 26
3.3 Results and discussion . . . 28
3.3.1 Experiment 1 . . . 28
3.3.2 Experiment 2 . . . 29
3.4 Future work . . . 32
3.5 Conclusions . . . 32

Chapter 4: **Haptic Time-to-Cue Requirements for Foot Placement Adjustment in Mobile Task** . . . 33
4.1 Wearable haptic wrist band . . . 33
4.1.1 Electronics . . . 33
4.1.2 Mechanical design and construction . . . 34
4.1.3 Motor vibration profile . . . 34
4.1.4 Spatial design choice . . . 34
4.2 User study . . . 35
4.2.1 Participants . . . 35
4.2.2 Apparatus . . . 35
4.2.3 Task . . . 36
4.2.4 Study protocol and design . . . 37
4.3 Data processing and analysis . . . 38
4.3.1 Stride length definition . . . 38
4.3.2 Centering of target foot index . . . 38
4.3.3 Normalization of stride length . . . 38
4.3.4 Statistical analysis . . . 40

4.4 Results . . . 40
4.4.1 Haptic cues enable changes of participants' self-selected stride at target foot (T) . . . 40
4.4.2 Haptic cues delivered at ST1, ST2, and ST3 enable timely change of target foot stride (T) . . . 41
4.4.3 Changes of stride are observed beyond the target foot . . . 41
4.4.4 Correlation of walking speed to stride length adjustments . . . 43
4.4.5 Qualitative reports . . . 45
4.5 Discussion . . . 47
4.6 Limitations and future work . . . 48
4.7 Conclusion . . . 49

Chapter 5: **Descending 13 Real World Steps: A Dataset and Analysis of Stair Descent** . . . 51
5.1 Methods . . . 51
5.1.1 Participants . . . 51
5.1.2 Sensors and data acquisition . . . 51
5.1.3 Protocol . . . 52
5.1.4 Data preparation . . . 52
5.1.5 Data analysis . . . 54
5.2 Results . . . 56
5.2.1 Kinematics . . . 56
5.2.2 Kinetics . . . 57
5.2.3 Foot placement . . . 58
5.3 Discussion . . . 60
5.3.1 Angular parameters . . . 60
5.3.2 Temporal parameters . . . 61
5.3.3 Intra and inter subject variability . . . 62
5.3.4 Foot placement position . . . 62
5.3.5 Symmetry . . . 63
5.4 Limitations and future work . . . 64
5.5 Conclusion . . . 64

Chapter 6: **Predicting Future Foot Placement** . . . 66

6.1 Dataset . . . 66
6.1.1 Data preparation . . . 66
6.2 Algorithm design . . . 68
6.2.1 Output features selection . . . 68
6.2.2 Input features selection . . . 68
6.2.3 Baseline algorithm selection . . . 71
6.2.4 LSTM algorithm selection . . . 72
6.3 Validation results: 10-fold cross-validation sets . . . 73
6.3.1 ARIMA . . . 73
6.3.2 LSTM . . . 73
6.4 Test results . . . 74
6.4.1 Test set 1 - anthropomorphic: 11 new participants . . . 74
6.4.2 Test set 2 - environmental: 1 participant on 3 new staircase dimensions 74
6.5 Discussion . . . 76
6.5.1 Safety concerns and translating predicted values to step shorter and step longer cues . . . 76
6.5.2 Baseline ARIMA vs LSTM algorithm . . . 78
6.5.3 Robustness across anthropomorphic variations . . . 80
6.5.4 Robustness across environmental variations . . . 80
6.6 Limitations and future work . . . 80
6.7 Conclusion . . . 81

Chapter 7: **Conclusion** . . . 82

Bibliography . . . 84

# LIST OF FIGURES


Figure Number Page

2.1 Vibration detection thresholds at 100Hz (white bar) and 200 (white bar). [1] 11

2.2 Mean detection rate and mean reaction time for stimulus at various body sites under four different conditions. [2] . . . . . 12

2.3 A lab motion capture system with cameras placed in the room and a user shown with body markers. [3] . . . . . 15

a Xsens motion capture system [4] . . . . . 16

b Moticon force sensor insole [5] . . . . . 16

2.5 Examples of commercially available wearable gait measurement systems. . . 16

3.1 Block diagram of the haptic feedback system. . . . . 22

3.2 Sensor insole with 6 FSRs shown without the top layer of shoe insert. . . . . 23

3.3 (a) Thigh band with 6 actuators; (b) 3D printed actuator housing; (c) piezoelectric actuator and the haptic driver board shown with a quarter US dollar coin for scale. . . . . 24

3.4 The stiff medical boot worn by the participants to minimize ankle flexion and plantar surface forces sensation. Positions of the FSR on the sensor insole at the bottom of the boot are marked accordingly. . . . . 26

3.5 The haptic feedback system worn by a subject during Experiment 2. . . . . 27

3.6 3-step staircase with a variable step-size hidden step. . . . . 27

3.7 (a) Perceived position for each given position shown as a confusion matrix; (b) Normalized confusion matrix of perceived location for each given location. 28

3.8 Position error shown for each given hidden step position with and without haptic feedback. . . . . 30

3.9 (a) Confusion matrix for trials without haptic feedback and (b) confusion matrix for trials with haptic feedback, given position calculated from actuator activation. . . . . 31

4.1 Wrist-worn haptic band. . . . . 34

4.2 Participant walking along the walkway with reflective markers and ground reaction forces shown as arrows normal to the contact. . . . . 35

4.3 Participant walking along the walkway. This configuration shows right foot as the first step on the first force plate. . . . . 36
4.4 Six haptic stimulation times (ST1-ST6) . . . . . 37
4.5 Centering of target foot (T) at the fifth index. Target foot can either be the second, third, fourth, or fifth right heel strike (RHS). . . . . 39
4.6 Mean right stride lengths for all 10 participants for all no stimulation (ST0) trials. . . . . 39
4.7 Normalized stride length of target foot (T) for each stimulation time (ST1-ST6) and stimulation condition (short and long) for all 10 participants. . . . 42
4.8 Normalized stride lengths of the right stride prior to target foot (T-2), the target foot (T), and 2 subsequent right strides after target foot (T+2, T+4) for each stimulation time (ST1-ST6) and condition (short and long) for all 10 participants. Step shorter and step longer foot strides significantly different with the stride length prior to haptic cues onset are denoted with * ($p < 0.05$). 44
4.9 Normalized absolute changes of target foot stride length ($SL$) given walking speed. The value for each trial is plotted as a dot, with a linear regression fit calculated for each stimulation time (ST1-ST6) and condition (short and long). The top row is for step short stimulation condition, and the bottom row is for step longer. $p$ value of the fit compared against the constant model for each ST is shown. . . . . 45
4.10 Post-trial questionnaire response from all 10 participants. The responses are on a Likert scale from 1-5. Red bar indicates negative (undesirable) responses, and green bar indicates positive responses. . . . . 47

5.1 a-c) Segmentation of stair descent data and d) Sensors worn by participant during trial. Foot $z$ position data for: a) a section of a trial consisting of stair ascent and descent; b) one entire flight of staircase during descent; c) one descent step representing 0-100% step. . . . . 53
5.2 Kinematic parameters during stair descent measured by the Xsens (% step from toe-off to toe-off). 'Flex' = Flexion, 'Ext' = Extension, 'Abd' = Abduction, 'Add' = Adduction, 'ER' = External Rotamation, 'IR' = Internal Rotation, 'PF' = Plantar-flexion, 'DF' = Dorsi-flexion, 'Eve' = Eversion, 'Inv' = Inversion. ($n = 101$). . . . . 56
5.3 Kinetic parameters, foot placement, and foot acceleration information during stair descent measured by the Moticon. (% step from toe-off to toe-off). 'COP' = Center of Pressure. ($n = 101$). . . . . 60
5.4 Staircase step edge position underneath the foot as measured from the toe (a) and the heel (b) for participants with varying shoe lengths. ($n = 101$). . . . . 61

6.1 Histogram of target foot placement values for train ($n = 90$) and test ($n = 11$) sets. . . . . 67
6.2 Target foot placement value as indicated by the most distal center of pressure value within 0.5s around toe-off. . . . . 69
6.3 Input sequence length and the relationship with target foot placement. We are predicting the foot placement in relation to the step edge (indicated by the time stamp at gold star). From Aim 2, the haptic cue has to be delivered at 1.5 steps prior to heel strike (indicated by the purple shaded region). The input sequence for machine learning prediction is selected to be 6 steps to 4 steps (grey shaded region) prior to the target foot (purple star). Note that the target output value is obtained during toe off, as opposed to heel strike, hence the discrepancy between the gold and purple stars. . . . . 70
6.4 LSTM architecture . . . . . 73
6.5 ARIMA prediction results and errors together with actual foot placement positions for the 10 validation sets. . . . . 75
6.6 Histogram of validation error for all predictions across all 10-fold cross validation sets using the best hyperparameters. Left: ARIMA result. Right: LSTM result. ($n = 90$). . . . . 76
6.7 Histogram of error for all predictions in unseen individuals (test set). ($n = 11$). 76
6.8 Histogram of error for all predictions in unseen staircases for Participant 8 (test set). ($n = 1$). . . . . 77
6.9 Example of thresholds for non-cue in the directions of step shorter and step longer. Green shaded region indicates no cue given. . . . . 78
6.10 Prediction result for Participant 49. Comparison of ARIMA and LSTM predictions for foot placement values with a trend. ARIMA predicts only the mean of the time-series, whereas LSTM is able to predict the trend. . . . . 79
6.11 Prediction result for Participant 4. Comparison of ARIMA and LSTM predictions for rapid up and down trends for consecutive time steps. ARIMA predicts the trend with a 1 time step lag, while LSTM is able to follow the trend without time lag. . . . . 79

# LIST OF TABLES


| Table Number | | Page |
|---|---|---|
| 2.1 | A summary of a portion of publicly available gait datasets. | 18 |
| 2.2 | A summary of work in biomechanical analysis for stair ambulation. | 19 |
| 2.3 | A summary of work in biomechanical analysis for stair ambulation (cont.). | 20 |
| 4.1 | Seven haptic stimulation times (ST0-ST6) explained | 37 |
| 4.2 | Percentage of correct stride adjustments for all 10 participants. | 41 |
| 4.3 | One-way ANOVA results comparing the effect of haptic cue onset timing (stimulation time) on stride length in foot stepping prior to the onset of haptic cue (T-2), and after the haptic cue at the target foot (T), 2 steps after the target foot (T+2), and 4 steps after the target foot (T+4). | 43 |
| 4.4 | Post-trial questionnaires from 10 participants (P1-P10). Green indicates favorable or positive responses, red indicates unfavorable or negative responses, and black indicates neutral responses. | 46 |
| 5.1 | Parameters of gait kinematics at the lower limb (Mean ± SD). $n = 101$. | 57 |
| 5.2 | Inter-subject and intra-subject parameters of (Mean ± SD (%)) of the maximum flexion, maximum extension, and joint angle averaged across time for the leading left and leading right limb. $n = 101$. | 58 |
| 5.3 | Symmetry reports of stair descent parameters. (Mean ± SD) (%). $n = 101$. | 59 |
| 5.4 | Foot placement and toe overhang with respect to the staircase edge (Mean ± SD). $n = 101$. | 59 |
| 6.1 | Hyperparameters tested and chosen for the final prediction algorithm. | 74 |

# Chapter 1

# INTRODUCTION

## *1.1 Motivation*

### *Smart technologies for mobility assistance*

The exponential growth of technology and the availability of information today influence human behaviors on a daily basis. How humans interact with other humans, how humans interact with technology, and how humans process this vast information generates cognitive burden for users of these technologies. Not all devices that are designed to help humans make an effort to reduce cognitive load. However, recent technological developments have created intelligent devices capable of interacting with humans in a revolutionized manner. The advent of the internet of things and ubiquitous computing, through integration of sensors, communication technology, and daily devices, has enabled the creation of smart devices such as smart homes, intelligent vehicles, and continuous wearable health monitoring devices [6, 7, 8, 9, 10]. As such, smart technology has become an integral part of human daily life, enabling humans to perform tasks in a simpler and easier manner.

While the concept of smart technology is starting to be widely applied for technology-related consumer applications, there has been minimal adaptation of smart technologies for fields that truly can augment human capabilities in a way that minimizes cognitive burden. When a human capability is absent, the ability to perform and complete a task in an intuitive manner is lost. Take for example the case of mobility impairment. There are various types of cognitive and physiological mobility impairments such as aging, amputation, cerebral palsy (CP), multiple sclerosis (MS), vision-impaired mobility, or even difficulties in physical functioning. The American Community Survey reported that 6.6% of the population in the United States has an ambulatory disability [11]. In addition, 7.1% of adults in the United States are unable to walk a quarter mile [12]. Mobility impairment introduces various side effects aside from the inability to ambulate, such as increased risk of depression and anxiety [13], as well as mortality [14].

In the case of lower limb amputation, there are 185,000 new amputations annually in the United States alone. This number is projected to reach 3.6 million total cases by 2050 [15]. Such a staggering number of people with amputation (PWA) has motivated research to focus

on better and more sophisticated prosthetic legs that enable PWA to walk. Nevertheless, most of the current state of the art research focuses on flat-ground walking, with minimal investigation on other types of ambulatory functions, including stair ambulation. I would like to tackle the problem of stair ambulation for PWA.

### *Action-advising wearable systems*

The use of wearable technologies for daily assistance is becoming increasingly prevalent [16, 17, 18]. In [19], Hänsel et al. argued that feedback presented to the users by wearable devices must be meaningful, beyond just the presentation of raw data. This motivates the development of *simpler* feedback systems that provide straightforward, instructional cues to users. Such systems have been developed for a variety of domains, such as health and lifestyle. FatBelt [20] inflates around the waist once over-consumption is detected, alerting the user to stop eating. [21, 22] developed haptic headbands to cue gaze direction to augment user attention.

With regards to mobility assistance [23, 24], wearable devices are frequently used for cases such as detection of freezing-of-gait for people with Parkinsons' disease (PD) [25, 26, 27], trip and fall prevention [28], posture correction [29, 30, 31], navigation guidance [32, 33, 34], and navigation with visual impairment [35, 36].

Cues may be especially useful as a way to augment attention to potential hazards during gait and prevent falls. Falls amongst older adults cost $50 billion each year [37] and is the leading cause of injury-related death. 1.9 million US adults suffer a fall-related injury every 3 months [38]. 61% of these falls were attributed to an environmental hazard such as a large object, surface contamination, and stairs or steps. Haptic cues delivered by wearable devices are well suited to draw attention to hazards, especially when auditory and visual channels are often occupied with other tasks. Moreover, wearable haptic devices can be worn discreetly, whereas auditory and visual cueing systems draw attention to the user in public settings which may be undesirable [39].

As such, it is imperative that I explore the use of a smart wearable system that can provide its users with distilled, action-advising cues for mobility assistance applications for PWA.

### *Importance of foot placement for ambulation*

Foot placement is a crucial element in ambulation [40, 41]. Unimpaired individuals with intact limbs possess proprioception, a sense of where in the world a specific part of the body is. However, for people with mobility impairments, proprioception is often also impaired,

making foot placement during gait challenging. The elderly population has a high risk of injury after a fall, making safe foot placement important [42].

For PWA, stair navigation remains a challenge due to: (1) the absence of proprioception and sensory information; as well as (2) the absence of ankle range of motion in the prosthetic ankle. Active prostheses are not targeted for stair descent and have yet to become a viable option for many PWA. As a result of these limitations, some PWA avoid stairs altogether. PWA with a unilateral amputation that are active community ambulators opt to walk downstairs using the *step to* technique, leading with the prosthetic side [43]. Experienced prosthesis users can walk downstairs using the *step over step* technique, utilizing both legs like unimpaired individuals would walk downstairs.

While using the *step over step* technique, they often compensate by employing the "overhanging toe" strategy during stair descent [44, 45, 46]. Such users will place the prosthetic foot such that the first metatarsal is approximately $3 \pm 2$cm from the step edge [47], and pivot the foot over the stair edge in a smooth rolling motion. This requires the prosthetic foot to be placed optimally on the stair edge. To achieve this, users will rely heavily on visual cues to place their prosthetic feet, hindering a smooth and easy stair descent process.

I am building *Smart Step*, a low-cost wearable system that helps users place their feet accurately and optimally in an intuitive manner while minimizing cognitive burden using simple action-advising haptic cues.

### *1.2 Research aims*

I envision to enhance the ability of people with lower limb amputation to perform daily tasks seamlessly with the specific goal of assisting stair descent ambulation. To achieve this goal, I am developing *Smart Step* utilizing the smart wearable haptic feedback system and machine learning algorithms described in the following aims.

#### ***Aim 1: Demonstrate the viability of providing direct haptic feedback on the thigh to "restore" the sensation of the prosthetic foot***

In Aim 1, I evaluate the feasibility of using haptic feedback as a sensory substitution scheme for the loss of sensation at the bottom of the prosthetic foot. I build a haptic thigh band with four distinct locations of vibration motors corresponding to four different step edge locations underneath the foot. I test: (1) the ability of users to distinguish four different vibration locations on the thigh; and (2) the ability of users to distinguish four different step edge locations with haptic feedback.

Results of Aim 1 are published in [48, 49]. As Aim 1 is targeted at sensory substitution, it introduces cognitive burden for the users as they have to process the vibration information and determine where on the foot to which it correlates. This extra layer of processing adds to the already cognitively demanding task of stair descent. Motivated by this, I propose shifting the cognitive load from the human to the device, creating a smart system that instead of relying on sensory substitution, provides direct simple instructional cues instructing the user in real-time how to achieve optimal foot placement. For example, one vibration may signal the user to take a longer step while a different vibration signals the user to take a shorter step. This leads to Aims 2 and 3.

### *Aim 2: Assessment of haptic timing of time-to-cue for foot placement adjustment*

To optimally deliver targeted cues for users, we require: (1) knowledge of where the user is going to place his/her foot on the following step(s); and (2) knowledge of the optimal timing with respect to gait phase to deliver a haptic cue such that user can modify his/her foot placement in time. With (1), I compare the predicted next step foot placement with an expert-recommended foot placement during stair descent. In this case, foot placement is represented by the distance of the foot center of pressure at toe-off as a proxy for the stair edge. Based on the difference, an appropriate cue is given within the time frame observed in (2). The first question is addressed in Aim 3, while the second question is addressed in Aim 2.

I want to investigate how haptic cues affect the timing at which users modify their foot placement during ambulation. This information is crucial for any situation in which a specific foot placement is desired, such as in stair ambulation, obstacle avoidance, and trip/fall prevention for the elderly population. Aim 2 is further divided into the two following sub-aims:

- **Aim 2a: Build a wearable bi-directional haptic device**

- **Aim 2b: Evaluate how timing related to gait phase in vibration cues affect foot placement**
  In this aim, I evaluate the instant during walking gait phase at which a haptic cue could effectively change the user's foot placement. I perform the experiment in flat-ground walking as proxy for stair descent.

Investigation and results for Aim 2 are to be published in [50].

***Aim 3: Predict future foot placement during stair descent using wearable sensors and machine learning algorithms***

Aim 3 is further divided into the two following sub-aims:

- **Aim 3a: Collect kinetics and kinematics data from 100+ adults walking downstairs using completely wearable sensors**
  Currently most gait data collection is constrained by the lab environment, with participants numbering less than 30. Performing stair navigation inside a gait lab is impractical as a staircase has to be built inside a gait lab while ensuring that the motion capture system is able to capture the entire height of the staircase. I perform gait data collection on a regular American with Disabilities Act (ADA) approved staircase using completely wearable sensors. Such a data set is important for this research and also for other stair-related research problems. No such stair ambulation database exists.

  Findings from Aim 3a are to be published in [51].

- **Aim 3b: Predict future foot placement during stair descent using a machine learning regressor**
  I build a machine-learning based algorithm to predict where the user is going to place the foot with respect to the edge of the staircase. The algorithm utilizes gait data collected in Aim 3a to provide a prediction.

  Results and findings from Aim 3b are to be published in [52]

### *1.3 Scope and future implementations*

Combining the results from Aims 2 and 3, I will build a system that predicts the next step's foot placement, compares it with the expert-recommended foot placement, and in turn sends appropriate vibration command to the motors worn on the wrist. This vibration command will be timed to match the result obtained in Aim 2. I envision the user will wear a haptic wrist band, a pair of insoles, and one or two inertial measurement units (IMU) on the legs or a smartphone with an integrated IMU inside the pants pocket.

This research will provide the necessary answers to the research questions required to achieve this final implementation. The final implementation of such real-time system for PWA is considered as an engineering cycle and will not be evaluated in this work.

### *1.4 Organization*

This manuscript is organized as follows:

- Chapter 1: Motivation and background to this research, aims, scope, and further implementation.
- Chapter 2: Current state of the art for this research in general as well as each of the three research aims.
- Chapter 3: Aim 1
- Chapter 4: Aim 2
- Chapter 5: Aim 3a
- Chapter 6: Aim 3b
- Chapter 7 Conclusion

# Chapter 2

# PRIOR ART

## *2.1 State of the art lower limb prostheses*

### *2.1.1 Restoring motion: active powered and microcontroller-ankle prostheses*

To date, most standard commercial prostheses prescribed clinically are passive prostheses made of composite materials. These prostheses possess an energy storing and releasing (ESR) function, in which energy is stored at the ankle during stance, and released at toe off, which is useful to help "propel" the leg forward during level-ground walking. Such a mechanism is spring-based hence completely passive.

In addition to the passive prostheses, there are active powered prostheses and microcontroller ankle prostheses, which are not yet widespread. Most of these prostheses are research products in early development.

The active powered prosthesis that is currently available is the Empower Ankle, Ottobock, Duderstadt, Germany (previously the BiOM [53], BionX Medical Technologies Inc, Bedford, MA, USA). The primary benefit of an active powered prosthesis is a powered foot-ankle system results "in metabolic energy costs, preferred walking velocities and biomechanical patterns that were not significantly different from people without an amputation" [53]. This means, when the prosthesis senses an increase in ankle joint torque, the actuator at the ankle increases its torque in mid-late stance phase, resulting in a net positive ankle work production to meet faster walking speeds. The BiOM is also equipped with a controller that adapts the actuator at the ankle to meet environmental constraints such as uneven terrain [54]. [55] investigated stair ascent with the BiOM and found that while it did restore power to the ankle joint, users exhibited the same strategy in the proximal joints as they did when wearing passive prostheses. However, there has been no investigation of the BiOM during stair descent. I suggest that active powered prostheses might be undesirable for stair descent due to the risk that increased power will compromise stability in stair descent.

Unlike active powered prostheses which focus on adding power or work to the device, microcontroller ankle prostheses set a dorsiflexion angle at the ankle specifically designed to assist slope and stair navigation. An example of such prosthesis is the PROPRIO Foot, Ossur, Reykjavik, Iceland. This type of prosthesis does not add power and simply prepositions the

ankle when its unloaded to normalize gait. The amount of dorsiflexion angle is set by the prosthetist during fitting, customized to each user depending on their needs and gait patterns. There is no accepted guideline on setting this particular angle, and purely depends on the prosthetist's expertise to tune the ankle such that stair descent results in more symmetrical gait [56]. The study by Alimusaj et al. [57] also found that with ankle dorsiflexion, knee kinetics and kinematics were improved.

Microcontroller-ankle prostheses that allow ankle dorsiflexion can help in stair descent as they allow the ankle dorsiflexion that is required for a smooth and easy stair descent. However, insurance practices and access to qualified prosthetists reduce the availability of these devices. On top of that, this prosthesis does not address the issue of sensory feedback for the users.

### *2.1.2 Restoring sensation: sensory feedback in prostheses*

Currently, there are no prostheses that provide sensory feedback. However, sensory feedback, especially proprioception, is important when a body part is replaced with a prosthetic limb, and especially for gait [58]. Saunders et al. [59] found that in upper limb prosthesis control, feedback is especially important for prosthesis users when they do not have the ability to estimate the state of their limbs.

Currently there are a variety of methods that are used to obtain "sensory feedback" in prostheses:

**Socket forces**. Users use forces exerted on the residual limb by the prosthetic socket to infer the terrain underfoot and the position of the prosthetic limb [60]. Anecdotally, users report they can discern the denomination of a coin merely by stepping on it with their prosthetic foot and feeling the forces in their socket.

**Skin-contact sensory substitution**. This consists of a sensory signal delivered by an actuator on the skin, via vibrating motor or electrodes. Information measured from the sensors are provided directly to users as a form of biofeedback.

**Implanted sensory substitution**. Instead of contacting the skin, the actuators delivering sensory signals are surgically implanted at or around nerves where they depolarize afferent fibers in order to induce meaningful perception. The actuators are linked to sensors at the prosthesis, such that users may have a sensed proxy for some important function of the prosthesis. This is most frequently done in the upper limb for grip force perception. This is a sensory substitution paradigm, thus the user's perception of the stimulus at the implanted region is rarely spatially or characteristically the same as the sensed stimulus at the sensor.

In the field of prostheses, most research in sensory feedback is performed for upper limb prostheses. While there has been a significant amount of work performed for sensory feedback in lower limb rehabilitation and gait assistance using exoskeletal and rehabilitation devices [61], little work on sensory feedback has been performed for lower limb prostheses. In [62], the authors build an insole with four sensors and a thigh band with four pneumatic actuators spaced at 90°. They found that these four actuation locations are distinguishable in static cases but did not test for dynamic (walking/stepping) cases. The work done in [63] focuses on providing loud auditory cues to users when gait asymmetries, detected using force-sensing insoles, are present, with the motivation of bringing gait training outside of the clinic. [64] performed a similar work with visual, auditory, and vibrotactile cues, delivered to users via a smartphone. The study reported that users prefer visual cues, but were also effective in modifying their gait to vibrotactile cues. In [65], the authors placed three vibration motors along the outer perimeter of the thigh, spaced at 90° on the thigh. Each motor vibrates corresponding to different phases in the gait cycle (heel strike, foot flat, and toe off), determined from a pressure sensor insole. During the experiment, the subjects are instructed to walk on a treadmill at the speed of 2km/h. Each vibration motor will vibrate for 100ms synchronously with the gait phase (heel strike, foot flat, and toe off respectively). The subjects are asked to report for missing vibrations and wrong vibrations. Performance from the subjects were good, but the tasks are deemed to be cognitively demanding.

### *2.1.3 Cognitive load imposed by sensory feedback*

To the best of my knowledge, few studies have been done to assess cognitive loads on users while externally-given sensory feedback is present. The only study that talks about cognitive burden is [65], while [2] indirectly investigates the effect of cognitive load and mobile task performance on the detection threshold of a vibrotactile stimulus.

In [65] (described in Section 2.1.2), the subjects reported that the task of identifying which stimulus is missing or wrong is cognitively demanding. It is even explicitly mentioned in the experiment instruction that the participants **"pay attention"** to the vibrotactile signals during the rehabilitation sessions.

Similarly, in [2], participants are asked to report if a vibrotactile stimulus is sensed under sitting and walking conditions. In the walking condition, participants demonstrated increased difficulties in detecting vibrotactile stimuli. Another testing condition is when participants are tasked with a visual workload analogous to the mental activity of a pedestrian keeping track of their surrounding. Introduction of visual workload does not affect stimulus detection, but significantly impairs reaction time. This suggests that the task of identifying external feedback stimuli adds to the user's cognitive burden, and vice versa, their ability to perceive external feedback stimuli is affected when a task with cognitive load is presented to the user.

Typically in an intact individual, sensation requires zero cognitive effort - sensing is done unconsciously and automatically. The sensory system uses highly evolved neural machinery to filter out noise and deliver the salient sensory information to one's awareness. With the introduction of externally-given sensory feedback, there is an assumption that such "sensation" will be seamlessly incorporated into the user's sensory experience over time. However, such sensory substitution takes an alternate pathway, and instead seems to rely on the user's cognitive effort to perform low-level filtering of the sensory information. This assumption that sensory substitution will seamlessly integrate with the sensory system and become an unconscious process has yet to be convincingly demonstrated, and research in this area rarely follows the users of these sensory substitution devices for a period of time sufficient for such an integration to occur.

This brings us to a point — the value that sensory feedback can bring is to enable error correction, something that is lost due to impairment. Rather than spend a user's valuable cognitive resources on filtering low level sensory information, the resources can be spent on attending to errors. Analagous to the sensory system's role in presenting salient and immediately useful information to the user's awareness, sensory devices should present meaningful information to the user, and filter out the noise.

#### *2.1.4 Conclusion*

Most of the work in sensory feedback uses real-time biofeedback of a calculated gait parameter. They are yet to predict future error and inform the user early enough to prevent the error from happening. In stair descent, predicting and correcting for a future error is necessary because an error on stairs might not only lead to a more difficult and awkward descent, but also to a fall and possibly death. *Smart Step* does not provide "biofeedback" of events already happening to its users, but instead provides a feedback information of the future that allows users to alter their gait hence perform error correction.

### ***2.2 Haptic feedback systems***

#### *2.2.1 Haptic feedback in human bodies*

Sensory feedback techniques for prostheses include visual, auditory, and haptic modalities. While visual and auditory cues can sometimes be useful for training or rehabilitation in a clinical environment, prosthesis users prefer inconspicuous options for daily wear as to not attract attention to themselves. This leads to haptic feedback being the modality of choice.

In terms of vibration frequency, there have been various investigations that suggest a frequency range from 100-450Hz provides the lowest threshold of detection [1, 66]. How-

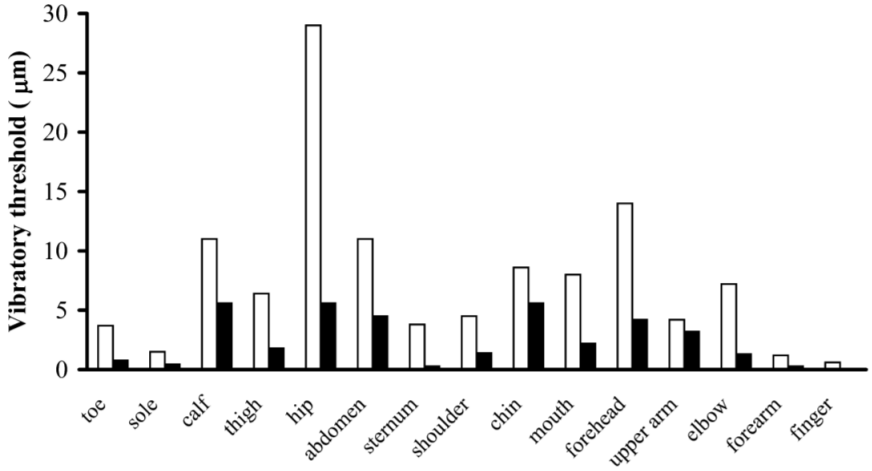


Figure 2.1: Vibration detection thresholds at 100Hz (white bar) and 200 (white bar). [1]

ever, most work has used frequency ranges around 200-250Hz as the preferred values for vibrotactile stimuli.

In [67], Jones et al. provide an exhaustive review of existing tactile displays implemented at the human bodies. In the review, most of the work suggested that the hand and forearm have the highest sensitivity for detecting tactile stimulus, followed by chest and shoulder, with the leg having less sensitivity (Figures 2.1 and 2.2). Moreover, the ability to localize a point of vibrotactile stimulation on the body is best when it is presented near anatomical points of reference such as the wrist, elbow, spine, or navel. [66, 68, 69].

While most of these studies focused on static tasks, some work have looked at vibrotactile haptic stimulation given during mobile tasks such as walking. [70] found that detection rate of haptic feedback are the bests for spatial placement at the spine and wrist, and worst at the feet. Walking significantly decreases detection rate and increases reaction time, in which these effects are the most prominent in thigh and foot. [71, 72] found that during walking and running, haptic stimulations at the distal parts of the body, especially ear, hand, foot, and wrist have the highest perception rating qualitatively rated by 10 participants. The studies also suggested that ear followed by hand and wrist are the ideal locations while the lower limb is impractical for walking purposes.

For the application of lower limb prostheses, providing vibrotactile feedback at the thigh is the most intuitive and practical, as it can be easily integrated with the socket as a single unit. However, these results report that a stimulus at the thigh has a higher threshold for detection, and also a slower reaction time. The latter factor is crucial in terms of providing users with a real-time cue for correction of a future error. Karuei et al. [2] also reported that

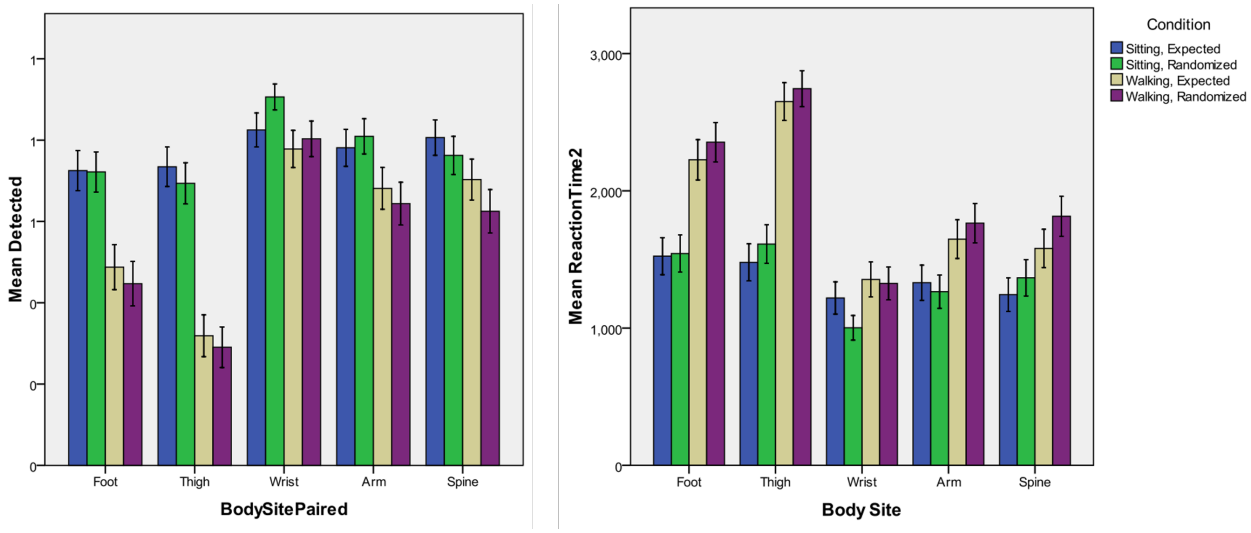


Figure 2.2: Mean detection rate and mean reaction time for stimulus at various body sites under four different conditions. [2]

the thigh is the least preferred and effective site of stimulus. These disadvantages of using the thigh as a vibrotactile locus lead to using the wrist as a more optimal choice.

### *2.2.2 Haptic guidance for timing-focused tasks*

The use of haptic feedback to promote timing accuracy in time-sensitive tasks (haptic guidance) such e.g. giving oral presentation [73], playing musical instrument [74], sports [75], time specific games [76] were investigated in the literature. This study focuses not on that, but instead on evaluation of the timing of the haptic cue itself. In order to affect users' behavior, when should the haptic cue be given?

### *2.2.3 Cueing for mobile tasks - visual, auditory, and haptics*

Cueing for mobility assistance has been implemented using auditory, visual, and haptic cues. The use of auditory and visual cues to alter walking characteristics has been thoroughly investigated in the literature, with conflicting results. Danion et al. [77] altered: (1) stride length using visual cue, displaying the walking stride as a signal that has to be kept within upper and lower bounds; (2) stride frequency using auditory cue with a metronome. This study reported that eight unimpaired participants successfully modulated their stride lengths and frequencies to follow the visual and auditory cues. Bonnard et al. [78] used auditory

and visual cues to intentionally shorten or lengthen one step, and then adjust the stride frequency/length of steady state gait for multiple steps. In contrast, Baker et al. [79] attempted to modify stride frequency and length by giving rhythmic auditory cues at 10% below preferred stride frequency, along with instructions of taking "a big step in time of the beat". Given these cues, they saw reduced step time variability in participants with PD, but increased variability in unimpaired participants. They suggest that these cues disrupt an otherwise stable self-selected gait pattern in uninmpaired participants, while participants with PD benefited by relying on external cues. Almarwani et al. [80] also found that rhythmic auditory cueing is detrimental for speed adjustments in unimpaired participants. Dixon et al. [81] compared the use of pre-planned and real-time external auditory cue to instruct older adults to make a left turn or a right turn at the intersection while walking on an uneven cross-shaped path. The real-time cue was given at the same location of the path for all participants, resulting in the ability to successfully turn at all times. However, the study found that the real-time auditory cue resulted in a longer delay of body segment reorientation as well as increased in COM acceleration. This study did not investigate the gait parameters affected by cues given at different locations of the path.

The use of haptic cues were investigated for altering stride frequency, in which rhythmic vibrotactile cues on the wrist and ankle have been shown to alter walking speed [82, 83, 84]. The work by Karuei and McLean [82] showed that 13 out of 15 participants can synchronize their stride frequency to the given vibrotactile rhythm. This speed was maintained for at least 30s after the cue was turned off. This is in contrast to the results of auditory cueing, and suggests that haptic cues may perform better than auditory cues for adjustment of gait.

While these studies demonstrated the use of cues to instruct changes in walking speed or stride frequency, no study has employed external cues to alter stride length.

### *2.2.4 Foot placement cueing*

The importance of foot placement in gait analysis, especially for balance related applications such as reducing trip and fall when negotiating obstacles, motivates studies of foot placement. Current work uses mathematical models of human bodies with kinematics measurement at the hip to determine foot placement using sensors in the gait lab [85, 86, 87], as well as wearable sensors [41, 88].

#### *Timing requirements for foot placement stride length adjustments*

The relationship between onset cue timing and the resulting change in walking behavior is unknown for all modalities. Walking is a phasic steady-state behavior in which balance is maintained despite constant forward progression outside the base of support. Adjusting

stride length disrupts this steady-state. The intrinsic dynamics of a phasic movement influence how coordinated changes like adjusting stride length occur [89, 90]. In light of the role that gait phase may play in determining ability to adjust stride length, reaction times to haptic cues in static or dynamic tasks [70] alone may not adequately describe how behavior changes during a phasic task like walking. Hence, knowledge of when haptic cues should be delivered during phasic tasks requires separate investigation.

As far as we know, the studies done by Matthis et al. [91, 92, 93, 94, 95] are the only ones performed to investigate how early cues (in this case, visual) have to be given to users to allow timely stride length adjustments. They examined during which point of the gait cycle visual information is integrated into feedforward motor planning of walking — that is using information about the upcoming path to establish the mechanical state of body. Target foot placements were made visible during windows specified by the user's gait cycle. They found that the most accurate steps were made when the target was visible in between the prior step's mid-swing and heel strike (1-1.5 steps prior). In other words, visual information presented during this window was readily integrated into feedforward planning of the next step. In contrast, haptics are typically used in feedback pathways, thus the timing of integration of haptic cues into feedforward planning of gait may differ from that of visual cues. Despite the enhanced feasibility of implementing haptic cues over visual cues in wearable mobility assistance devices, nobody has characterized how haptic cues integrate into gait planning.

#### *2.2.5 Conclusion*

I want to ask the same question when haptic cues are given instead of visual cues. For the purpose of stair descent, we want the users to step on the optimal position at the step edge, allowing the use of "overhanging toe" strategy. Instead of presenting visual cues, how can haptic cues be presented to the users such that a target foothold is achieved. For the case of lower limb prosthesis users, they have visual cues of where the step edge location is, but have to combine this cue with the visual cues of where the prosthetic foot is. For intact individual, the latter part comes in the form of proprioception, which requires minimal cognitive load. Prior to implementing haptic cues to adjust foot placement for PWA, I want to answer the question of how the timing of haptic cues relative to gait phase affects the foothold of users. This will be tested for a level-ground walking task.

### *2.3 Gait modeling, analysis, and estimation*

Human gait analysis is a very important study in the field of biomechanics. The parameters of interest in gait analysis can be divided into: (1) anthropometric data that consists of physical human measurements; (2) kinematic data which includes body segments and joints

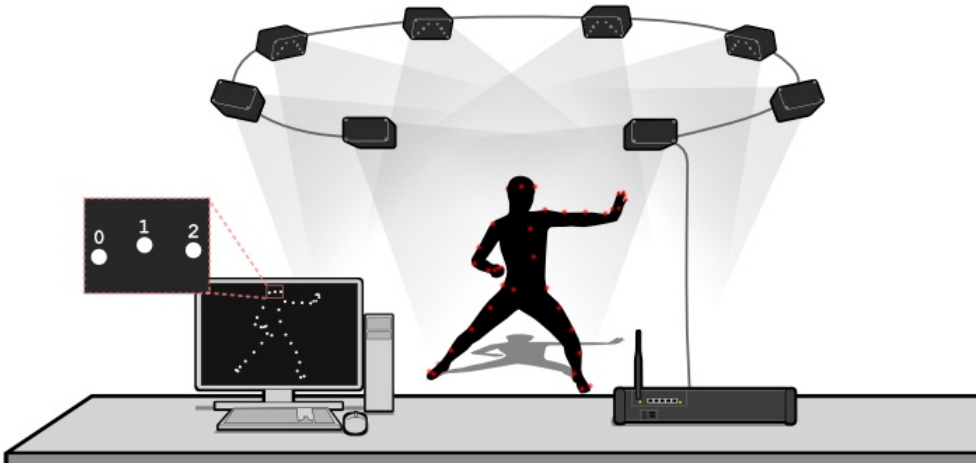


Figure 2.3: A lab motion capture system with cameras placed in the room and a user shown with body markers. [3]

positions at its derivatives; (3) kinetic data which is mainly ground reaction forces at the feet; and (4) spatiotemporal data derived from kinematics and kinetics such as body center of pressure (COP), balance, cadence, symmetry, and many others [96].

### *2.3.1 Gait measurement techniques*

The gold standard method for raw human gait data collection is using a motion capture system to collect kinematics data and force plates to collect kinetics data (Figure 2.3). The motion capture system consists of multiple cameras placed in a room, with the user wearing whole body markers. These markers are placed such that they coincide with anatomical landmarks, allowing cameras to infer the positions and orientations of markers, from which 3 degree-of-freedom (DOF) joint angles and 3DOF body link positions can be derived mathematically. The force plates are installed on the floor of the same room, in which 3DOF ground reaction forces are measured. Such data collection that is constrained to a lab environment has four problems: (1) difficult setup; (2) complicated pipeline for marker identification, reconstruction, and clean up; [97] (3) homogeneous population of participants; and most importantly, (4) a limited experimentation time window and space that fails to capture the full range of human movements and behaviors [98, 99, 100].

One way to perform data collection outside of the lab is to employ wearable devices (Figure 2.5) [101, 102, 103, 104]. Currently, there are non-marker (non-motion capture) based kinematic measurement system, such as custom [105, 88, 41, 106] or commercial [107, 108, 109, 110, 111, 112] inertial measurement units (IMU) mounted at joints, electromyography

Xsens motion capture system [4]


Moticon force sensor insole [5]

Figure 2.5: Examples of commercially available wearable gait measurement systems.

(EMG) electrodes mounted on the skin [113, 114, 115], goniometer encoder [116], ultrasound sensors [117, 118] to measure stride length, ultrawide-band (UWB) radio signals [119] and electric field height sensor [120] to measure toe clearance. Examples of wearable kinetic measurement systems include custom [121, 122, 123, 124, 48] and commercial [5, 125, 126, 127, 128] 1DOF force insoles, and 3DOF ground reaction force (GRF) shoes [129, 112].

With wearables, human gait data can be obtained while humans are performing their day to day activities, allowing collection of vast amounts of data.

### *2.3.2 Gait analysis*

*Model-based methods for gait analysis*

After measurement of gait data using the techniques described above, analysis and processing from raw data to useful gait parameters are typically done using biomechanics software such as OpenSim or Visual3D.

These estimation methods of kinetics parameters from kinematics parameters and vice versa are achieved by building a mathematical model of the human gait system and solving for its inverse rigid-body dynamics or multi body dynamics (MBD) solution [130]. These types of solutions, although precise and exhaustive, are subject-dependent, mathematically complex, and time consuming [131, 97]. Most importantly, obtaining precise models for human gait is challenging as human bodies are deformable and possess huge temporal and person-to-person variation [132]. Moreover, such solutions are not applicable for real-time estimations and cueing. Challenges in model-based estimation methods lead to investigations using model-free and data-driven methods.

*Model-free data-driven methods for gait analysis*

Currently, most model-free data-driven methods use machine learning algorithms to estimate various types of gait parameters, with lots of emphasis on force and moments at joints in the leg, and some on predicting kinematic trajectories. While some variations of algorithms such as support vector machine (SVM), random forest (RF), decision trees (DT), and hidden Markov model (HMM) are used, neural-network based algorithms, especially the artificial neural network (ANN) remains one of the most popular baseline algorithm used that shows the best performance most frequently, especially when dealing with prediction of non-sequential variables (e.g. parameters at every time step as input and output, discrete features extracted over a gait cycle as inputs).

A common variable predicted using model-free method is the force and moment at the knee using neural-network algorithms based on complete kinetic and kinematic data collected in the gait lab for the purpose of knee rehabilitation [133, 115, 114, 134]. Similar work using a model-based method is performed based on gait lab [135] and wearable sensors data [136, 129] using linear mixed models and inverse dynamics, respectively. Some work predicts full 6DOF ground reaction forces (GRF) based on kinematics data capture in the gait lab [137, 131] using a neural-network. Similar prediction was performed based only on normal force data from wearable insoles using linear regression [121] and inverse dynamics [138].

### *2.3.3 State of the art for gait analysis*

*Publicly available gait datasets and analyses*

As data science techniques continue to improve, the utility of collected data can be amplified by making it publicly available [139, 140]. Public dissemination of datasets facilitates reproducibility and allows secondary analysis that might not have been conceptualized by the collectors of the data. It also creates the potential to aggregate data from many sources, facilitating analysis and new applications.

In Table 2.1, we surveyed currently available public datasets of typical gait. Publicly available datasets exist for level-ground walking [141, 142, 143, 144, 145, 146, 147, 148, 149], running [150, 151, 145], and some other tasks such as side shuffle, v-cut [152], and Activities of Daily Living (ADL) [142, 153, 154, 155, 156, 157, 158, 159]. However, there are fewer publicly available datasets for stair ambulation [160].

Table 2.1: A summary of a portion of publicly available gait datasets.

| Authors | Population | Activities | Environment | Sensors | Outcome |
|---|---|---|---|---|---|
| CGA Normative Gait Dataset | 5-22 Children and Adults | Walking | Laboratory | MoCap | Kinetics, kinematics, EMG |
| CMU Graphics Lab MoCap Database | 144 for all; <10 per task Adults | Walking, Sports, Interaction, Random Tasks, ADL | Laboratory | MoCap | Kinematics |
| Fukuchi et al. 2018 | 42 Adults and Seniors | Treadmill Walking | Laboratory | MoCap | Kinetics, kinematics |
| Schwartz and Rozumalski 2008 (Gillette Children's Hospital) | 166 Children | Walking | Laboratory | MoCap | Kinematics |
| Fukuchi et al. 2017 | 28 Adult Runners | Running | Laboratory | MoCap | Kinetics, kinematics |
| Dorn et al. 2012 | 9 Adult Runners | Running | Laboratory | MoCap | Kinetics, kinematics, EMG |
| Neptune and Wright 1999 | 10 Adults | Side shuffle, V cut | Laboratory | MoCap | Kinetics, kinematics, EMG |
| Besier et al. 2009 | 27 Patello Femoral Pain + 16 Adults | Walking, Running | Laboratory | MoCap | Kinetics, kinematics, EMG |
| Chang et al. 2014 (from Physionet) | 93 Parkinsons' + 73 Adults | Walking | Laboratory | MoCap | Kinetics, kinematics |
| Fregly et al. 2012 | 6 Instrumented Knees | Walking | Laboratory | MoCap | Kinetics, kinematics, EMG |
| **Human ID (Gait challenge, CASIA, Soton, OU-ISIR)** | **>100 each Aged 19-59; 4000 Aged 1-94** | **Walking** | **Indoor and Outdoor** | **Video recording with various view angles** | **Human recognition from gait** |
| 61 articles reviewed by Benson et al. 2018 | 1-20; ~100; ~3000 Adults, Seniors, Targeted | 47 Walking; 13 Running; 1 Walking and Running | Indoor and Outdoor | Accelerometers | Cadence; step length, speed, acceleration; time |
| 76 articles reviewed by Shull et al. 2014 | Adults, Targeted | Walking, ADL | Most laboratory; some unconstrained environment | IMU, goniometer, accelerometer, FSR | Kinetics, kinematics |
| 12 Fall datasets reviewed by Casilari et al. 2017 (DLR, MobiFall, tFall) | 2-57 Aged 18-75 | ADL (stairs included) | Indoor home and office; outdoor | Single IMU unit (from Xsens or cell phone) | Fall classification |
| **Action dataset (USC-HAD, UCB WARD, 30 articles reviewed by Ahad et al. 2011)** | **~tens** | **ADL, varieties of gestures** | **Indoor and Outdoor** | **Video recording, MoCap, wearable sensors** | **Action recognition** |

*Current scientific understanding of stair ambulation*

To date, studies of typical gait on stairs have used laboratory-built staircases, generally 4-5 steps long, including 10-33 participants. In Tables 2.2 and 2.3, we provide a summary of studies of gait on stairs, including the population, measurement, and a brief overview of analysis. One notable study was performed with 25 young adults and 70 older adults, on an instrumented 7-step laboratory staircase [161]. In this study, a variety of kinematic and dynamic parameters were used to create a multivariate characterization of stepping behavior.

The current challenges with examining stair decent include; 1) Steady-state gait on stairs is not achieved until after the fourth step [162], thus, there is a need to study gait behaviors on full-flight staircases beyond the fourth step. 2) Behavior and performance may be affected by laboratory conditions [98, 99, 100]. 3) The gold standard gait measurement system requires expensive laboratory-based equipment, as well as intensive time dedicated by trained personnel for data processing and analyses [97]. These factors provide motivation to measure typical stair ambulation gait on long full-flight staircases outside of the laboratory. Such measurement is made possible by employing wearable sensors [101].

Table 2.2: A summary of work in biomechanical analysis for stair ambulation.

| Authors | Population | Staircase | Measurement | Feature Analysis | Application |
|---|---|---|---|---|---|
| Ackermans et al. 2019 | 25 adults;<br>70 older adults | 7-step custom lab staircase<br>Self-selected speed<br>Step-over-step no handrail | MoCap: full body kinematics and GRF | 1. COM<br>2. Foot clearance, %foot in contact with stairs<br>3. Friction<br>4. Cadence | Clustering of fallers and non-fallers |
| Livingston et al. 1991 | 15 adult women | 3 5-step custom lab staircase<br>0.58, 0.73, 0.88m stride<br>(only Steps 2-4 considered)<br>Self-selected speed | High speed video camera | 1. Temporal parameters: stance vs swing phase, speed (0.5, 0.7, 0.8m/s), cadence<br>2. Hip, knee, ankle angles<br>3. Anthropomorphic relationship<br>Right side only | Analyze lower limb kinematics for varying stair dimension across short, medium, and tall women |
| Riener et al. 2001 | 10 adults | 5-step custom lab staircase<br>(only Steps 2-4 considered)<br>Self-selected speed | MoCap: full body kinematics and GRF | 1. Temporal parameters<br>2. Hip, knee, ankle angles, moments, power<br>3. Foot placement angle: forefoot strikes ground first on stair walking<br>4. Angle when subject switches from level-walking gait pattern to stair-walking | Compare biomechanical parameters for 3 stair inclinations |
| Protopapadaki et al. 2007 | 33 adults | 4-step custom lab staircase<br>0.67m stride step<br>Self-selected speed<br>Step-over-step | MoCap: full body kinematics and GRF | 1. Temporal GC parameters: time and speed in ascent and descent = 0.56m/s<br>2. Hip, knee, ankle joint angles and moments<br>3. GRF | Compare biomechanical parameters in ascent vs descent |
| Adiputra et al. 2015 | 10 adults | 2-step custom lab staircase | MoCap: full body kinematics and GRF | 1. Temporal: hip, knee, ankle joint velocities<br>2. Hip, knee, ankle angles and moments<br>3. Tall vs short height comparison | Recreate work by Protopapadaki with different stair dimension |
| Cluff & Robertson 2011 | 17 adults | 5-step custom lab staircase<br>0.72m stride step<br>Self-selected speed<br>Step-over-step | MoCap: full body kinematics and GRF | 1. Temporal: self-selected speed 0.53m/s, speed progression with gait cycle<br>2. Hip, knee, ankle moments, power, and work | Lower extremity mechanics, progression of velocity, #gait cycle to attain steady-state |
| Bonifacio et al. 2018 | 16 adults with orthoses | 1-step lab step<br>Self-selected speed | MoCap: full body kinematics, GRF, EMG | 1. Hip, knee, ankle angles and moments<br>2. Abductor hallucis EMG<br>Dominant side only | Effect of foot orthoses on patellofemoral pain |
| Andriacchi et al. 1980 | 10 adults | 3-step custom lab staircase<br>0.33m stride - 25.5cm run, 21cm rise | MoCap: full body kinematics, GRF, EMG | 1. Kinematics - sagittal plane angle of hip, knee, ankle<br>2. Mean and max values of sagittal plane kinematics<br>3. Mean and max values of joint reaction moments, external moments | Compare biomechanical parameters in ascent vs descent |
| Zachazewski et al. 1993 | 11 adults<br>(3 male, 8 female) | 4-step custom lab staircase<br>0.33m stride<br>(1st step 2.5cm rise) | MoCap: full body kinematics and GRF | 1. Temporal parameters<br>2. Kinematics data shown as a "sample" and not presented as a whole<br>3. COM displacements in ascent and descent<br>4. GRF | Compare biomechanical parameters in ascent vs descent |
| Bergmann et al. 2010 | 14 adults<br>(9 male, 5 female) | 4-step staircase<br>0.29m stride | MoCap and Wearable MoCap (Xsens) | NA | Determine initial contact during stair ascent using wearable sensors |
| Queen et al. 2014 | 42 older adults with THA<br>(22 male, 20 female) | 4-step custom lab staircase<br>0.34m stride<br>Self-selected speed<br>Step-over-step | MoCap: full body kinematics and GRF | Peak hip kinematics and kinetics during pre-op, 6-weeks post-op,<br>and 1-year post-op during ascent and descent | Compare symmetry during stair ascent and descent after THA |
| Liikavainio et al. 2007 | 27 older adults with knee OA<br>(6 male, 21 female) | 4-step custom lab staircase<br>0.36m stride<br>Self-selected speed<br>Step-over-step | MoCap: full body kinematics, GRF, EMG | 1. Temporal parameters<br>2. Max 3D GRF and EMG information<br>3. Symmetry (ASI) | Compare impact loading and symmetry during level and stair walking for older adults with asymptomatic knee OA |
| Onodera et al. 2011 | 46 older adults with and without diabetic neuropathy (18 male, 28 female) | 5-step staircase<br>0.36m stride | EMG, Electrogoniometer | 1. EMG values during ascent and descent<br>2. Kinematics in sagittal plane (hip, knee, ankle) for control and target groups | Compare EMG and kinematics values for diabetic and non diabetic adults |

*Gait prediction during stair ambulation*

For gait prediction and classification , most model-free methods are implemented for level-ground walking tasks [163, 164]. Most work that tackles stair ambulation is related to event-based classifications useful for prostheses control [165, 166, 167]. The work that is

Table 2.3: A summary of work in biomechanical analysis for stair ambulation (cont.).

| Authors | Population | Staircase | Measurement | Feature Analysis | Application |
|---|---|---|---|---|---|
| Paquette et al. 2014 | 20 older adults (10 male, 10 female) | 3-step instrumented staircase + 2 additional custom steps<br>Variable step width limited by masking tape<br>Self-selected speed<br>Step-over-step | MoCap: full body kinematics and GRF | 1. Speed 0.57±0.06m/s<br>2. Peak GRF across 3 SW<br>3. Knee kinematics and kinetics (peak values and time to reach peak values) across 3 SW | Effects of staircase step width on frontal knee biomechanics on older adults |
| Ramstrand et al. 2009 | 10 unimpaired adults; 10 transtibial amputation older adults | 5-step custom lab staircase<br>Rise 17cm, Run 29cm (0.34m stride) | MoCap: full body kinematics | 1. Temporal parameters: cadence, step width, speed 0.73m/s (control) and 0.48m/s (impaired)<br>2. Foot placements (4 params each for ascent and descent) – reports no overhang | Compare FP strategies of unimpaired and individuals with transtibial amputation |
| Hamel et al. 2005 | 12 adults;<br>10 older adults | 7-step staircase<br>0.33m stride - 17.8cm rise, 27.9cm run | MoCap on the foot only, ambient lighting for different illumination | 1. Clearance for steps 1,3,5,7 of the staircase for young and older adults, under different lumination | |
| Muhaidat et al. 2011 | 10 adults | 4-step custom lab staircase<br>0.30m stride | MoCap on foot only | 1. Percent foot overhang 16% (6 standard deviation)<br>2. Landing Clearance and Passing Clearance | Determine FP, FC, TC during stair descent |
| Mian et al. 2007 | 13 men;<br>15 older men | 3-step custom staircase<br>0.33m stride<br>Controlled cadence 90steps/min | MoCap: full body kinematics and GRF | COM and COP distances relationship | Compare COP and COM separation between young and older adults |
| McFadyen & Winter 1988 | 3 male | 5-step custom lab staircase<br>0.36m stride | MoCap: full body kinematics, GRF, EMG | 1. Kinematics (joint angles), kinetics (GRF, moments, and muscle power), and EMG parameters for Hip, Knee, Ankle, during ascent and descent<br>2. Inter and intra subject variabilities of the above parameters | Report full biomechanical analysis of 3 male subjects during stair ambulation |
| Novak & Brouwer 2010 | 23 adults;<br>32 older adults | 4-step custom lab staircase<br>15cm rise, 26cm run<br>Self-selected speed<br>Step over step | MoCap: full body kinematics and GRF | 1. Temporal parameters<br>2. Joint moment peak values in sagittal and frontal planes, joint moment plots<br>3. Intra and inter subject variability for joint kinematics | |
| Telonio et al. 2013 | 17 adults | 5-step custom lab staircase<br>18.8cm rise, 30cm run<br>Self-selected speed | Mocap on the foot only | 1. Speed 0.71m/s<br>2. Distribution of foot clearance (not placement!) over step progression | |
| Zietz et al. 2011 | 8 adults;<br>7 low-risk (of falling) older adults;<br>8 high-risk older adults | 5-step custom lab staircase<br>17cm rise, 27cm run<br>Self-selected speed | MoCap: full body kinematics | 1. Vertical and horizontal foot clearance<br>2. Step width, step length<br>3. Distance between COM and ankle<br>4. COM acceleration<br>5. Walking speed 0.81m/s | Comparing effects of foot and toe clearance across different age groups, illumination, stair edge contrast |
| Den Otter et al. 2011 | 6 adults<br>(3 male, 3 female) | 10-step actual staircase<br>18cm rise, 28cm run | Eyetracker | | Studies gaze during stair descent |
| Vallabhajosula et al. 2011 | 10 adults | 4-step custom lab staircase<br>18cm rise, 28cm run | MoCap: full body kinematics and GRF, photocell for speed | 1. Joint moment and torques analyses<br>2. Sagittal plane moment and power over gait phase | Determine the differences in the joint moments and powers when one begins stair ascent after achieving a comfortable gait speed compared to beginning stair ascent from a static position directly in front of the stairs |
| Bosse et al. 2012 | 13 adults;<br>13 older adults | 2-step staircase<br>17cm rise, 30cm run<br>Self-selected speed<br>Step-over-step | MoCap: full body kinematics and GRF | 1. Dynamic stability (COM x, xdot), Joint kinematics (sagittal) during initiation of double support phase and single support phase<br>2. COM xdot relationship with ankle and knee angular impulse during double support phase | Examine dynamic stability control in younger and older adults during stair descent |
| Rao and Carter 2012 | 15 adults | 7-step staircase<br>19.5cm rise, 28.75cm run | Pedar | Peak pressure, force, contact time: stair ascent, descent, level ground, for: heel, midfoot, medial forefoot, central forefoot, lateral forefoot, hallux | Analysis related to plantar pressure data recorded using Pedar and its comparison with force plates |

closely related to assisting users in real time about their stair descent performance is the work done in [168], in which stair descent cases are classified into normal or anomalous, but

this is only useful when a trip or fall event has happened, which is not practical in real life. The work done in [169, 170] helps determine gait parameters that may lead to a fall, hence it could be used for providing a more timely cue to prevent a fall. Aside from the cases of fall prevention, there has been, to the best of my knowledge, minimal investigation of how to assist people with difficulties walking downstairs complete stair descent in an easier and a more intuitive manner.

### *2.3.4 Conclusion*

While prediction and estimation of gait parameters are used for a complete biomechanical analysis, as well as for designing control systems for prostheses, most of the times they are not metrics that are directly applicable and interpretable for human day to day applications. Moreover, in stair descent, making an error is very dangerous."Reactive" error corrections are not always available during stair descent — a missed step may result in a fall before the user can react."Proactive" error correction – or correcting the error before it occurs – is the safest solution. This entails predicting when an error will occur, and informing the user such that they have time to react and adjust their foot placement or stride before risking a fall.

For my application of assisting stair descent through cueing of optimal foot placement, I propose using wearable sensors for gait measurement such that data collection is not constrained to a lab environment and can be performed in an actual ADA staircase. With such setup, collection of stair descent gait data can be expanded to a larger group of participant, in the order of hundreds instead of tens, allowing availability of more data that represents the population better.

With this, I also propose using model-free machine learning algorithms based on neural-networks for predicting future foot placement. This proposed method may not be able to provide a complete biomechanical analysis at a gold standard level of precision, but is far more suitable for the use case.

# Chapter 3

# PROVISION OF DIRECT HAPTIC FEEDBACK ON THE THIGH AS SENSORY RESTORATION OF PROSTHETIC FOOT

This chapter describes Aim 1 of this research, in which I describe the initial approach for assisting stair descent: the sensory restoration paradigm of using direct haptic feedback on the thigh to represent forces underneath the prosthetic foot. The background related to Aim 1 is described in Section 2.1.2. The hardware and system design of this aim has been published in [48], while experimental testing and evaluation is published in depth in [49].

## *3.1 Device design*

We present the initial design of our haptic feedback system in [48]. It is fully wearable and consists of a sensor insole, an actuator thigh band, and an on-board embedded processing system (Figure 3.1). We modified the sensory insole from our initial design to use four force sensitive resistors instead of five.

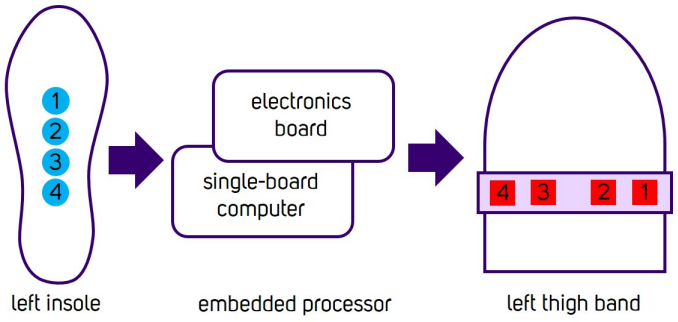


Figure 3.1: Block diagram of the haptic feedback system.

### *3.1.1 Sensor insole*

In the sensor insole, four force-sensitive resistors (FSR) (FlexiForce A401, Tekscan, South Boston, MA, USA) are placed in between two off-the-shelf shoe inserts. The FSRs are aligned along the longitudinal axis of the foot. We use four sensors in this design iteration to distinguish four different foot "overhang" positions on a staircase, which will be explained in Section 3.2.2. Electrical signals from the FSRs are sent to separate voltage dividers on the electronic board which then interfaces with the on-board processor. Exact calibration between electrical signals and force values measured by the FSR is not necessary because precise force values are not required to accomplish a simple edge discrimination task. Figure 3.2 shows the sensor insole with 6 FSRs. The insole is attached to the bottom sole of a medical boot to address foot size variations among participants, however in future applications the insole can be made to size.

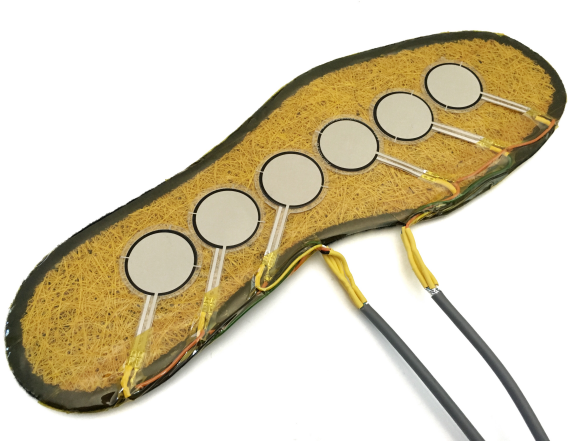

Figure 3.2: Sensor insole with 6 FSRs shown without the top layer of shoe insert.

### *3.1.2 Actuator thigh band*

The actuator thigh band (Figure 3.3) consists of four piezoelectric actuators (Samsung Electro-mechanics, South Korea) encased in a 3D-printed housing made of PLA plastic. The actuators are sewn on an elastic strap with a spacing of 1.5in between Actuators 1 and 2, and Actuators 3 and 4. Actuators 2 and 3 are spaced at a distance of 3in. The strap is worn around the upper thigh with the actuators placed from medial to lateral (as shown in Figure 3.1). The actuators contact the skin through the custom housing. A Velcro strap enables easy adjustment. Each actuator activates independently with an amplitude of vibration that responds linearly to the amplitude of force sensed by the corresponding FSR.

Vibration frequency of the actuator is set to be in the range of 200-500Hz [171] in software. Vibration commands to the actuators are sent using I2C communication protocols from the embedded processor through an I2C multiplexer (TCA9548A, Texas Instruments, Dallas, TX, USA) and a haptic motor driver (DRV2605L, Texas Instruments, Dallas, TX, USA).

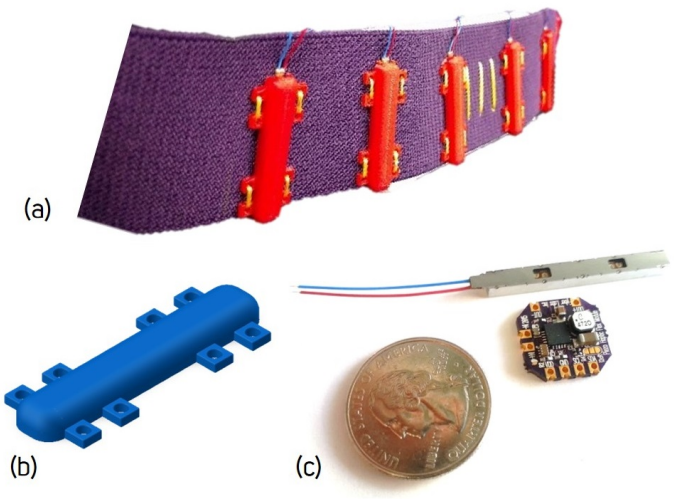


Figure 3.3: (a) Thigh band with 6 actuators; (b) 3D printed actuator housing; (c) piezoelectric actuator and the haptic driver board shown with a quarter US dollar coin for scale.

### *3.1.3 On-board embedded processor*

A BeagleBone Black (BeagleBoard.org, Oakland, MI, USA) performs on-board processing. Signal processing of insole data and processing of actuation commands are accomplished in two separate electronic boards stacked on the BeagleBone Black and sewn to the thigh band, respectively. During startup, the BeagleBone Black is activated through a wired-USB connection to a PC. Once the wireless connection (through WiFi) is established, the BeagleBone Black can be disconnected from the PC and the haptic feedback system is fully wireless and wearable.

### *3.1.4 Haptics actuation scheme*

The haptic feedback system transmits force information at the bottom of the foot to vibrotactile actuators on the thigh. Each actuator is mapped to one FSR, according to the numbering scheme shown in Figure 3.1. FSR signals in the anterior-posterior direction on

the foot are mapped medio-laterally to take advantage of increased two-point discrimination acuity in the medio-lateral direction [172].

We explored two modes of actuations. First, Proportional Mode is defined as when vibration amplitude of the actuators is directly proportional to the magnitude of force sensed by the FSR. This scheme is designed to induce body ownership towards the device through direct mapping of forces to the thigh. Second, we tested the Edge Detection Mode, in which analysis of FSR data reveals the position of the staircase edge with respect to FSR Position 1, 2, 3, or 4. In this mode, only the single actuator that corresponds to the position of the staircase edge will vibrate at a constant maximum amplitude and cue the user as to the position of the staircase edge. While the Proportional Mode may induce embodiment of the prosthesis, it may also create a sensory overload for the user, masking useful vibration information that is critical for an easier stair descent. In contrast, the Edge Detection Mode provides clear and direct information without attempting to substitute the sensory experience of the amputated limb. Edge Detection Mode requires the participant to localize stimuli, whereas in Proportional Mode the participant must also gauge the intensity of the stimuli. However, different areas of the thigh have different sensitivities to vibration. To minimize the effect of sensory biases, we used Edge Detection Mode. We would like to explore additional actuation modes in future studies.

## *3.2 Experimental protocol*

To assess the performance of our haptic feedback system, we performed two experiments.

### *3.2.1 Experiment 1 - benchtop verification*

Experiment 1 demonstrated each participant's capability to differentiate distinct vibration positions on the thigh. We performed Experiment 1 across $n = 15$ unimpaired participants. The participant wore only the actuator thigh band and did not wear the sensor insole and on-board processor. The actuators were adjusted such that they lay in the transverse plane along the posterior of the thigh, and aligned such that the participant could individually discriminate actuators. While wearing the actuator thigh band, discrete forces were applied manually to a single FSR (given position) on the insole, causing the corresponding actuator worn on the thigh to vibrate. The participant was instructed to report the position of vibration (perceived position as illustrated in Figure 3.1). The vibration amplitude was set to be uniform across the four actuators regardless of the amount of force applied to the FSR. Each participant completed 120 repetitions, in which the sequence of FSRs were randomly generated. Given and perceived positions of vibration were recorded.

### *3.2.2 Experiment 2 - hidden step experiment*

Following Experiment 1, the participants were asked to perform Experiment 2. The thigh band was worn continuously during the transition between experiments. If the participant needed to remove the thigh band, it was donned in its original location and orientation.

Experiment 2 investigated each participant's capability to indicate the staircase edge position at the bottom of the foot without visual feedback and plantar sensation. We performed Experiment 2 across $n = 13$ unimpaired participants. The participant wore a stiff medical boot (Maxtrax$^{TM}$, DJO LLC, Vista, CA, USA) (Figure 3.4) on the left leg to eliminate ankle flexion and to minimize sensation on the bottom of the foot. The medical boot simulated the range of motion constraints at the ankle of a lower limb prosthesis. The sensor insole was attached to the outer surface of the underside of the boot, and the on-board processor was attached to the shank of the boot. The participant wore the actuator thigh band on the left thigh as in Experiment 1. Setup of the haptic feedback system worn by the participant is shown in Figure 3.5.


Figure 3.4: The stiff medical boot worn by the participants to minimize ankle flexion and plantar surface forces sensation. Positions of the FSR on the sensor insole at the bottom of the boot are marked accordingly.

For this experiment, we built a custom 3-step staircase (Figure 3.6) from 80-20 aluminum bars (T-slotted aluminum bar, 80/20 Inc., Columbia City, IN, USA) and plywood. The lowest step of the staircase was flush with the platform. The step was covered with a piece of flannel cloth to visually obstruct the edge of the step. The position of the hidden step was manually adjusted such that it coincided with Positions 1, 2, 3, or 4 of the FSR at the insole.

During each trial, the participant stood on the platform with both feet straddling the


Figure 3.5: The haptic feedback system worn by a subject during Experiment 2.

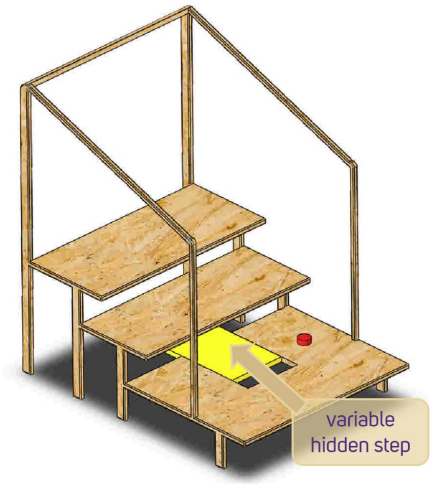


Figure 3.6: 3-step staircase with a variable step-size hidden step.

hidden step. The participant then placed the boot within a marked box on the hidden step. Subjects were instructed to not adjust the positioning of the boot once they had stepped onto the hidden step. In between each trial, the hidden step was manually adjusted such that it coincided with FSR Positions 1, 2, 3, or 4 in a randomized order. Haptic feedback on the thigh was enabled for half of the trials, also in a randomized order. The participant was asked to verbally report the number (1-4) of the perceived position of the edge of the staircase under the foot based on the vibration information given by the actuators on the thigh. The experiment was repeated 120 times each per participant. Actual sensor force and actuator signal data, as well as given and perceived positions of the hidden step edge were recorded.

## *3.3 Results and discussion*

### *3.3.1 Experiment 1*

The perceived positions of stimulation in Experiment 1 for all 15 participants are plotted as a confusion matrix. Figure 3.7a displays the raw number of guesses while Figure 3.7b displays the normalized values as a percentage of guesses for each given position.

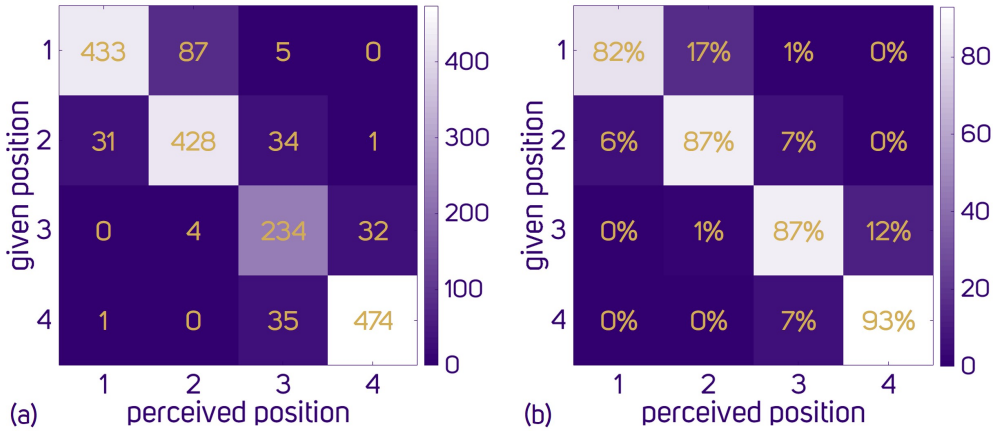


Figure 3.7: (a) Perceived position for each given position shown as a confusion matrix; (b) Normalized confusion matrix of perceived location for each given location.

As seen in Figure 3.7, the participants correctly distinguished the position of vibration with a minimum accuracy of 82% for every given position. All participants demonstrated the lowest accuracy in localizing stimuli in Position 1 (closest to toe). The actuator for Position 1 is located on the inner thigh, which may be less sensitive to vibration than the

posterior or lateral thigh. In a lower limb prosthesis user population, additional effort may be necessary to ensure that each actuator is individually distinguishable, depending on the sensory characteristics of the lower limb after amputation.

We observed that even though we delivered the exact same vibration amplitude and frequency commands to all four actuators, participants reported that the strength of vibration was different among the four actuators. Subjects reported that Actuators 1, 3, and 4 had similar vibration strength, whereas Actuator 2 was weaker. To achieve uniform vibration amplitude and frequency, the actuators must be calibrated such that the physical representation of the software command is correct. Calibration could be performed by measuring vibration amplitude and frequency using a vibration meter, or by performing impedance matching characterization [173].

The variation in vibration strength (amplitude and frequency) among the actuators might contribute to variations in distingushability of stimulus position. We suspect that this is the cause for the observation we had for stimuli given at Position 2, in which the participants reported these as stimuli given at either Position 1 or 3.

For stimuli at Position 3, participants mistakenly guessed Position 4 for 12% of trials, and only 1% at Position 2. This discrepancy in errors may be explained by the placement of the actuators, in which Actuators 2 and 3 are separated by a distance of 3in while Actuators 3 and 4 are only 1.5in apart.

The participants reported a higher accuracy when localizing stimuli given at Position 4. This observation may suggest that participants have higher two-point-discrimination sensitivity on the lateral thigh.

### *3.3.2 Experiment 2*

The results of Experiment 2 are depicted in Figure 3.8. The $x$-axis shows the 4 hidden step staircase edge positions with respect to the position of the FSR on the insole (Figs. 3.1 and 3.4). Position 1 is closest to the toe and Position 4 is closest to the heel. The $y$-axis shows the absolute error value between the given position of the staircase edge and the perceived position of the staircase edge (3.1). In (3.1), $e$ is error and $p$ is position. For example, when the given position of the staircase edge is 1, and the perceived position is 4, the error is 3.

$$e = |p_{stepedge,given} - p_{vibration,perceived}| \tag{3.1}$$

There are 3 error bars plotted for each hidden step position. The first bar in dark purple represents the trials with haptic feedback in which the error is calculated between given and perceived hidden step edge positions as in (3.1). However, two situations arose in which

the system detected the step at a different position than intended (e.g. FSR/Actuator 2 is active when the step is in Position 1). First, the participant's placement of the boot on the hidden step varied, despite the guide markings on the step. Second, the curvature of the boot sole (as seen in Figure 3.4) made the system sensitive to the angle at which the participant placed the boot down. Thus, the second bar in light purple represents the trials with haptic feedback in which error is calculated between perceived position and the active actuator as verified through extraction of actuation commands and FSR readings (3.2). This accounts for errors in edge detection due to boot placement. The third bar in gold represents the trials with no haptic feedback.

$$e = |p_{actuator,active} - p_{vibration,perceived}| \tag{3.2}$$

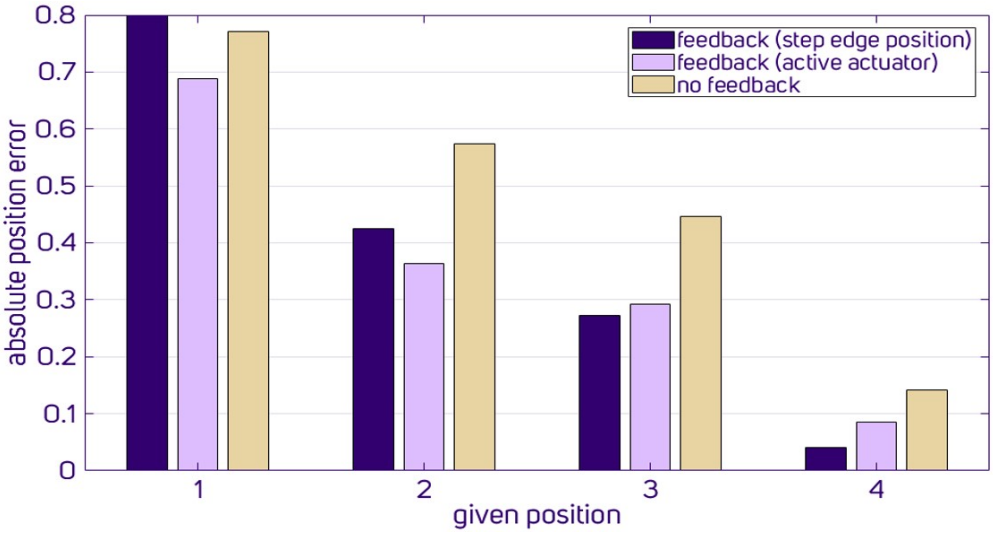


Figure 3.8: Position error shown for each given hidden step position with and without haptic feedback.

Figure 3.8 reveals a general trend that the position error between actual and perceived hidden step positions, regardless of haptic feedback, decreases as the edge of the hidden step is moved from the toe (Position 1) to the heel (Position 4). This trend may be explained by changes in body dynamics as the step edge moves posteriorly towards the center of mass, thus rolling the foot over the step edge and inducing the sensation of "falling over." This may cue the participant to the position of the hidden step.

Figure 3.9 shows the percentage of guesses in both trials with feedback and without feedback. Each given position is determined from the active actuator ($p_{actuator,active}$). Consistent with Figure 3.8, participants demonstrated increased accuracy in localizing the step edge

when haptic feedback is present. In particular, error between Positions 2 and 3 was reduced in the presence of haptic feedback, potentially indicating that the increased spacing between Actuator 2 and 3 enhanced discriminability between these positions beyond that of other adjacent actuator pairs.

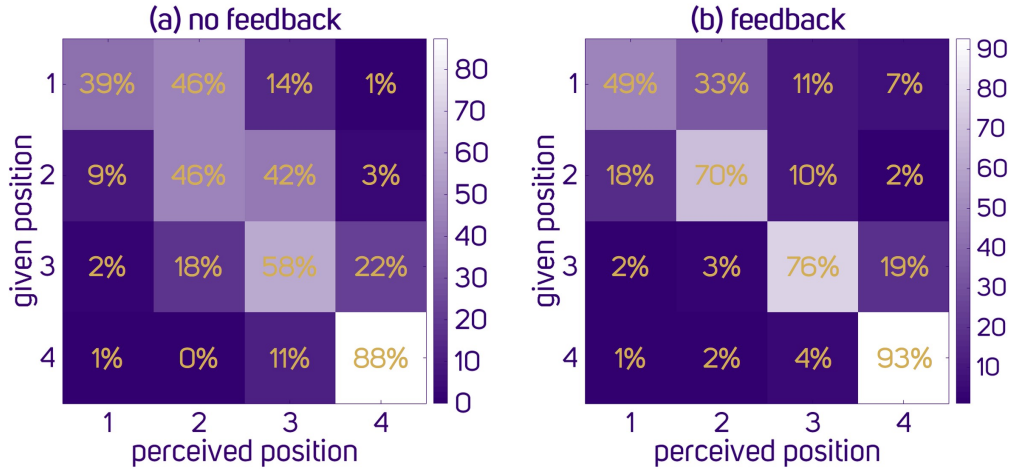


Figure 3.9: (a) Confusion matrix for trials without haptic feedback and (b) confusion matrix for trials with haptic feedback, given position calculated from actuator activation.

The participants demonstrated reduced position error and increased success in perceiving hidden step position when haptic feedback is provided. However, in performing the paired t-test statistical analysis to compare trials for each position when feedback is absent and present, only Position 2 shows a statistically significant reduction in position error with feedback ($p = 0.0213$). Nevertheless, this result by itself is promising because it shows that our haptic feedback system improves the participants ability to "feel" and perceive information on foot placement in the absence of plantar sensation. It should be noted that even though haptic feedback reduces error, the participants do not require haptic feedback to remain somewhat capable of discriminating step position, which makes Position 4 easily identifiable without haptic feedback. It must also be taken into account that this result may not generalize to lower limb prosthesis users, who have altered sensory pathways.

Experiment 2 shows that, without access to visual cues and the sensation of plantar forces, participants wearing the haptic feedback system are able to localize the position of the hidden step edge based on vibration information delivered to the thigh.

### *3.4 Future work*

This experiment may be fine tuned in future work to include a stiffer boot with a flat bottom to completely remove sensation of plantar forces, better mimicking the simulation of lower limb prostheses. The experiment may be broadened to include lower limb prosthesis users and full stair descent tasks. Future device designs may prioritize sensorizing areas in which feedback proves more beneficial for step edge discrimination. In fact, providing cognitively demanding haptic feedback may be unnecessary when proprioceptive cues are available.

Future work in this domain requires further characterization of stair mobility kinematics in impaired populations. New feedback devices and actuation schemes should be evaluated with respect to the benefits they provide to impaired users. Stair descent performance remains a challenging construct to measure due to the variety of gait and balance strategies used by those with impairments, and demands further research to enable rigorous evaluation of new interventions.

### *3.5 Conclusions*

We have demonstrated the feasibility of haptic feedback as a method to sense the stair step edge without a visual aid. The utility of haptic feedback is highlighted in the absence of interoceptive sensation, or when biological feedback pathways are unavailable or absent.

*Despite this promising result, four different locations of vibrations caused increased cognitive burden for the participants especially during locomotion. This problem prompted the design of the new system which shifts the cognitive load from the human to the device. Instead of directly mapping sensors to feedback, we make a system that intelligently predicts the users behavior to deliver simplified cues. This way, instead of restoring sensation, we are providing simple bidirectional cues with the hope of reducing cognitive load to facilitate integration of Smart Step in daily live. This leads to Aims 2 (Chapter 4) and 3 (Chapters 5 and 6).*

# Chapter 4

# HAPTIC TIME-TO-CUE REQUIREMENTS FOR FOOT PLACEMENT ADJUSTMENT IN MOBILE TASK

This chapter describes Aim 2, investigating how timing of haptic cues can effectively alter human foot placement behavior. This information is crucial such that during stair descent, the haptic cue can be given in a timely manner (not too early, and not too late) such that user can step at the desired foot placement with respect to the stair edge. This aim is parallel to Aim 3 in Chapters 5 and 6, which is focused on predicting where the original unaltered foot placement is going to be such that a cue can be given to alter it if an error is predicted.

The work in Aim 2 is highly motivated and based on existing haptic feedback technologies and cognitive load associated described in Sections 2.2.1 and 2.1.3, and foot placement investigations in Section 2.2.4. Publication for this aim is underway in [50].

## *4.1 Wearable haptic wrist band*

Our wrist-worn wearable device (Figure 4.1) consists of two haptic eccentric-rotating-mass (ERM) motors (Vibrating Mini Motor Disc 1201, Adafruit, New York City, NY, USA), one placed on the dorsal side of the wrist, and another on the palmar side. When the motor is vibrating, the participant is instructed to adjust foot placement of the following right footed step. Vibration on the palmar side cues a shorter step, while vibration on the dorsal side cues a longer step.

### *4.1.1 Electronics*

The motors are controlled using an Adafruit Feather M0 Adalogger microcontroller (2796, Adafruit, New York City, NY, USA), connected through a TCA9548A $I^2C$ multiplexer (Texas Instruments Incorporated, Dallas, TX, USA) and two DRV2605 haptic motor drivers (Texas Instruments Incorporated, Dallas, TX, USA). This system is interfaced to a computer via a serial bluetooth (SPP) communication protocol using the HC-05 transmitter (Shenzhen HiLetgo Technology Co., Ltd, Shenzhen, China). A 3.7V lithium-ion (LiPo) battery is used to power the system.

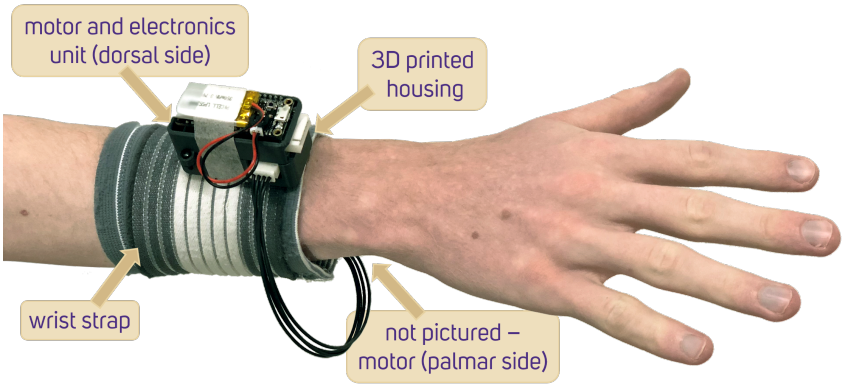


Figure 4.1: Wrist-worn haptic band.

### *4.1.2 Mechanical design and construction*

The wrist band is an off-the-shelf elastic band that can be tightened with Velcro. The dorsal motor is encapsulated together with the electronics and microcontroller boards, using a 3D-printed Acrylonitrile Butadiene Styrene (ABS) case. This casing is secured to the elastic band using Velcro. The palmar motor is secured within the elastic band.

### *4.1.3 Motor vibration profile*

The vibration profile of both motors are set based on the DRV2605 Waveform Library List [174]. The motor has a response time of 20ms. When activated, the motor will vibrate with Waveform 14 (Strong buzz, 100% — a step command with vibration frequency of 120Hz), pulsed every 100ms for a total duration of 2s.

### *4.1.4 Spatial design choice*

Dim, Karuei, and Machida et al [70, 71, 72] found that detection rate and time of vibrotactile cues are optimized when delivered to the distal or bony anatomy (ear, wrist, hand, spine, foot), with lower anatomy (foot) undesirable for walking applications. We picked the wrist as it aligns with user preferences while maximizing detection rate of cues for walking applications. In addition, wrist-worn wearable systems are commonly available and used in the market and hence allow easy adaptation and integration with existing wearables.

## 4.2 User study

### 4.2.1 Participants

We recruited 10 participants (5 male, 5 female) aged 21.6 ± 2.5years, height 167.56 ± 10.08cm, weight 62.91 ± 8.02kg, with no mobility impairments, following the Institutional Review Board (IRB) protocol conducted at the University of Washington.

### 4.2.2 Apparatus

Each participant wore a full-body set of motion capture markers for measurement of body kinematics (Qualisys AB, Göteborg, Sweden), and a haptic wrist band on the right wrist that delivers two distinct haptic cues on the palmar and dorsal side. We also recorded ground reaction forces during walking using four force plates levelly-mounted on the walkway (Kistler Group, Winterthur, Switzerland).

Figure 4.2 shows the 36 reflective markers on user's anatomical landmarks and 10 clusters of 4 markers on the upper arm, fore arm, thigh, shank, and foot. The right heel marker is highlighted, with user stepping on force plates 1 and 2 (red arrows denote normal ground reaction forces sensed by the force plates).

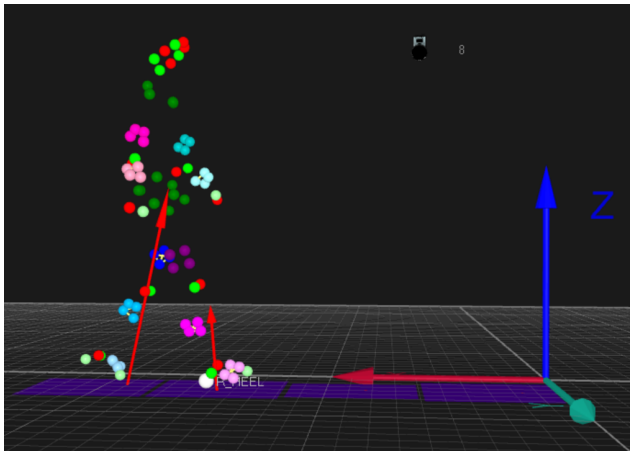


Figure 4.2: Participant walking along the walkway with reflective markers and ground reaction forces shown as arrows normal to the contact.

The motion capture system and force plates are used to determine real-time gait events, while the haptic wrist band is used to deliver haptic vibrotactile cues to the participants.

The motion capture system is also used to record and measure stride length information during the trials.

### *4.2.3 Task*

The participant is instructed to walk in a straight line along a 10m walkway in the forward pass. The starting position is approximately 5 steps prior to the first force plate, and is determined for each participant such that participants natural stride will result in each step striking a separate force plate prior to the haptic stimulus. Trials in which steps prior to haptic stimulus landed on multiple force plates at once were discarded and repeated. The first foot step on the first force plate can either be the left or the right foot (Figure 4.3).

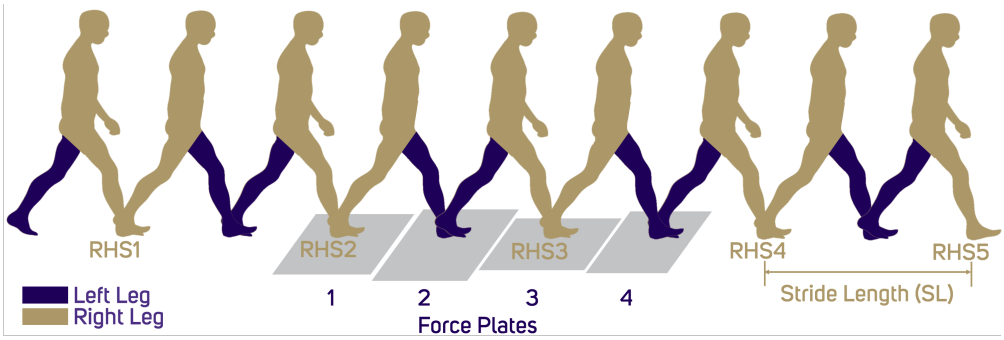


Figure 4.3: Participant walking along the walkway. This configuration shows right foot as the first step on the first force plate.

During the forward pass, a haptic stimulus is given to the participant. The participant is instructed to adjust the stride length of the next right foot once the haptic cue is felt. If the haptic cue is felt on the palmar side, the participant is to take a shorter step with the next right foot. Likewise, if the haptic cue is felt on the dorsal side, the participant is to take a longer step with the next right foot. We have chosen to only perform the experiment for the right sided stride to reduce experimental complexity.

We instruct the participants to walk at a self-selected walking speed, and to refrain from stopping should they require time to think about the haptic cue and the appropriate response. Participants are not given instruction regarding how much to adjust their stride by, nor whether to continue or cease the adjustment in subsequent steps. As such, the amount of stride adjustments observed are self-selected by the participants. At the end of the trial, we ask the participant to complete a questionnaire.

### *4.2.4 Study protocol and design*

We provide one condition without any haptic stimulation (ST0) and two stimulation conditions (step shorter and step longer) at six stimulation times (ST1-ST6). These stimulation times correspond to different events in the gait cycle (Figure 4.4). The target foot (T) is the right heel strike that we want participants to change (e.g. step longer or step shorter). The six stimulation times and their timing corresponding to the target foot (T) are described in Table 4.1. For each participant, we collected 84 trials, in which one trial consists of a single forward pass over the force plates. There are 12 trials each for ST0-ST6. For ST1-ST6, there are 6 trials for each condition (step long and step short).

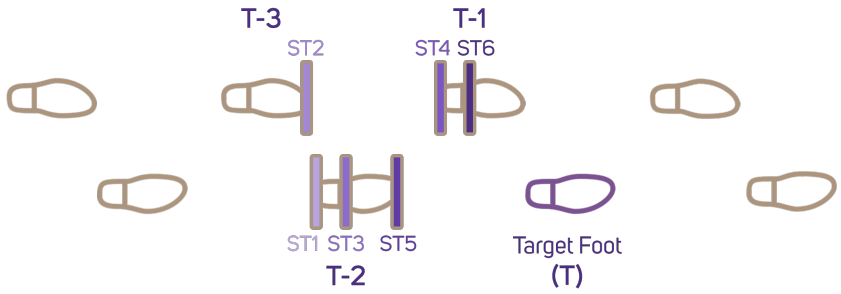


Figure 4.4: Six haptic stimulation times (ST1-ST6)

Table 4.1: Seven haptic stimulation times (ST0-ST6) explained

| | *Corresponding gait event* | *Relationship to target foot (T)* | *No. of steps prior to T* |
|---|---|---|---|
| **ST0** | No stimulation | | |
| **ST1** | Right heel strike | At T-2 | 2 |
| **ST2** | Left toe off | Leading to T-1 | 2 |
| **ST3** | Left mid swing | Leading to T-1 | 1.5 |
| **ST4** | Left heel strike | At T-1 | 1 |
| **ST5** | Right toe off | Leading to T | 1 |
| **ST6** | Right mid swing | Leading to T | 0.5 |

The gait events are determined in real-time based on marker position and ground reaction forces given by the motion capture system and the force plates. Once a gait event corresponding to the timing condition (ST1-ST6) is detected, the firmware will send a command to the microcontroller on the wrist band to activate either the palmar or the dorsal

motor, cueing the participants. The stimulation is delivered at a random location along the walkway to prevent participants from memorizing the spatial location at which they have to adjust their stride.

## *4.3 Data processing and analysis*

After the user study, we determine the resulting stride length of all participants and trials before and after the haptic cue based on the heel marker position captured by the motion capture system.

### *4.3.1 Stride length definition*

As we instruct the participants to adjust their right footed step, we limit our scope of analysis to the right strides. In this study, one stride is defined to begin at right heel strike and end at the next right heel strike. Hence, **stride length** is defined as right heel position at current right step (T), subtracted by right heel position at the previous right step (T-2). This is not to be confused with **step length**, which is defined as beginning at right heel position and ending at left heel position.

### *4.3.2 Centering of target foot index*

For each trial, we recorded 5 right heel strikes along the walkway. The first right heel strike is selected to be the one prior to stepping on the first force plate (Figure 4.3). With the experimental configuration in which cues are given at random locations along the walkway, the target foot (T) can either be the second, third, fourth, or fifth right heel strike (RHS). During analysis, we center the target foot (T) to be the fifth index, allowing recording of at most 4 right heel strikes prior to the target foot (T-2, T-4, T-6, T-8) and 3 right heel strikes after the target foot (T+2, T+4, T+6) as illustrated in Figure 4.5.

### *4.3.3 Normalization of stride length*

For each trial, there are 5 right heel strikes, resulting in 4 right stride lengths (SL). For all no stimulation trials (ST0), we calculated for each participant the mean stride length for the first, second, third, and fourth strides (Figure 4.6). There are variations in mean stride length for each participant and minor variation within each participant between each stride index.

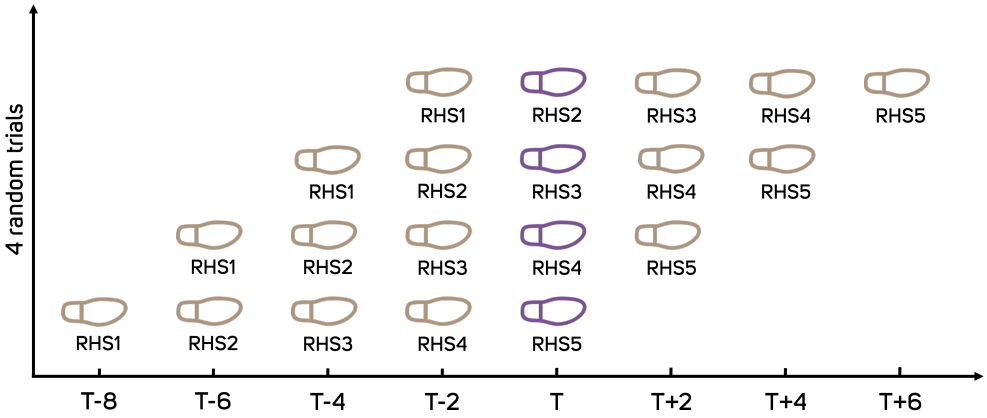


Figure 4.5: Centering of target foot (T) at the fifth index. Target foot can either be the second, third, fourth, or fifth right heel strike (RHS).

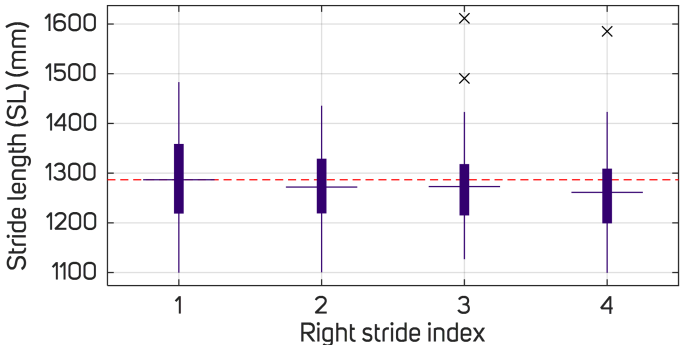


Figure 4.6: Mean right stride lengths for all 10 participants for all no stimulation (ST0) trials.

To account for variation in self-selected stride lengths across participants, we normalize the stride lengths for each participant and each trial (4.1). $SL$ is stride length; $i$ is the stride length index from 1 to 4. This allows variation along stride progression to be taken into account with the normalization. $SL_{mean,ST0}(i)$ is the mean stride length obtained from the no stimulation trials (ST0). It is important to note that $SL_{mean,ST0}(i)$ is the unique mean stride length of that particular stride index for that particular participant.

$$SL_{norm}(i) = \frac{SL(i)}{SL_{mean,ST0}(i)} \tag{4.1}$$

#### *4.3.4 Statistical analysis*

We performed a one-way ANOVA to compare the effect of haptic timing (stimulation time) on stride length in foot stepping to steps occurring at the onset of the haptic cue (T-2), after the haptic cue at the target foot (T), 2 steps after the target foot (T+2), and 4 steps after the target foot (T+4). We repeated the ANOVA 12 times for each of the 6 stimulation time, ST1-ST6, for step shorter and step longer trials. The significance level is set to be $\alpha = 0.05$. We performed post-hoc comparisons using Tukeys Honestly Significant Difference test to compare the pre-haptic cueing group (T-2) and the post-haptic cueing groups (each T, T+2, T+4).

We used Matlab `fitlm()` to test the correlation between speed and changes in stride length. The linear fit is compared to a constant fit, and we picked an $\alpha = 0.05$ to determine significant differences between the linear fit and the constant fit, suggesting that there is a significant correlation between walking speed and changes in stride length.

### *4.4 Results*

#### *4.4.1 Haptic cues enable changes of participants' self-selected stride at target foot (T)*

We calculated the normalized stride length of the target foot (T) for each trial. For the step shorter trials, values smaller than 1 are correct. For the step longer trials, values greater than 1 are correct. For the no stimulation trials, we counted the number of trials with values greater than 1.

Table 4.2 shows the percentage of trials in which correct adjustments are made in aggregate. The percentage of correct stride adjustments for both step shorter and step longer cues are highest during ST1 and ST2, with mean values ranging from 77% to 91%. As the stimulation is delivered later in the gait cycle and closer to the target foot heel strike, we observe a reduced ability to adjust stride length. During ST5 and ST6, the mean values for both step longer and step shorter cues drop to around 50%. During ST3 and ST4, we observe mixed success.

These results demonstrate that users can perceive haptic cues and adjust their stride lengths. For the step short condition, this holds if the cue is delivered at or before ST2. For the step long condition, the cue has to be delivered at or before ST3. Cues that were delivered later than ST3 did not alter the following stride length.

Table 4.2: Percentage of correct stride adjustments for all 10 participants.

| *Condition* | *ST1* | *ST2* | *ST3* | *ST4* | *ST5* | *ST6* |
|---|---|---|---|---|---|---|
| **Short** | 83.05 | 77.59 | 59.65 | 65 | 50.88 | 55.93 |
| **Long** | 91.07 | 82.46 | 64.41 | 40 | 48.21 | 53.45 |

### *4.4.2 Haptic cues delivered at ST1, ST2, and ST3 enable timely change of target foot stride (T)*

We plotted the normalized stride length of the target foot (T) for each stimulation time in Figure 4.7. A normalized stride length of 1 indicates that the stride length is equal to the mean stride length for that particular stride index and participant. Stimulation times ST1 and ST2 resulted in normalized stride lengths greater than 1 for step longer trials and smaller than 1 for step shorter trials. At ST3, only step longer trials resulted in a change, while step shorter trials trended to the mean. Step shorter trials in ST4 show a minor trend towards shorter strides, but not to the same degree as ST1 through ST3 conditions. ST5 and ST6 do not reveal any changes in stride lengths.

### *4.4.3 Changes of stride are observed beyond the target foot*

In addition to the target foot (T) stride lengths above, we calculated the stride lengths of the right foot before and after the target foot at four points denoted by its relation to the target foot.

In Figure 4.8, as expected, participants successfully adjusted their stride lengths under stimulation times ST1 and ST2. However, in following strides participants exhibited continued adjustment to their stride lengths such that every cue resulted in participants adjusting at least two consecutive strides (T and T+2, or T+2 and T+4).

In both the step shorter and step longer trials, there are significant effects at the $p < 0.05$ level for all 4 conditions (T-2, T, T+2, and T+4) in all 6 stimulation times, as shown in ANOVA result in Table 4.3.

In the step shorter trials, for ST1 and ST2, there are significant differences between stride length prior to the haptic cue (T-2) and after the haptic cue immediately at the target foot (T), as well as after the haptic cue at 2 steps after the target foot (T+2). There are no significant differences between the stride length prior to the haptic cue (T-2) and after the haptic cue at 4 steps after the target foot (T+4). For ST3-ST6, there are no significant differences between stride length prior to the haptic cue (T-2) and stride length after the

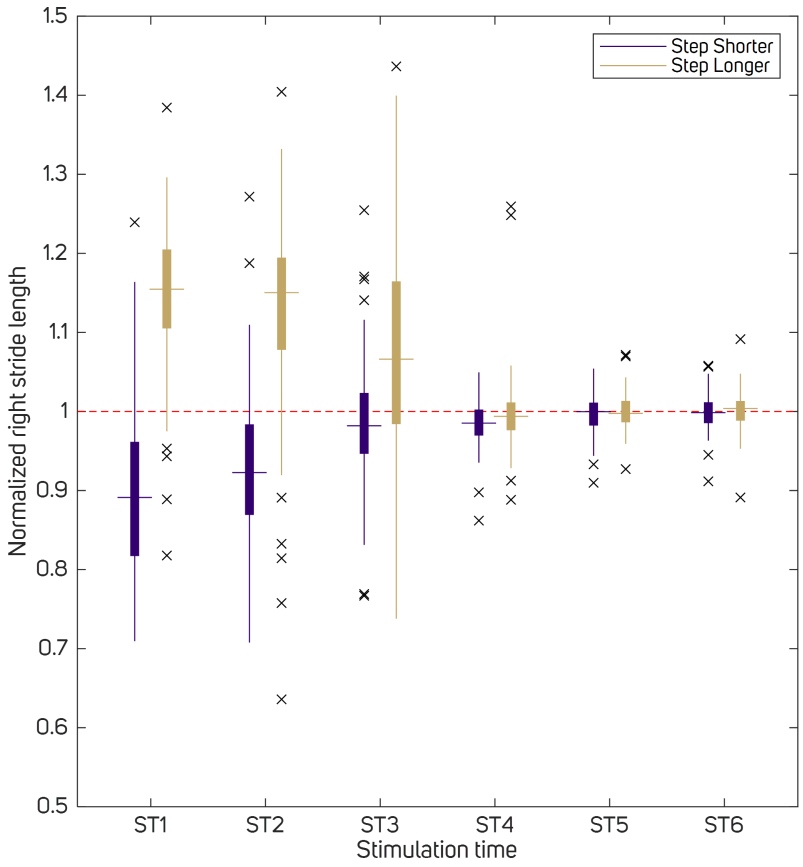


Figure 4.7: Normalized stride length of target foot (T) for each stimulation time (ST1-ST6) and stimulation condition (short and long) for all 10 participants.

haptic cue at target foot (T). However, there are significant differences between stride length prior to the haptic cue (T-2) and stride length after the haptic cue at 2 steps after the target foot (T+2). For ST4 only, there are also significant differences between stride length prior to the haptic cue (T-2) and after the haptic cue at 4 steps after the target foot (T+4).

In the step longer trials, for ST1, ST2, and ST3, there are significant differences between stride length prior to the haptic cue (T-2) and stride length after the haptic cue at the target foot (T) and 2 steps after the target foot (T+2). For ST4, ST5, and ST6, there are significant differences between T-2 and T+2. For ST6, there are significant differences between T-2 and T+4 as well.

This suggests haptic cues to adjust a single stride may entail further adjustments of later strides. When designing a haptic cueing system, it is necessary to deliver cues before mid-

Table 4.3: One-way ANOVA results comparing the effect of haptic cue onset timing (stimulation time) on stride length in foot stepping prior to the onset of haptic cue (T-2), and after the haptic cue at the target foot (T), 2 steps after the target foot (T+2), and 4 steps after the target foot (T+4).

| *Step Shorter* | | |
|---|---|---|
| **ST1** | $F(3, 203) = 10.43$ | $p = 2.04 \times 10^{-6}$ |
| **ST2** | $F(3, 160) = 11.1$ | $p = 1.17 \times 10^{-6}$ |
| **ST3** | $F(3, 196) = 31.60$ | $p = 1.05 \times 10^{-16}$ |
| **ST4** | $F(3, 206) = 61.25$ | $p = 2.39 \times 10^{-28}$ |
| **ST5** | $F(3, 195) = 82.85$ | $p = 1.60 \times 10^{-34}$ |
| **ST6** | $F(3, 202) = 27.30$ | $p = 7.26 \times 10^{-15}$ |
| *Step Longer* | | |
| **ST1** | $F(3, 193) = 47.27$ | $p = 5.96 \times 10^{-23}$ |
| **ST2** | $F(3, 151) = 14.13$ | $p = 3.65 \times 10^{-8}$ |
| **ST3** | $F(3, 202) = 6.23$ | $p = 0.0005$ |
| **ST4** | $F(3, 207) = 5.23$ | $p = 0.0017$ |
| **ST5** | $F(3, 192) = 12.98$ | $p = 9.29 \times 10^{-8}$ |
| **ST6** | $F(3, 199) = 22.55$ | $p = 1.31 \times 10^{-12}$ |

swing of the prior step to change stride length. This adjustment may last 2 strides after the target stride (T+4).

### *4.4.4 Correlation of walking speed to stride length adjustments*

We hypothesized that walking at a faster speed diminishes one's ability to adjust stride length in a timely manner. To test this, we calculated the normalized absolute value of target foot stride adjustment (4.2). $SL$ is the stride length value of the target foot. $SL_{mean}$ is the average stride length of that stride index obtained using the aforementioned method described in Section 4.3.3. The value $\Delta SL_{norm}$ represents the absolute value of stride change for that particular trial, normalized for each participant. Then, we calculated the average walking speed for each trial from RHS0-RHS5 (4.3).

$$\Delta SL_{norm} = \frac{|SL - SL_{mean}|}{SL_{mean}} \tag{4.2}$$

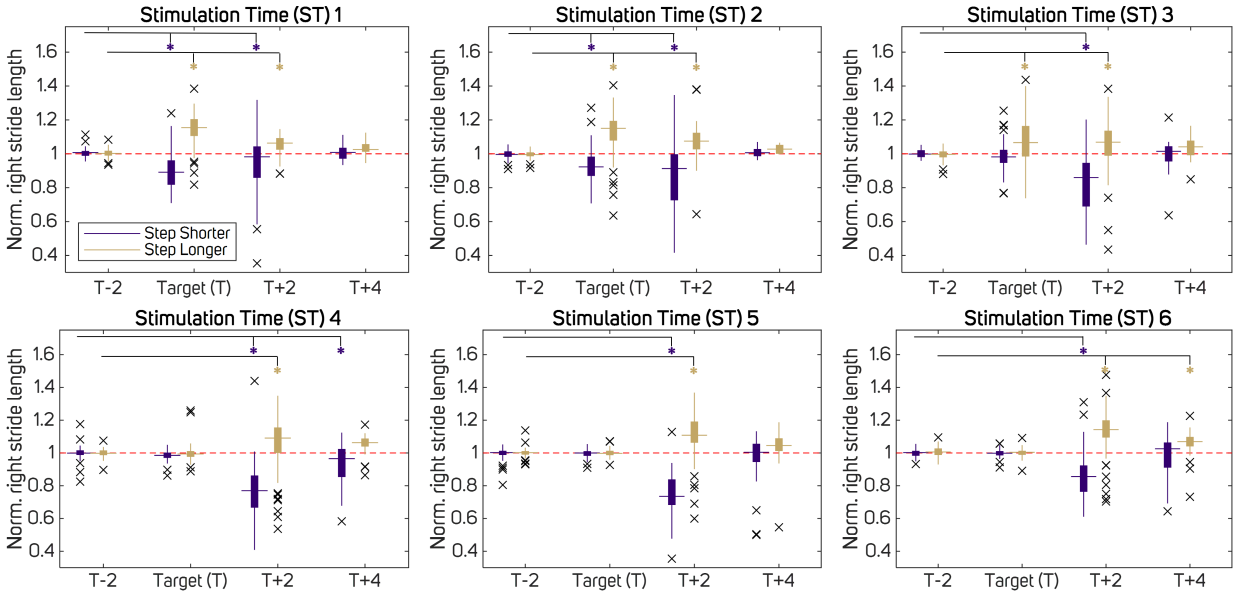


Figure 4.8: Normalized stride lengths of the right stride prior to target foot (T-2), the target foot (T), and 2 subsequent right strides after target foot (T+2, T+4) for each stimulation time (ST1-ST6) and condition (short and long) for all 10 participants. Step shorter and step longer foot strides significantly different with the stride length prior to haptic cues onset are denoted with * ($p < 0.05$).

$$Speed = \frac{pos_{Heel,RHS5} - pos_{Heel,RHS0}}{time_{Heel,RHS5} - time_{Heel,RHS0}} \tag{4.3}$$

We plotted the speed against normalized stride adjustment values for every trial and performed a linear regression (Figure 4.9). For the step shorter trials, the linear fit for ST1, ST3, ST4, and ST5 are significantly different from their respective constant fits ($p < 0.05$). For the step longer trials, statistical significance is observed for all stimulation trials except ST2 ($p < 0.05$).

In Figure 4.9, downward slopes indicate that as walking speed increases, the amount of self-selected stride length adjustments are smaller. In ST3, faster walking speed yields to almost no adjustment in stride lengths, suggesting that depending on walking speed, haptic cues given at ST3 might or might not influence stride length adjustments. In ST4, ST5, and ST6, there is little effect of walking speed because under these conditions participants were not able to modify their stride lengths in a timely manner.

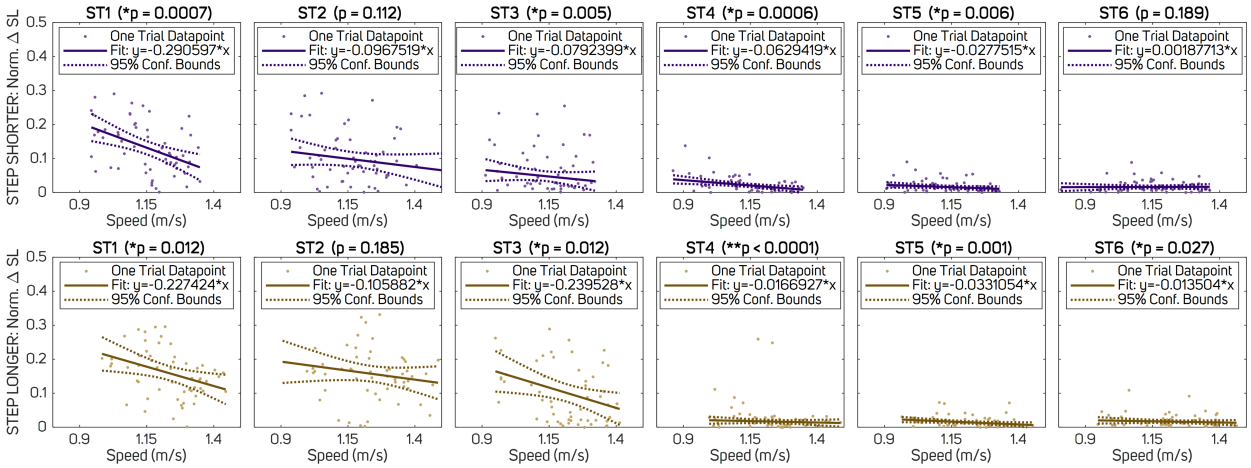


Figure 4.9: Normalized absolute changes of target foot stride length ($SL$) given walking speed. The value for each trial is plotted as a dot, with a linear regression fit calculated for each stimulation time (ST1-ST6) and condition (short and long). The top row is for step short stimulation condition, and the bottom row is for step longer. $p$ value of the fit compared against the constant model for each ST is shown.

### *4.4.5 Qualitative reports*

After the walking trials, we asked the participants a set of *Likert*-scale questionnaires that are adapted from the NASA TLX:

**Q1** How much mental effort did it take to accomplish the task? **1: None at all, 5: Maximum effort**.

**Q2** How much was your gait disrupted after feeling the haptic cue? **1: None at all, 5: Maximum disruption**.

**Q3** How much physical fatigue did you experience during the experiment? **1: None at all, 5: Maximum fatigue**.

**Q4** How much mental fatigue did you experience during the experiment? **1: None at all, 5: Maximum fatigue**.

**Q5** Rate this statement: I could distinguish between the two haptic cues **1: Not at all, 5: Very clearly**.

**Q6** How is the comfort of the device? **1: Not comfortable, 5: Very comfortable**.

**Q7** Given mobility impairment, would you use this device in your daily live for assisting your mobility? **1: Not at all, 5: A lot**.

We explained to the participants that Q1 mental "effort" is similar to cognitive load, such as doing math in your head. Whereas Q4 mental "fatigue" means tiredness after completing the study. For Q7, we instructed the participant to think about being occupied (talking on the phone, or carrying boxes) while walking.

Responses from all 10 participants are summarized in Table 4.4 and Figure 4.10. Notably, participants reported a moderate mental effort to use the device. Three participants reported that mental effort decreases with the number of trials. Although we did not investigate the effect of cognitive load on user ability to adjust stride length, it remains an important determinant of the practicality of designing and implementing such a device.

Table 4.4: Post-trial questionnaires from 10 participants (P1-P10). Green indicates favorable or positive responses, red indicates unfavorable or negative responses, and black indicates neutral responses.

| | *P1* | *P2* | *P3* | *P4* | *P5* | *P6* | *P7* | *P8* | *P9* | *P10* |
|---|---|---|---|---|---|---|---|---|---|---|
| **Q1** | 2 | 3 | 3 | 2 | 4 | 4 | 4 | 2 | 2 | 4 |
| **Q2** | 1 | 3 | 2 | 3 | 2 | 3 | 2 | 3 | 2 | 3 |
| **Q3** | 1 | 1 | 2 | 1 | 2 | 3 | 2 | 2 | 1 | 2 |
| **Q4** | 2 | 3 | 2 | 2 | 4 | 3 | 2 | 4 | 2 | 3 |
| **Q5** | 4 | 3 | 4 | 4 | 4 | 4 | 3 | 4 | 4 | 4 |
| **Q6** | 5 | 3 | 3 | 4 | 5 | 3 | 3 | 4 | 4 | 4 |
| **Q7** | 4 | 3 | 3 | 2 | 4 | 3 | 2 | 4 | 4 | 4 |

Participants reported that their gait was minimally disrupted by responding to the haptic cue. One participant reported that at the beginning of the study he/she had to stop to think about the cue but eventually he/she could react more quickly without stopping. Another commented that when used in unprompted daily settings, when he/she felt the vibration, he/she might need to stop before reacting. Two participants reported that they had the tendency to correct their subsequent steps after the target foot due to the stride adjustments at target foot. Two participants indicated that it was easier to step longer than to step shorter.

Participants also reported some difficulties with distinguishing between the two haptic cues, and suggested increasing the amplitude of vibration, or placing the two vibrations at the left and right wrist instead of the same wrist would help them respond to the cues quicker. One participant mentioned that if the device is used in daily settings without any prior

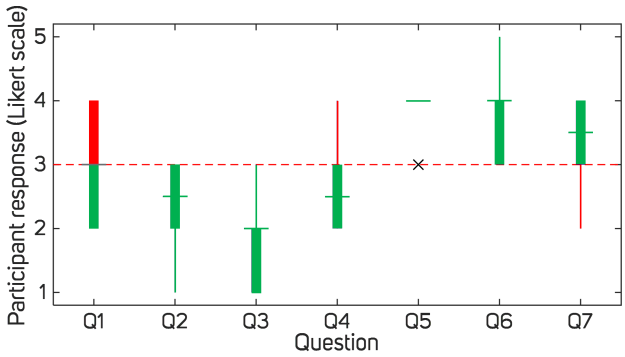


Figure 4.10: Post-trial questionnaire response from all 10 participants. The responses are on a Likert scale from 1-5. Red bar indicates negative (undesirable) responses, and green bar indicates positive responses.

knowledge on when the cue will occur, he/she might completely miss it. Four participants reported that occasionally they had to guess the vibration location, and realized after the fact that they had made the wrong guess and the wrong stride adjustments. One of the four reported that they would made the wrong adjustments even though they perceived the correct vibration.

## *4.5 Discussion*

We demonstrate that a wrist-worn wearable haptic device can be used to cue participants to adjust stride length. Cues that are delivered at or before toe off of the prior step (ST2) for step shorter, and at or before mid-swing of the prior step (ST3) for step longer may be perceived and acted upon in time to alter stride length. In general, when a cue is delivered earlier, participants are able to generate larger adjustments to their stride length. Considering that steady gait is a precise pattern of movement that prioritizes balance and the conservation of energy, intentional disruptions to steady gait require anticipatory movement patterns to stabilize against resulting balance disturbances. Given more time to anticipate the disturbance, participants are able to make larger adjustments to their stride without exiting the gait cycle.

We also found that changes to stride length persisted beyond the target foot. This may be due to the different movement strategies employed to achieve stride lengthening and shortening. Varraine et al. found that shortening a right stride creates a rapid forward displacement of the head, arms, and trunk, which necessitates taking a short left stride to prevent a forward fall, which is then followed by a long right stride to recover forward momentum [89]. In contrast, longer strides requires an increase in propulsive forces and a

prolonged swing phase, which is followed by both a long left stride and a long right stride. This effect is important to note if the adjustment is only intended for a single stride. In our study, this persistence effect was stronger for the step longer condition, in which stride length continued to be longer than the mean for up to 3 consecutive strides (statistically significant with $p < 0.05$, as shown in Figure 4.8), whereas for the step shorter condition, the effect was less clear. Under the step shorter condition, participants exhibited increased variation in stride length, which agrees with the claim made by Varraine et al. that the following same side stride (T+2 for ST1 and ST2; T+4 for ST3-ST6) will be longer than the preceding stride (T for ST1 and ST2; T+2 for ST3-ST6).

When comparing timing requirements of haptic cues, our results contrast with the results of previous work on timing requirements of visual cues. In [91, 92, 93, 94], Matthis et al. found that visual cues could be displayed after mid-swing of the prior step (ST3 or later). From our results, haptic cues should be displayed before mid-swing (before ST3 for step longer) and before toe-off (before ST2 for step shorter) of the prior step. This may relate to how motor planning of gait may integrate visual information naturally while haptic information is typically of little use for feedforward control. As a result, haptic cues may need to be delivered earlier to be useful for planning the next step.

As suggested from qualitative interview with the participants, it is also important to ensure that when designing a wearable haptic system for mobility assistance, special attention should be paid to ensure cues are salient and distinguishable to avoid imparting cognitive load.

We observed that participants made smaller stride adjustments when walking at a higher speed. This may be due to the shortening of time in between the onset of haptic cue and the heel strike of the target foot at higher speeds. This may suggest requirements that faster walkers are cued earlier in the gait cycle than slower walkers.

## *4.6 Limitations and future work*

We performed this study in a laboratory setting, in which participants were aware that a haptic stimuli would be given during the forward pass of every trial. When the system is taken outside of the laboratory setting for daily use, users' attention would likely be engaged elsewhere and they would have no prior expectation of receiving a haptic cue, thus increasing reaction time. One possible solution is to amplify the vibrotactile cues such that users can distinguish and perceive them better.

Participants in our study were also instructed to adjust the right stride only. In real world scenarios, users may be wearing the device for both sides, which may further increase reaction time as users must decide both which side stride to adjust and how to adjust it.

This difference may alter the optimal timing for a haptic cue. Future research should focus on non-laboratory environment applications.

We did not account for the effect of training in our study. We argue that the effect of training during our one-time user study is minimal due to the randomization of cue location. However, as users increase experience with the wearable system, cued stride behavior may change.

In our implementation in the lab, participants were also able to choose how much to shorten or lengthen their target strides. Smaller or larger amplitude modifications may result in different timing requirements. For instance, a larger amplitude modification may require an earlier cue as it requires increased anticipatory movement to maintain balance.

This study presents the timing requirements for unimpaired participants but results may vary across populations. For instance, the intrinsic dynamics of gait are fundamentally altered after amputation of a lower limb and requires its own investigation to support our results. Individuals with underlying sensorimotor impairments such as Parkinsons may also exhibit significantly different stride length modulation behavior. Future research should focus on implementation in target populations, such as older adults or people with lower limb amputation who may receive the most benefit from such an intervention.

Furthermore, we did not investigate the effects or contributions from haptic cues placed at different spatial locations of the body, and different options for presenting two distinct "step shorter" and "step longer" cues. We also suspect that inherent reaction times to haptic cues might could contribute to variations in timing at which foot stride can be adjusted.

Lastly, this study investigated the timing requirements for level-ground walking scenarios. Our broader application for *Smart Step* is focused on stair ambulation and stair descent. Although we argue that the result from this study translates to the case of stair descent, the exact timing requirement for stair descent might be different from that of level-ground walking. Additional experimentation should be performed to further evaluate the case of stair descent.

## *4.7 Conclusion*

Wearable haptic devices present an enticing opportunity to assist mobility on a daily basis. This study informs design guidelines of timing requirements for haptic interfaces used during walking. This is the first study to investigate the feasibility of haptic cues to adjust stride length during walking. We quantified the optimal time-to-cue with respect to phases of gait and found that cues delivered before mid-swing of the prior step resulted in successful stride length adjustments. This adjustment is inversely proportional to walking speed. Shortened and lengthened strides persisted after the target step, albeit by varying amounts.

Understanding gait as a phasic movement guided by balance and energy constraints is key to designing a cueing system that integrates seamlessly with a user's motor plan.

*The key finding of this aim — cues delivered before mid-swing of the prior step resulted in successful stride length adjustments — answers one of the two compulsory parameters in designing Smart Step. Now that we answered the question of when a haptic cue should be given in order for its user to adjust the foot placement in time, we discuss the second question of what should be the appropriate haptic cue is, in the following aim (Chapters 5 and 6).*

# Chapter 5

# DESCENDING 13 REAL WORLD STEPS: A DATASET AND ANALYSIS OF STAIR DESCENT

As I am using model-free data-driven methods to predict foot placement during stair descent, I need a vast amount of stair descent gait data. Most gait data available is collected for level-ground walking. Existing work that investigate stair descent scenarios are not publicly available, and are collected in laboratory environment with less than 7-steps and less than 30 participants (Section 2.3.3). With these gaps in current literature, building a data set specialized for stair ambulation is inherently valuable. This chapter includes Aim 3a, in which a publication is underway in [51].

## *5.1 Methods*

### *5.1.1 Participants*

We recruited 111 unimpaired adult participants according to a University of Washington Institutional Review Board approved protocol. The exclusion criteria were any physical impairment and recent injuries on the lower limb. Data from 10 participants were not included in this manuscript due to file corruption and error. This work includes data collected from 101 participants (54 male and 47 female; aged 18-35, mean 23.17 $\pm$ 4.12 years; height 171.16 $\pm$ 10.21 cm; weight 65.68 $\pm$ 12.17 kg; shoe length 25.46 $\pm$ 2.01 cm).

### *5.1.2 Sensors and data acquisition*

We employed fully wearable sensors for measuring gait data. We collected full body kinematics using the Xsens wearable motion capture system (MTw Awinda, Xsens Technologies B.V., Enschede, Netherlands), and normal forces underneath each foot using the Moticon insoles (Moticon SCIENCE ver. 2, Moticon ReGo AG, Munich, Germany) (Figure 5.1).

The Moticon insoles are sized for European shoe size 44/45 (US 9 Men). Participants with shoe size equal or larger than the insole wore it inside their athletic, flat bottom shoes with the heel of the insoles flush with the heel of the shoes. Participants with shoe size

smaller than the insole wore rubber overshoes (SRM1111, SR Max Slip Resistant Shoes, New Castle, DE, USA) with the same size as the insole, with the insole inserted in between their foot and the overshoe. The overshoe is secured to the foot using self-adherent wrap (Coban, 3M, St Paul, MN, USA).

### *5.1.3 Protocol*

Each session is conducted on the same 13-step staircase at the University of Washington (rise 15.5 cm and run 33 cm). Participants are instructed to walk down and up the staircase at their own comfortable pace step-over-step, without instruction to begin on a specific foot. Trials ranged from 20 to 50 descents and ascents. Participants took breaks after 10 or 15 descents.

### *5.1.4 Data preparation*

#### *Preprocessing*

The Xsens data is reprocessed in HD according to the Xsens data processing guide, and then exported as a comma-separated-value (CSV) file using the Matlab (MathWorks, Natick, MA, USA) plugin for Xsens. The Moticon data is stored onboard the insole during the data recording session, and then downloaded to the PC as a text (TXT) file. Both Xsens and Moticon recorded time series data of gait parameters, including joint angles, body segment positions, forces under the foot, foot acceleration, and foot center of pressure. Note that in the Xsens and Moticon coordinate system, the $x$ axis represents the **transverse** plane, the $y$ axis represents the **frontal** plane, and $z$ axis represents the **sagittal** plane.

#### *Sampling, syncing, and filtering*

The Xsens and Moticon data are recorded with a sampling rate of 60Hz and 50Hz respectively. The Moticon data is resampled to 60Hz to match the Xsens data.

Once resampled, the Xsens and Moticon data are synced. The syncing procedure is done through a physical marker, in which at the beginning of the data collection prior to the first descent, the participant will stomp their right foot for five times. The time instance at which this event occured are then manually marked based on the right foot $z$ position data from Xsens and the right foot total force data from Moticon.

Center of pressure (COP) values measured by the Moticon are set to zero when the foot is in mid-air.

*Segmentation*

The gait dataset is segmented such that the data represent 1 step cycle from toe off of one foot at one step to the toe off of the same foot at the next step. Note that this terminology is slightly different than that of Chapter 4. In this Chapter, one step is referred to as the stair step that is taken by the same foot side. In Chapter 4, this is referred to as one stride (heel strike to heel strike on the same foot). The absence of clean ground reaction force readings from force plates prohibits the ability to accurately determine the toe-off event.

To segment the dataset this way, we used the $z$ position data of the left and right foot as references. Figure 5.1 shows the $z$ position data for a portion of a trial, which are segmented into data per descent, and then further segmented into data per step.

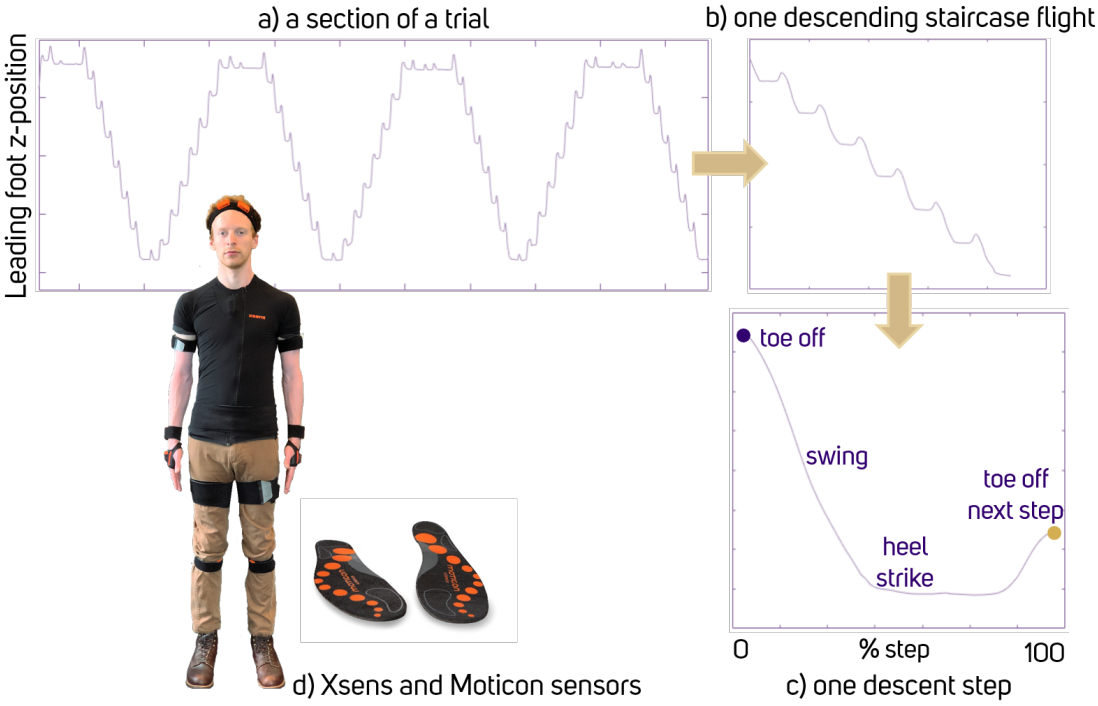


Figure 5.1: a-c) Segmentation of stair descent data and d) Sensors worn by participant during trial. Foot $z$ position data for: a) a section of a trial consisting of stair ascent and descent; b) one entire flight of staircase during descent; c) one descent step representing 0-100% step.

**Descent segmentation.** The beginning and ending of each descent from the $z$ position data are determined using a combination of Matlab's `findpeaks()` command with `MinPeakProminence` value of 1 and a smoothing filter with a moving average span of 200 (`smooth`). The resulting start and end indices for each descent are stored as `topX` and `botX`.

**Step segmentation.** Each descent is further segmented into steps. We used Matlab's `findpeaks()` command with `MinPeakProminence` of 0.2 to detect the peaks of foot $z$ position at every step, which closely correlates to the toe-off event. This automatic detection algorithm might not accurately determine the exact point of toe-off, but is closely aligned to the moment shortly after toe-off. We chose this method as it provides a simple and automatic annotation strategy that would otherwise be laborious for the amount of data (13,300 left and 14,485 right steps) and participants (101) that we have.

After the automatic toe-off detection using `findpeaks()`, we manually verified that the peaks detected are accurate. We would add or remove peak indices by hand. Some of the times the foot $z$ position was not recorded correctly due to the multi-level rendering error from the Xsens software. In these cases we removed the detected step indices accordingly.

*Normalization to percent step*

In this manuscript, the gait kinematics and kinetics parameters are presented based on 0-100% step, which is from toe-off (0%) to the next toe-off (100%) of the same foot (Figure 5.1c). As the length of trials in terms of duration (s) could be different from one step to others, we perform normalization of parameters per step from 0 to 100%. This normalization is used for presentation of data in this manuscript, but is not reflected in the data stored in the repository.

### *5.1.5 Data analysis*

*Variability*

We calculate coefficient of variation (CV), which is defined by standard deviation (SD) divided by mean. For both the CV and SD, we calculate the values for the hip, knee, and ankle angles of both the leading left and leading right limbs. We also calculate the corresponding CV and SD values during maximum flexion, maximum extension, and at each instant of step cycle averaged across time. We repeat these calculations for both intra-subject (CV and SD values across all trials averaged per subject, and then these averages are averaged across all participants), and inter-subject (CV and SD values averaged across all trials and all participants).

Example calculation of the inter-subject CV for left hip flexion is as follows. First, we have an array of left hip joint angles in the sagittal plane for all trials (13,243 full steps). We calculate the maximum flexion angle for each of the trials, determined by the maximum hip joint angle value in the sagittal plane. We then compute the CV of these 13.243 values (Table 5.2). For the intra-subject value, for each participant, we calculate the maximum

flexion angle for each trial and stored them into an array. We take the CV of this array and the resulting value is a single value of CV for that participant. We repeat this for all participants, and we compute the mean and standard deviation of the 101 CV values.

For inter-subject CV for left hip across time, we calculate the CV of all 13,243 full steps at each timestep (1-100) in the step cycle, and take the mean and standard deviation of these CV values. For intra-subject, we calculate the CV of all trials per subject at each timestep. Then we average this array of 100 CV elements per subject (averaged across time). We repeat this for all 101 participants, and take the average across all participants.

*Foot placement position*

Foot placement position is defined as the distance from the leading step edge to the heel for each step. Moticon sensors are used to determine foot placement position. We take the COP value at the moment of toe-off, and select the maximum value across a 30-timestep window (0.5s). To our knowledge, our work is the first to report such information in real-world long staircases.

*Symmetry*

Symmetry measures of temporal and angular gait parameters were calculated using methods laid out in [175]. For the temporal parameters, the Absolute Symmetry Index (ASI) was used based on [176] (Equation 5.1). A higher ASI means less symmetry, and an ASI of less than 10% is considered symmetric gait.

$$\begin{gathered} ASI(\%) = \frac{X_r - X_l}{0.5\,(X_r + X_l)} \times 100\% \\ X_r = \text{parameter for left limb} \\ X_l = \text{parameter for right limb} \end{gathered} \tag{5.1}$$

Angular parameters were analyzed using the statistical method of analyzing symmetry based on [175, 177]. We consider $\alpha = 0.05$ as statistically significant differences for the paired t-test result between the left and right limb (i.e. $p < 0.05$ results to asymmetry).

*Repository*

The dataset described in this work will be made publicly available in Harvard Dataverse. Organization and formatting of data will be elaborated in the dataset.

## 5.2 Results

### 5.2.1 Kinematics

Figure 5.2 shows the lower limb kinematics parameters normalized for 0-100% step ($n$ = 101). The solid line represents the median across all participants and all steps, with the shaded region representing the 25$^{th}$, 50$^{th}$, 75$^{th}$, and 90$^{th}$ percentiles.

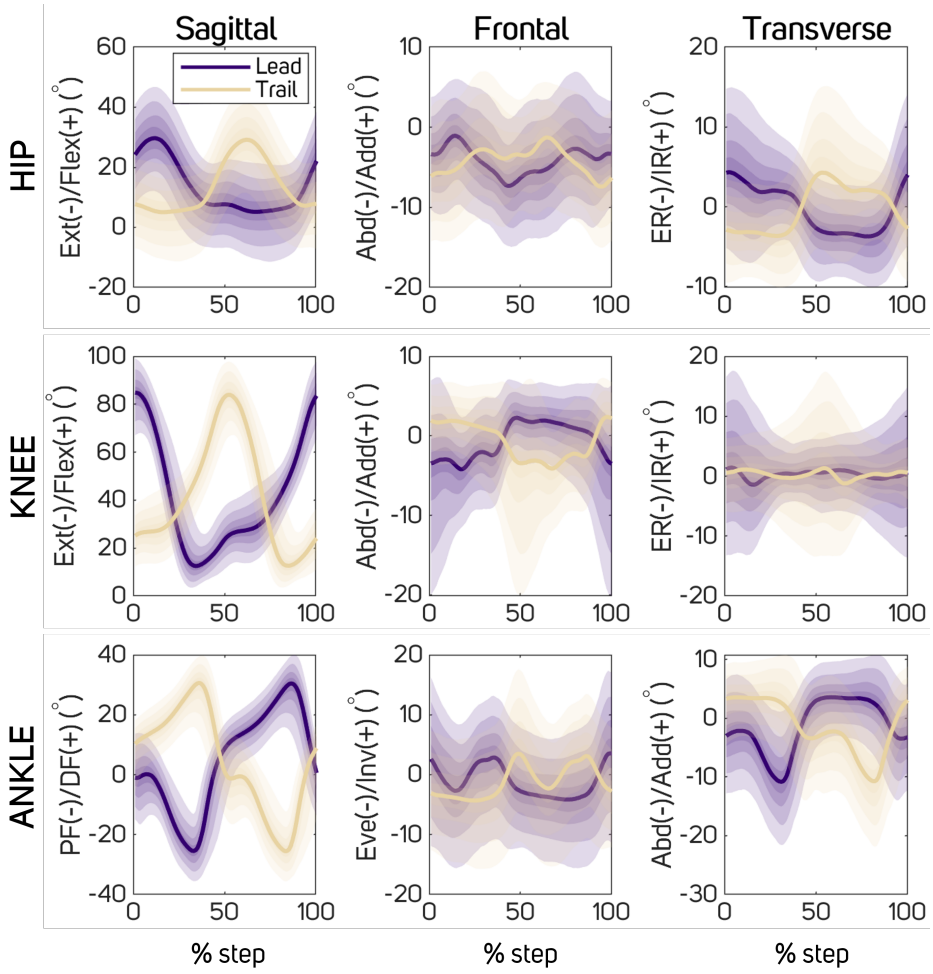


Figure 5.2: Kinematic parameters during stair descent measured by the Xsens (% step from toe-off to toe-off). 'Flex' = Flexion, 'Ext' = Extension, 'Abd' = Abduction, 'Add' = Adduction, 'ER' = External Rotamation, 'IR' = Internal Rotation, 'PF' = Plantar-flexion, 'DF' = Dorsi-flexion, 'Eve' = Eversion, 'Inv' = Inversion. ($n = 101$).

The maximum flexion and extension angles for the hip and knee, as well as maximum

dorsi-flexion and plantar-flexion angles for the ankle are shown in Table 5.1a. We report the temporal parameters in Table 5.1b.

Table 5.1: Parameters of gait kinematics at the lower limb (Mean ± SD). $n = 101$.

*a) Maximum ranges of joint angles*

| | | Joint Angles (°) | |
|---|---|---|---|
| | | Left | Right |
| Hip | Flexion | 30.69 ± 10.23 | 29.67 ± 9.96 |
| | Extension | 7.96 ± 5.89 | 7.91 ± 5.53 |
| Knee | Flexion | 85.94 ± 9.14 | 85.26 ± 10.20 |
| | Extension | 11.21 ± 5.95 | 10.64 ± 5.79 |
| Ankle | Dorsi-Flexion | 30.91 ± 6.61 | 31.85 ± 8.37 |
| | Plantar-Flexion | 27.98 ± 6.01 | 28.11 ± 6.14 |

*b) Temporal parameters*

| | Left | Right |
|---|---|---|
| Cycle Duration (s) | 0.9632 ± 0.1791 | 0.9689 ± 0.1763 |
| Speed (m/s) | 0.7893 ± 0.1560 | 0.7891 ± 0.1535 |
| Cadence (steps/s) | 1.0824 ± 0.2140 | 1.0821 ± 0.2105 |

We present the coefficient of variation (CV) (Table 5.2a) and standard deviation (SD) (Table 5.2b) for the hip, knee, and ankle joints. We calculate the CV and SD for the maximum and minimum angles at the sagittal plane, as well as the CV and SD for the sagittal plane angle averaged across time during one step cycle.

We report the symmetry behavior of the angular parameters at the lower limb using paired t-test (Table 5.3a), and the temporal symmetry characteristics using ASI (Table 5.3b) .

### *5.2.2 Kinetics*

Figure 5.3 shows the kinetic parameters recorded using the Moticon insole. The normal ground reaction force (GRF) is shown as the total force underneath the insole. The COP $y$ value indicates the COP along the heel-toe direction, whereas the COP $x$ value indicates COP along the medial-lateral direction in the frontal plane. Acceleration of the foot in the $x$ (transverse), $y$ (frontal), and $z$ (sagittal) directions are shown.

Table 5.2: Inter-subject and intra-subject parameters of (Mean ± SD (%)) of the maximum flexion, maximum extension, and joint angle averaged across time for the leading left and leading right limb. $n = 101$.

*a) Coefficient of variation (CV)*

| Joint Angles | | Inter-Subject CV (%) | | Intra-Subject CV (%) | |
|---|---|---|---|---|---|
| | | Left | Right | Left | Right |
| Hip | Flexion | 33.33 | 33.57 | 13.67 ± 9.63 | 14.13 ± 9.82 |
| | Extension | 74.03 | 69.93 | 45.40 ± 24.00 | 44.96 ± 23.27 |
| | Across Time | 102.92 ± 51.35 | 101.03 ± 49.01 | 145.53 ± 329.75 | 122.26 ± 269.50 |
| Knee | Flexion | 10.64 | 11.96 | 3.58 ± 2.94 | 3.96 ± 7.23 |
| | Extension | 53.09 | 54.39 | 28.98 ± 15.02 | 30.96 ± 17.71 |
| | Across Time | 31.11 ± 15.81 | 31.79 ± 14.55 | 21.18 ± 59.52 | 19.03 ± 36.41 |
| Ankle | Dorsi-Flexion | 21.38 | 26.27 | 9.64 ± 7.35 | 10.15 ± 7.27 |
| | Plantar-Flexion | 21.49 | 21.84 | 9.39 ± 4.82 | 9.70 ± 6.88 |
| | Across Time | 411.23 ± 1097.83 | 964.84 ± 3615.85 | 125.18 ± 124.48 | 205.77 ± 487.46 |

*b) Standard deviation (SD)*

| Joint Angles | | Inter-Subject SD (°) | | Intra-Subject SD (°) | |
|---|---|---|---|---|---|
| | | Left | Right | Left | Right |
| Hip | Flexion | 10.23 | 9.96 | 3.71 ± 2.09 | 3.66 ± 1.49 |
| | Extension | 9.39 | 9.12 | 2.84 ± 1.69 | 2.80 ± 1.21 |
| | Across Time | 9.93 ± 0.55 | 9.65 ± 0.64 | 3.70 ± 2.02 | 3.62 ± 1.46 |
| Knee | Flexion | 9.14 | 10.20 | 3.03 ± 2.37 | 3.06 ± 3.42 |
| | Extension | 6.11 | 6.40 | 2.83 ± 1.68 | 2.78 ± 1.75 |
| | Across Time | 10.00 ± 1.49 | 10.35 ± 1.90 | 4.75 ± 3.11 | 4.68 ± 3.33 |
| Ankle | Dorsi-Flexion | 6.61 | 8.37 | 2.77 ± 1.64 | 3.20 ± 2.97 |
| | Plantar-Flexion | 6.03 | 6.62 | 2.52 ± 1.10 | 2.51 ± 1.09 |
| | Across Time | 8.15 ± 1.52 | 8.96 ± 1.69 | 4.07 ± 2.26 | 4.27 ± 2.51 |

### *5.2.3 Foot placement*

There are a total of 15,942 left and 14,934 right foot placements. Ninety left and 177 right foot placements are removed due to noise (e.g. foot placement positions incorrectly computed as below the origin of the COP coordinate system or above 100% foot length).

Table 5.3: Symmetry reports of stair descent parameters. (Mean ± SD) (%). $n = 101$.

*a) p values (paired t-test between the left and right maximum angular parameters)*

| | | $p$ |
|---|---|---|
| Hip | Flexion | 0.0070 |
| | Extension | 0.9444 |
| Knee | Flexion | 0.2940 |
| | Extension | 0.3722 |
| Ankle | Dorsi-Flexion | 0.0795 |
| | Plantar-Flexion | 0.8217 |

*b) Absolute symmetry index for temporal parameters*

| | ASI (%) |
|---|---|
| Contact time (time per step) | 3.66 ± 4.52 |
| Speed | 0.75 ± 0.70 |
| Cadence (step frequency) | 0.75 ± 0.70 |

The relationship between foot length (rounded closest to the numerical representation of US shoe sizes) and foot placement positions are reported, measured from the toe (Figure 5.4a) and the heel (Figure 5.4b).

The mean staircase edge position with respect to the heel across 101 participants is 210.69 ± 9.37mm. The mean normalized toe overhang across 101 participants is 17.06 ± 6.67% (Table 5.4).

Table 5.4: Foot placement and toe overhang with respect to the staircase edge (Mean ± SD). $n = 101$.

| | Left | Right | Combined |
|---|---|---|---|
| Foot placement (mm from heel) | 210.46 ± 9.14 | 210.94 ± 9.60 | 210.69 ± 9.37 |
| Normalized toe overhang (%) | 17.08 ± 6.59 | 17.03 ± 6.75 | 17.06 ± 6.67 |

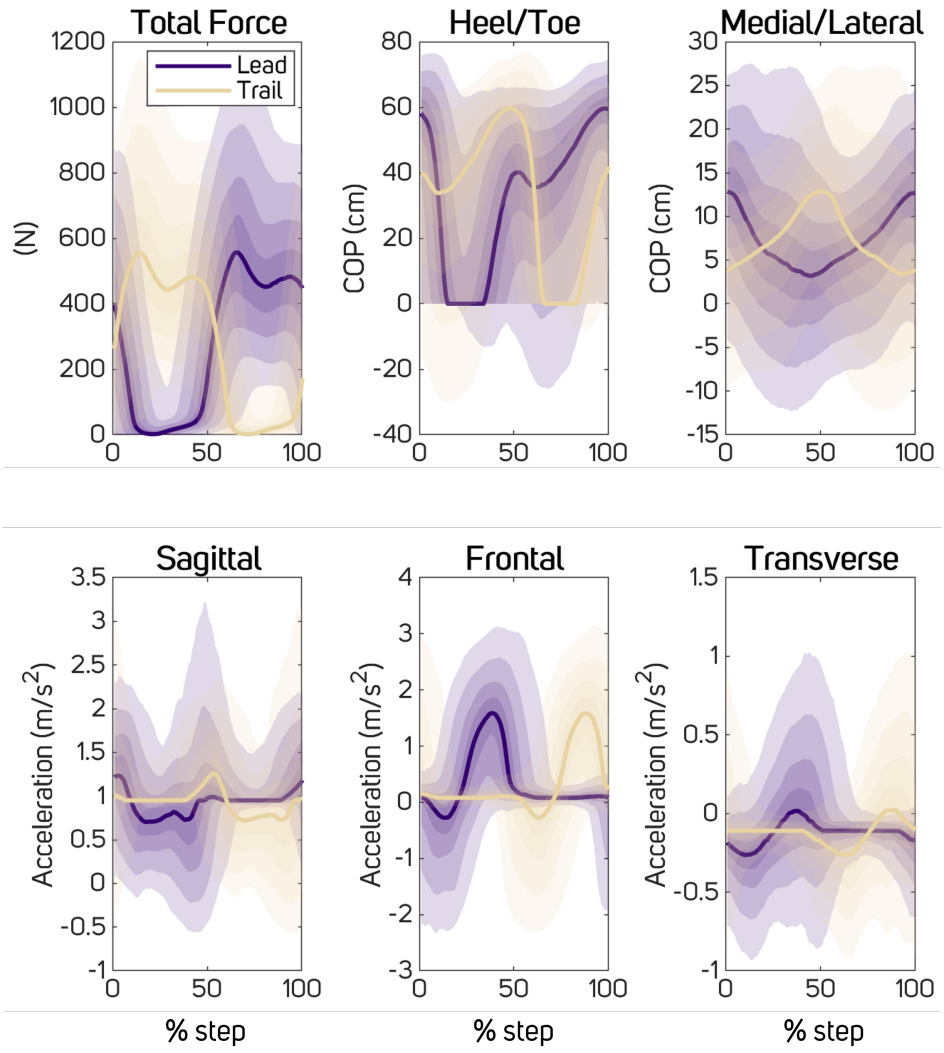


Figure 5.3: Kinetic parameters, foot placement, and foot acceleration information during stair descent measured by the Moticon. (% step from toe-off to toe-off). 'COP' = Center of Pressure. ($n = 101$).

## *5.3 Discussion*

### *5.3.1 Angular parameters*

These maximum and minimum angles in the sagittal plane for the lower limb are not directly comparable to other work in the literature such as [178] and [177] as our staircase inclination (25.16°) is different than the two (17°, 34°, 45°). However, our standard deviation (SD)

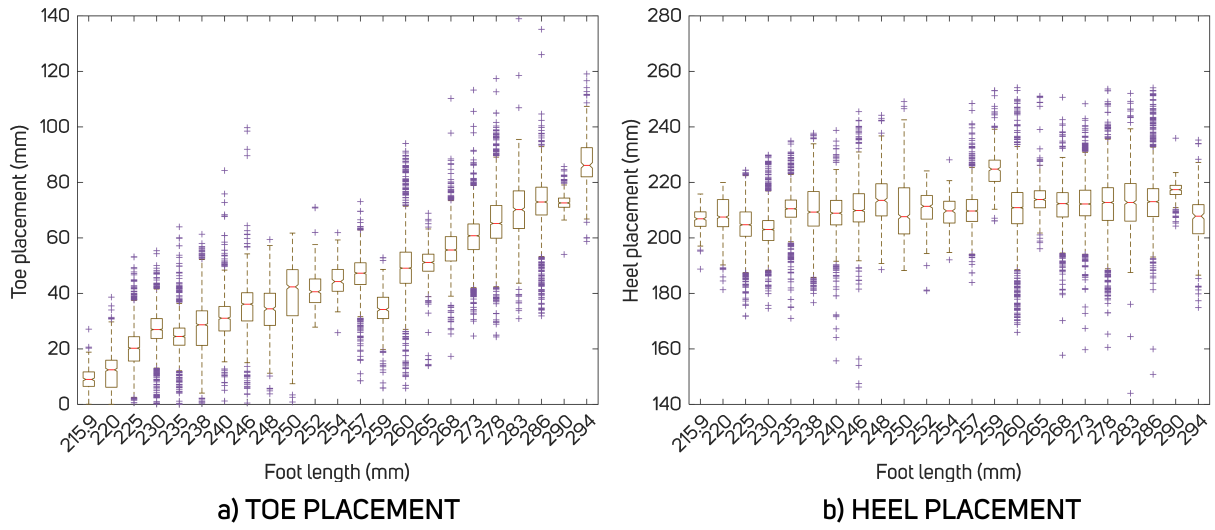


Figure 5.4: Staircase step edge position underneath the foot as measured from the toe (a) and the heel (b) for participants with varying shoe lengths. ($n = 101$).

values are larger than that of [178], arguably because we do not segregate our participants into groups of short, medium, and tall based on height, causing higher values of SD. Similarly, the work in [177] with 33 participants without height segregation also demonstrates SD of comparable values to our dataset.

### *5.3.2 Temporal parameters*

The cycle duration is in the range of 0.96s, which is faster than similarly inclined staircase from [179] (1.41s). Compared to the cycle duration from [178], our results are similar but slightly faster than 1.0-1.1s ranges. However, the staircase inclinations from [178] are not similar to our dataset.

The mean self-selected speed from our dataset is 0.78m/s, which is higher than [177] (0.56m/s) and [162] (0.53m/s), but lower than [178] (0.6-0.9m/s). The cadence from our dataset is 1.08 steps/s, which is higher than [161] (0.95 steps/s), but lower than [178] (1.78-2.33 steps/s) and [176] (1.53 steps/s).

We hypothesize that the faster cycle duration and speed is due to the fact that our staircase consists of 13 steps instead of only 4-5 steps, allowing participants to reach steady state and hence increases familiarity and speed with the staircase [162]. In addition, our data collection is in a regular staircase outside of the lab environment, which we suspect

decreases tension and "carefulness" of the participants.

### *5.3.3 Intra and inter subject variability*

It is important to note that [179] reports inter-subject CV of each joint angle across time, whereas we report the CV of each joint angle at maximum flexion and extension. Inter-subject CV across time from our dataset are 9.9462° and 9.6644° for left and right hip, 10.0131° and 10.3603° for left and right knee, and 8.1610° and 8.9763° for left and right ankle. These numbers show highest variability in the knee joint, followed by the hip and ankle joints. We argue that taking CV measures across time across gait cycle is not as representative because it would wash out the differences.

From Table 5.2, inter-subject variability is higher than intra-subject variability. For both cases, the hip and knee extension angle CVs are higher than flexion angle CVs, whereas ankle dorsi-flexion and plantar-flexion angle CVs are similar. If we look at the flexion angles (and ankle dorsi-flexion) only, the knee exhibits the lowest variability compared to hip and ankle, which agrees with Protopapadaki et al. [177]. Comparing extension angles (including ankle plantar-flexion), the ankle exhibits the smallest variability. It is interesting to note that even though the flexion angle CVs demonstrate similar patterns with that of [177], the absolute CV values are highly variable. Protopapadaki et al, [177] has intra-subject CV values ranging from 2.90-5.77% for hip, knee, and ankle flexion, whereas our dataset has CV values from 3.97-14.11% for flexion angles.

The SDs of the maximum flexion and maximum extension of joint angles indicate that the hip has the largest SD and thus largest variability compared to the knee and the ankle. This agrees with Riener et al. [179] and MacFadyen & Winter [180]. However, it is important to note that in [179], the SD values are calculated as average across time, which are lower than 9° for hip, and lower than 7° for knee and ankle. If we look at the SD values averaged across time from Table 5.2, we have around 10° for hip and knee, and around 8-9° for ankle, with knee having the highest variability.

### *5.3.4 Foot placement position*

Foot placement is important in adaptive gait to ensure safe navigation across obstacles [181, 182]. During stair decent, foot placement strategy is unknown. The heel placement could be prioritized, assuring heel clearance from the previous stair step and keeping the base of support of the foot constant or toe placement could be prioritized, assuring constant overhang and perhaps easier visual confirmation of the foot placement.

Individual foot placements could be generated by different priorities. For example, if a

particular individual places their foot so that the heel is 15 mm from the back of the stair, it is not clear whether that is because heel placement, or toe placement, or the fulcrum position on the foot, etc., is prioritized. However, given observations from a variety of participants with different sizes of feet, we can look for commonalities that could shed light into the strategies used.

One key finding which is an important variable in stair ambulation is the relation of the foot with the staircase step, which can be described by foot clearance and foot placement. Simoneau et al. [183] indicated that foot placement on, and clearance over, the step are important for understanding the mechanisms of a fall on stairs. We found three studies that reported foot placement during stair descent. Ramstrand et al. [184] reported very limited toe overhang. The distance from markers placed on the metatarsals to the stair edge was reported to be $0.03 \pm 0.02$ m, for 10 unimpaired young adults descending a 5-step staircase in laboratory conditions. This appears short and it is likely that at least some people in some conditions, overhang their foot over the stair edge more than this. Ackermans et al. [161] reported 80.7% percent foot in contact with the stair. Muhaidat et al. [46] reported 16 $\pm$ 6% of the foot overhanging the stair edge for 10 adults on a 4-step laboratory staircase.

Reporting foot placement in terms of percentage of foot overhanging the stair edge might not be appropriate, because it obscures the effect of foot size and assumes that toe placement relative to the stair edge is the important, or controlled, variable. In this study, we suggest that placement of the heel relative to the vertical edge of the previous stair step could be more carefully controlled (Figures 5.4a and 5.4b).

We find a similar percentage of foot overhang ($17.06 \pm 6.67\%$) as previous literature, but we observe that only 6% of heel placement variation is explained by foot size, while 79% of toe placement variation is explained by foot size (Figure 5.4). This indicates that the percentage of the foot overhanging the stair edge could be largely explained by constant heel placement combined with foot size. We discovered a significant mild linear correlation ($R = 0.2474, p = 0$) between heel placements and foot lengths. On the other hand, toe placement across foot lengths demonstrate a significant strong correlation ($R = 0.8899, p = 0$). These suggest that, in stair descent, heel placement may be the controlled variable rather than toe placement, as participants have a relatively constant heel placement across all foot sizes.

### *5.3.5 Symmetry*

Symmetry is often assumed for unimpaired populations [185], with asymmetries attributed to gait pathology [185, 186, 187]. However, more recent studies that gait asymmetry exists in in healthy adults [188]. While symmetry measures have been analyzed for stair ambulation in [189, 176], most of this work examined impaired participants. In this study, we report symmetry findings for unimpaired participants.

The paired t-test results (Table 5.3a) show that the maximum angular parameters of the lower limb in the sagittal plane are symmetrical ($p > 0.05$) except for the maximum hip flexion angle ($p = 0.0033$). This result disagrees with the commonly assumed symmetry in the literature, as well as with the result reported by Protopapadaki et al. [177]. In [177], the left and right limb are combined as paired t-test results show no significant differences ($p = 0.45$). The staircase is counter-clockwise when descending, suggesting that visual cues of a left turn might contribute to asymmetry.

The ASI for the temporal parameters (Table 5.3b) are well below 10%, indicating symmetry. This agrees with [176], but with much lower ASI or a higher symmetry results.

## *5.4 Limitations and future work*

We would like to expand our work for to include a wider variety of staircases with different rise and run parameters. We suspect that the gait parameters resulting from staircases with different rise and run values would be different, especially with extreme staircases that are non ADA compliant.

We also would like to see such dataset collected from target population (e.g. people with prosthetic limbs, children or elderly population). In order to accurately advise rehabilitation parameters for target population, we have to understand how different and/or similar the gait parameters are exhibited as compared to healthy intact individuals.

## *5.5 Conclusion*

This is the first quantitative observation of gait data from a large number ($n = 101$) of participants descending an unconstrained 13-step real world staircase outside of a laboratory environment (total of 27,785 steps). These data provide important but heretofore-unmeasured gait characteristics such as self-selected walking speed and foot placement in a real world setting. The dataset is a resource for understanding stair descent in unimpaired individuals.

The novel finding reflected in this dataset pertains the foot placement behavior during stair descent. Contrary to the literature, we found that foot placement strategy during stair descent emphasizes on heel placement relative to the stair edge, instead of toe placement relative to the stair edge. This finding could heavily influence rehabilitation strategies placed for PWA, especially in guiding users on how to optimally step while descending the stairs.

*This dataset encompasses a relatively large sample size of the population, with a relatively large number of step samples. This dataset enables the use of data-driven methods to analyze and predict movement behaviors during stair descent. In particular, for Smart Step, we are*

*interested in predicting foot placement in the future, particularly at least 2 steps ahead based on the time-to-cue requirements obtained in Chapter 4. Data, results, and findings obtained in this aim are directly implemented in the development of the regressor algorithm in Aim 3b (Chapter 6).*

# Chapter 6

# PREDICTING FUTURE FOOT PLACEMENT

This chapter describes the second portion of Aim 3: obtaining the knowledge of what to cue users during mobility tasks. The dataset obtained in Aim 3a (Chapter 5) is used to develop a machine learning algorithm for predicting future foot placements during stair descent. The primary novelty of this contribution is the capability of looking ahead, forecasting, and predicting a future event. Such a capability provides an opportunity to correct user behavior to prevent future error.

The work described in this chapter is going to be published in [52].

## *6.1 Dataset*

One of the biggest questions in terms of data availability in data science remains unknown: *how much data is enough data?*. There is a vast number of studies that utilize gait information for machine learning prediction of gait and human recognition [190, 148, 159]. These studies use "large" datasets (such as the CASIA [191] or SOTON [192], among many others [142, 160]), in which the number of participants are typically 100+. We use this number as a guide for the number of participants that we need in order to have enough data for a good machine learning prediction, although with the recognition our problem is significantly different.

These publicly available large datasets do not typically contain the full-body gait information that is required to perform typical gait analyses such as predicting foot placement, like in our application. This need motivated the number of participants involved in Aim 3a (Chapter 5). We utilized the dataset collected in Aim 3a (Chapter 5), consisting of kinematics and kinetics parameters of 101 unimpaired adults during stair descent. More details on the description of this dataset can be found in Chapter 5).

### *6.1.1 Data preparation*

We used the dataset obtained and described in Section 5.2. We have 101 comma-separated values (`.csv`) files, where each file corresponds to data from one individual.

*Outlier processing*

Outlier for the target foot placement value is defined as values beyond the 1.5 inter-quartile range below the $25^{\text{th}}$ percentile and above the $75^{\text{th}}$ percentile. The values beyond these thresholds are capped at the thresholds, which are 46.755 mm for the lower threshold (1.5 inter-quartile range below the $25^{\text{th}}$ percentile), and 91.382 mm for the upper threshold (1.5 inter-quartile range above the $75^{\text{th}}$ percentile). If a foot placement value is below or above the thresholds, that foot placement is already deviating from an optimal foot placement value and hence would need to be cued. Hence, predicting a foot placement value that is beyond the threshold as equal to the threshold value would fulfill our objective of cueing purposes, while making the task of prediction future foot placement less difficult for our algorithm to learn.

*Train - test split*

We split the dataset into train and test sets. The test set consists of data from 11 distinct individuals that are randomly selected such that the output distribution is similar to that of the training set of 90 individuals. The target foot placement values of the train and test sets are shown in Figure 6.1.

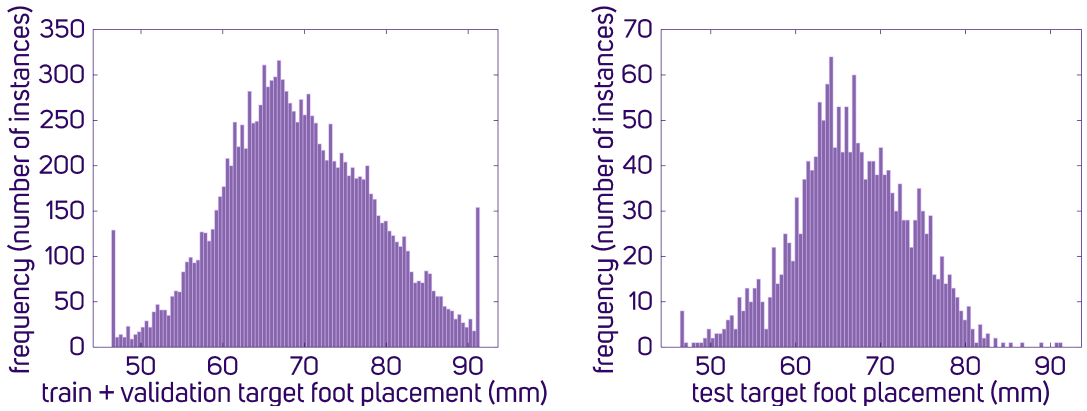


Figure 6.1: Histogram of target foot placement values for train ($n = 90$) and test ($n = 11$) sets.

The train set is further split into validation sets using the 10-fold cross-validation techniques. The 10-fold train and validation sets remain constant throughout the training and tuning process.

## *6.2 Algorithm design*

We want to design an algorithm that takes in biomechanical data as inputs, and generate a prediction that enables us to cue foot placement.

### *6.2.1 Output features selection*

The output of this algorithm has to answer the question: what is the cue to give to the users?

We could frame this problem into classification or regression. In classification, we would predict if the users' future foot placement will be optimal or non-optimal. This results in a cue when a non-optimal foot placement is detected, and a non-cue when an optimal foot placement is detected. We want to guide the users to reach the optimal foot placement, thus the cue has to be more informative. For this, we could classify if the future foot placement will be ahead, behind, or on the optimal foot placement. This way we could provide either a step shorter, a step longer, and a non-cue for the user.

This output framework aligns with our objective, but diminishes the detail of actual foot placement information that could be critical. For instance, judging the appropriate cue threshold between a step that is too ahead versus optimal may vary from user to user. We propose a regression algorithm, in which the exact future foot placement position in millimeters is predicted. This value can then be compared with the optimal foot placement position for each user, in order for the appropriate step shorter, step longer, or non-cue to be delivered.

The future foot placement information is obtained from the center of pressure measurement along the proximal-distal direction underneath the foot (Figure 6.2. The most distal center of pressure value within 30 timesteps (0.5s) around toe-off is taken as the ground truth information to represent the target value of foot placement prediction.

### *6.2.2 Input features selection*

Our dataset consists of time-series of 183 kinematics and kinetics variables during stair descent, that have been parsed into full-flight descents and then into steps.

Some key questions include:

1. **Variables to select.** Among the 183 variables, we picked the variables of interest based on four factors: (1) practicality; (2) expert recommendation; (3) correlation

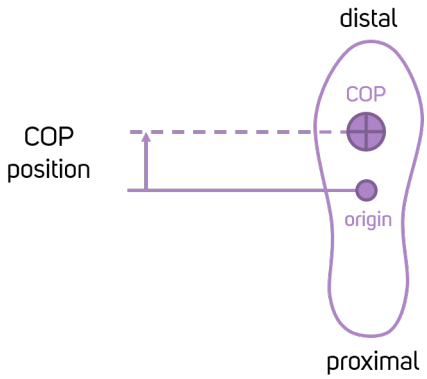


Figure 6.2: Target foot placement value as indicated by the most distal center of pressure value within 0.5s around toe-off.

with output target; and (4) correlation between features.

For practicality, we are looking at the ability to measure the input variables for our use case. While we collected full-body gait data in our dataset, in real-life it is ideal that users wear only one or two sensor units on the lower limb. For this we pick only variables at the lower limb.

For expert recommendation, we consulted with prosthetics and biomechanics experts on what variables may be important in determining future foot placements.

For correlation, we are looking at the Spearman's correlation among all the input features and between each input feature with our target output variable. We picked variables that are highly correlated with the output, and removed variables that are highly correlated with each other, keeping only those highest correlated with the output.

2. **Time series vs. multiple single-data points in time.** One option for featurizing the time series data would be to take data points at specific instances in gait such as at 0%, 25%, 50%, 75%, and 100% of the gait cycle, or other specific defining characteristics of the data such as at the maximum and minimum flexion angle of each input joint. This option could significantly simplify the input dimensionality. However, we argue that in order to capture future foot placement information well, the entire sequence in the time-series has to be considered. Thus, we use full time-series gait data in our input.

3. **Length of time-series sequences and relation to time with respect to target output.** To make a useful prediction of the future foot placement value, the prediction

has to happen prior to the target foot step. We investigated in Aim 2 how far behind the target this prediction has to happen. We discovered that a haptic cue has to be given at the latest at toe off of the contralateral foot leading to the target foot step. This time point expressed in the foot $z$-position plot during stair descent is shown as the purple shaded region in Figure 6.3. This suggests that the prediction has to occur prior to the purple shaded region. Another consideration is the length of the input sequence. How many steps should the input sequence consist of? We performed a grid search of the input sequence length for length of 0.5 step (4.5 steps to 4 steps prior), 1 step (5 steps to 4 steps prior), 2 steps (6 steps to 4 steps prior), 3 steps, as well as an adaptive window sizing that increases with the number of steps taken. The best result is given by the input sequence length of 2 steps (6 steps to 4 steps prior to the target foot step).

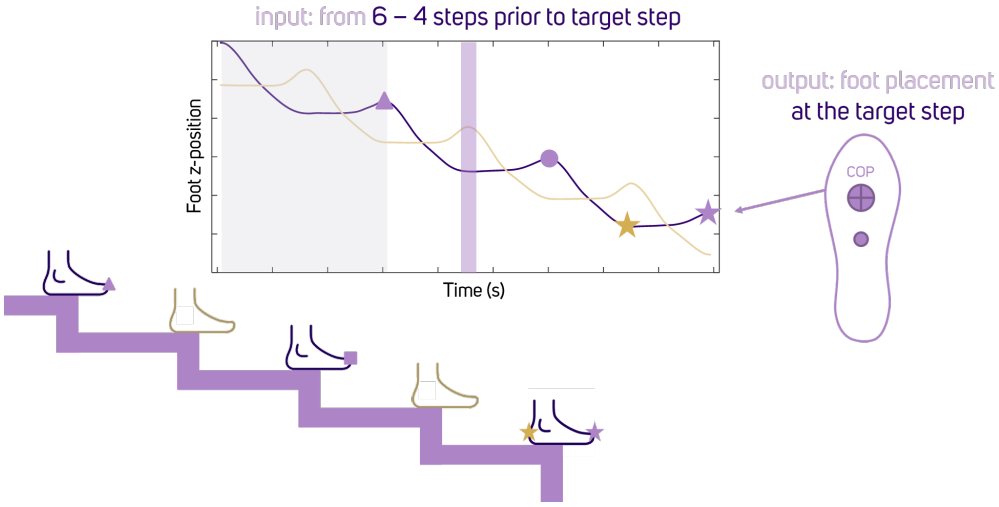


Figure 6.3: Input sequence length and the relationship with target foot placement. We are predicting the foot placement in relation to the step edge (indicated by the time stamp at gold star). From Aim 2, the haptic cue has to be delivered at 1.5 steps prior to heel strike (indicated by the purple shaded region). The input sequence for machine learning prediction is selected to be 6 steps to 4 steps (grey shaded region) prior to the target foot (purple star). Note that the target output value is obtained during toe off, as opposed to heel strike, hence the discrepancy between the gold and purple stars.

The final input feature includes 8 input sequences of ipsilateral: hip, knee, and metatarsal-phalangeal sagittal joint angles; metatarsal-phalangeal frontal joint angle; total forces underneath the foot; foot sagittal acceleration; foot distal-proximal, medial-lateral center of pressure. The length of the input sequence is selected to be from 6 steps to 4 steps prior

to the target foot step (grey shaded region in Figure 6.3). Starting the input sequence at 4 steps prior instead of right before the purple shaded region allows hardware latency for cue delivery.

In addition, we also include the sequence of past foot placement values. This history grows with time, as more data and more step information is recorded. The history value is reset for a new individual. The time dimensionality of the foot placement history is different than the 8 other input sequences, as one single value is logged for each input sequence.

### *6.2.3 Baseline algorithm selection*

In selecting a baseline algorithm for this future prediction problem, there are several methods that we can pick. Our goal is to predict foot placement value at the fourth step ahead.

The simplest solution is by setting the future foot placement value to be equal to the current foot placement value. In this case, the predicted value is equal to the current "history" shifted by 4 steps. However, this method takes into account information from one step only. Imagine if the current step is a bad step, then our prediction of the fourth future step would be bad as well.

One improvement from the solution above is by taking the average (mean) foot placement values of that particular individual, and output this average value as the predicted fourth step foot placement. On top of this, there are several techniques that improve the regular averaging technique, namely the moving average algorithm and its variants. Typically, these algorithms take into account size of the moving window, trend, and seasonality. The most common time-series forecasting method based on the moving average technique is the Auto Regressive Integrated Moving Average (ARIMA). We pick the ARIMA time-series forecasting method as our baseline for this prediction problem.

For each participant, we append the foot placement values for each step as a time series, with each time step equal to one foot stepping at each staircase step. The length of the time series will grow as more steps are recorded. This time series is reset for a new participant. We use the ARIMA method to forecast the foot placement value at the fourth time step ahead (fourth foot step in the future). Predicting the fourth foot step in the future is based on result in Chapter 4, in which haptic cues have to be delivered before mid-swing of the second step prior to the target foot. Further explanation as to why the fourth step ahead is chosen can be found in Section 6.2.2.

The ARIMA method consists of three parameters: $p$ (AR — number of lag observations included in the model), $d$ (I — degree of differencing), and $q$ (MA — size of the moving average window). To determine the optimal values for $p$, $d$, and $q$, we perform a grid search using the values of $p : [0..6]$, $d : [0..4]$, and $q : [0..4]$. We pick the parameters that result in

the lowest value of mean-squared-error ($MSE$) for all foot placement values as a time-series in the training and validation datasets. The optimal parameters are $p = 1$, $d = 0$, and $q = 1$, with $MSE = 0.00337563$. Note that the parameter combination with the smallest $p$ value is chosen, as a larger $p$ value results in a longer training time.

### *6.2.4 LSTM algorithm selection*

The ARIMA algorithm provides a great baseline for time-series forecasting problems. Nevertheless, the ARIMA algorithm does not take into account other factors that could help in predicting a future information. With input variables obtained from the biomechanical measurements of the human user as described above, we can utilize a neural-network based algorithm to predict the future foot placement value.

Based on the constraints determined while selecting the input features, namely the importance of preserving the time-series nature of the input parameters, we selected a neural-network algorithm that works well with time series inputs. Recurrent Neural Networks (RNN) are a good candidate except they suffer from vanishing and exploding gradients. We picked the Long-Short Term Memory (LSTM) algorithm, which behaves similarly, but does not suffer from vanishing and exploding gradients like the RNN.

The final architecture is composed of 2 parallel LSTMs. We separated the kinematics and kinetics input features from the history of past foot placement values, due to the difference in dimensionality of the two input types. The first LSTM takes in the 8 input features of time-series information of lower limb kinematics and kinetics. The input dimension of the training data for the first LSTM is (8996, 115, 8). The second LSTM takes in 1 input feature of past target foot placement information. This is a bi-directional LSTM algorithm. The bi-directional LSTM is chosen over the regular LSTM as it provides a better prediction with lower MSE over the 10-fold cross validation datasets. Note that length of the history increases with time. The input dimension of the bi-directional LSTM is (8996, 274, 1). The final architecture of the algorithm is shown in Figure 6.4.

Both LSTM inputs are padded with -10.0, and then masked during training to prevent the algorithm from learning the padded value. Each LSTM output is connected to a dropout layer of 20% to reduce overfitting. Finally, the outputs from the 2 dropout layers are concatenated and connected to a final Dense network to predict a single value of future foot placement at 4 steps ahead.

We trained the algorithm and determined the best configurations and hyperparamters using the 10-fold cross validation sets described in the earlier sections. We evaluated the hyperparameter values including number of hidden units, batch size, and activation function for the bi-directional LSTM using a manual grid-search. We also implemented an early stopping with patience of 500 epoch, given initial epoch of 1500 to avoid overfitting. The

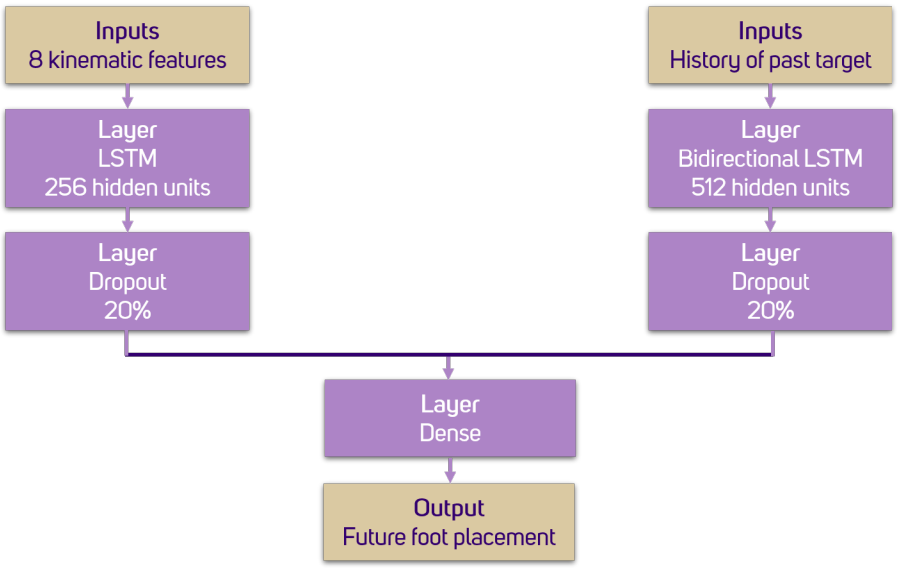


Figure 6.4: LSTM architecture

final hyperparameter values are shown in Table 6.1. Once the optimal hyperparameters are chosen, we retrained the LSTM algorithm using all train and validation data to allow the algorithm to learn from the maximum amount of data available. Finally, we implemented the final algorithm to predict future foot placement values on unseen data to evaluate robustness across unseen individuals and unseen staircases.

## *6.3 Validation results: 10-fold cross-validation sets*

### *6.3.1 ARIMA*

The ARIMA algorithm ($p = 1$, $d = 0$, and $q = 1$) is used to predict foot placement position of the fifth foot step in the future for all 10 validation sets. Prediction results and error are shown in Fig. 6.5. The mean and standard deviation of the $MSE$ for all 10 validation sets is 5.7138 $\pm$ 0.4473mm (Fig. 6.6).

### *6.3.2 LSTM*

Using the optimal hyperparameters above, the resulting validation error for all predictions in the 10-fold cross-validated training dataset is shown in Figure 6.6. The Root Mean Squared

| LSTM | |
|---|---|
| Hidden Units | 256 |
| Batch Size | 100 |
| Epoch | 70 |
| Dropout Rate | 20% |
| **Bi-directional LSTM** | |
| Hidden Units | 512 |
| Activation Function | ELU |
| Dropout Rate | 20% |
| **Concatenated** | |
| Optimizer | Adam |
| Learning Rate | 0.001 |
| $\beta_1$ | 0.9 |
| $\beta_2$ | 0.999 |
| Early Stopping | Patience 500 epoch |

Table 6.1: Hyperparameters tested and chosen for the final prediction algorithm.

Error (RMSE) is 4.6924 ± 0.5221mm. This RMSE value is 17.88% lower than the RMSE obtained using the ARIMA algorithm.

## *6.4 Test results*

### *6.4.1 Test set 1 - anthropomorphic: 11 new participants*

We implemented the LSTM algorithm described above to predict foot placement of unseen individuals, obtained from the set-aside test dataset of 11 individuals. The resulting RMSE (4.2355 ± 1.94mm) for all predictions for all 11 individuals are comparable to that of the validation sets (Figure 6.7).

### *6.4.2 Test set 2 - environmental: 1 participant on 3 new staircase dimensions*

To test the robustness of the LSTM algorithm to predict foot placement at different environmental conditions (staircases of different geometries), we collected additional data from

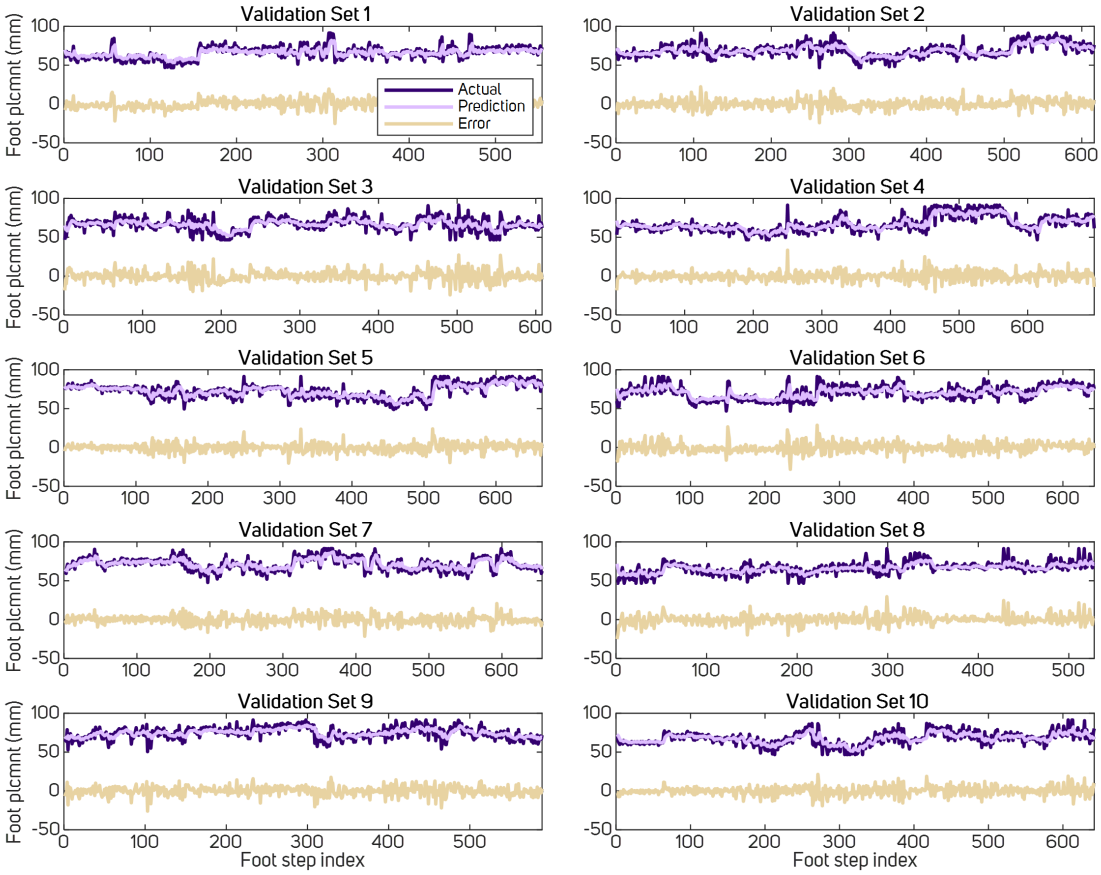


Figure 6.5: ARIMA prediction results and errors together with actual foot placement positions for the 10 validation sets.

Participant 8 descending 3 staircases with different dimensions from the primary staircase in our dataset. The original staircase in our dataset has a rise of 15.5cm and a run of 33cm.

Staircase A (rise = 10cm, run = 42cm), Staircase B (rise = 12cm, run = 35cm), and Staircase C (rise = 9cm, run = 40cm) provide distinct rise, run, and inclination values, thus representing different staircase dimensions encountered in real life. For each staircase, Participant 8 performed 30 sets of descent, the same amount of data as the primary staircase. Prediction results for all foot placements in Staircases A, B, and C demonstrate comparable result to the primary staircase, with RMSE values of 3.571mm, 3.6743mm, and 4.4147mm for Staircases A, B, and C respectively (Figure 6.8). This result shows that the algorithm is capable of generating prediction even for unseen staircases.

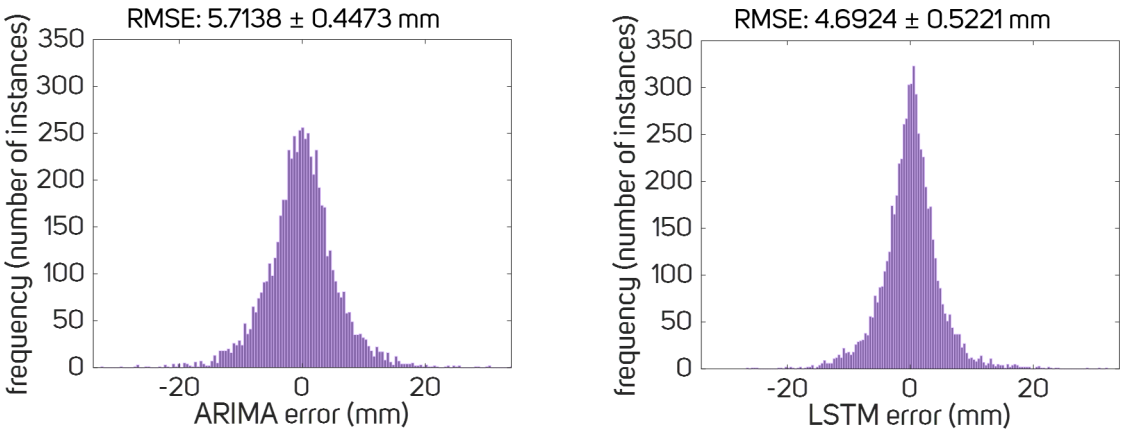


Figure 6.6: Histogram of validation error for all predictions across all 10-fold cross validation sets using the best hyperparameters. Left: ARIMA result. Right: LSTM result. ($n = 90$).

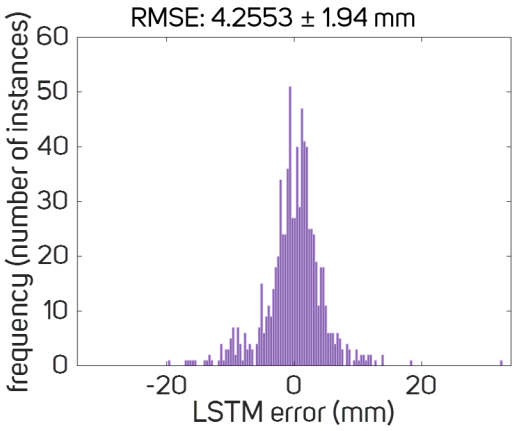


Figure 6.7: Histogram of error for all predictions in unseen individuals (test set). ($n = 11$).

## *6.5 Discussion*

### *6.5.1 Safety concerns and translating predicted values to step shorter and step longer cues*

Once a future foot placement value is predicted, we need to determine if the predicted placement is deviating from an optimal foot placement. The optimal foot placement value could be an expert or clinician-prescribed value that is dependent on the prosthesis. If the predicted value is deviating from the optimal, we need to then determine if it is deviating far enough to merit a step shorter or a step longer cue.

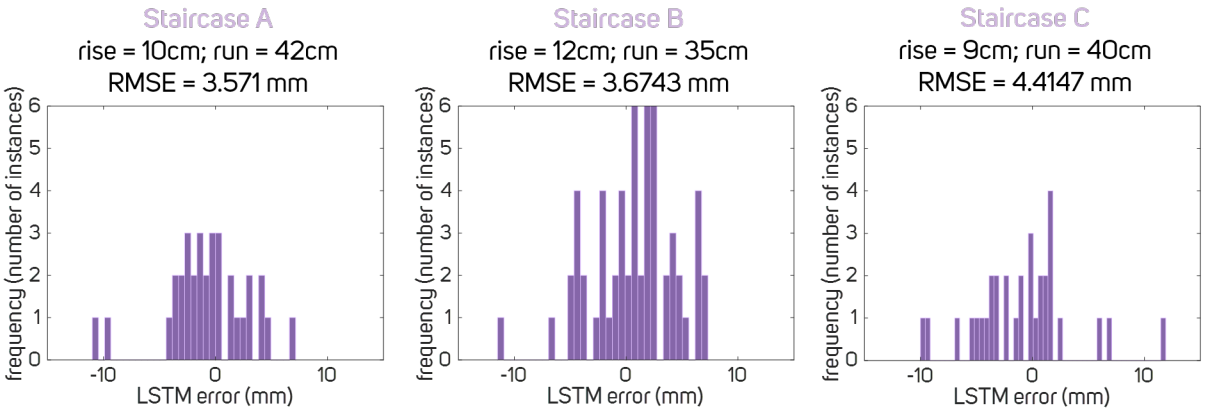


Figure 6.8: Histogram of error for all predictions in unseen staircases for Participant 8 (test set). ($n = 1$).

The range of "safe" or "correct" foot placement values should be set carefully to minimize false positives (non-cue situations that are considered as cues) while at the same time minimizing false negatives (cue situations that are considered as non-cues) and maximizing the true positives (cue situations that are considered cues). By minimizing false positives, we are erring on the safer side, preventing cueing users to either step shorter or step longer that could result in a trip from the previous step or a fall from missing the next step.

For illustration, if we want to be conservative on the step longer cue to prevent missing a step and a catastrophic fall, the safety threshold could be set to 20mm on the step longer direction and 5mm on the step shorter direction. Hence, any predicted foot placements that fall within the green region would be considered as non-cue, and anything in the gold region will be cued as step longer, and anything in the purple region will be cued as step shorter (Figure 6.9).

As a general safety concern, a different method of phrasing the predicted output could be used. In the Algorithm Selection method above, we discussed about phrasing this problem as a regression problem, predicting an actual foot placement value in terms of distance from the heel. We could feed this output into a classifier that decides the correct cue to give based on a given optimal foot placement. In this scenario, the safety thresholds can be represented as different weights for predicting any particular cues to be step shorter or step longer. This is an important issue to be further investigated while this algorithm is being deployed in real-life use cases.

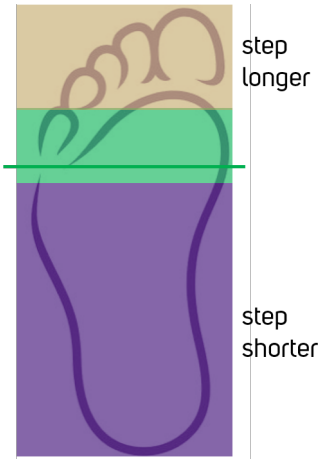


Figure 6.9: Example of thresholds for non-cue in the directions of step shorter and step longer. Green shaded region indicates no cue given.

### *6.5.2 Baseline ARIMA vs LSTM algorithm*

Both ARIMA and LSTM algorithms are capable of predicting foot placement values at 4 steps ahead with an accuracy of 5mm, with the LSTM algorithm having 17.88% less error than that of the ARIMA baseline algorithm. If we look at the prediction result in closer detail, we can see some other factors at which the LSTM algorithm outperforms the ARIMA algorithm in addition to a lower RMSE.

Figure 6.10 shows the prediction result using ARIMA and LSTM algorithms for Participant 49. From this example, we can see that even though the RMSE for the ARIMA and LSTM predictions are comparable, the ARIMA predicts only the mean of the foot placement, and fails to capture the trend in the data.

Furthermore, we can see another example from Participant 4 (Figure 6.11). As ARIMA is based on a moving-average algorithm, there is inherent lag in the algorithm, which might be problematic when there is rapid movement of values below and above the mean at consecutive time steps. In the zoomed in region of Figure 6.11, we can see that the ARIMA prediction of the up and down trends are lag by 1 time step, whereas the LSTM prediction follows the trend of the actual foot placement values. While such prediction capabilities result in similar root mean squared error, they might result in different cues generated for step modification. For example, setting the threshold for the step shorter cue to be 10mm and for the step longer cue to be 10mm, the resulting LSTM predicted cues are correct, whereas the resulting ARIMA cues are the opposite of the correct cues. It is important to note that this example provided is for an unimpaired individual with a researcher-selected threshold. More user research has to be done to determine the appropriate user-specific threshold depending on

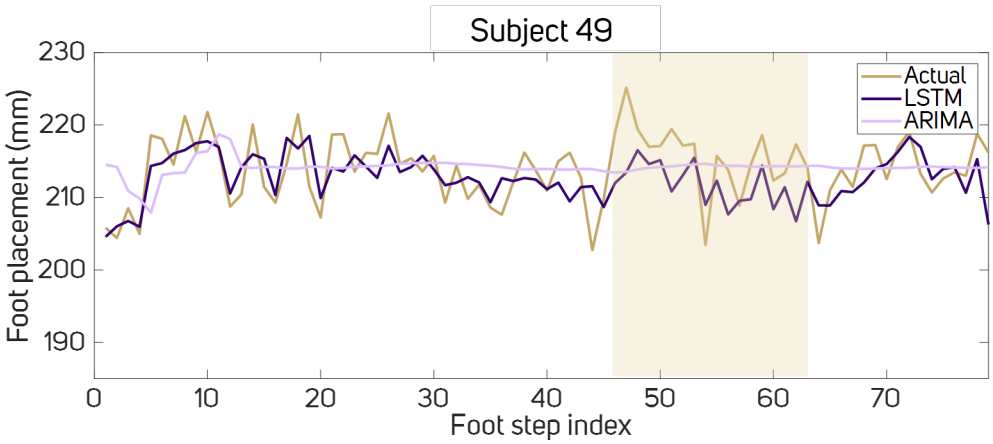


Figure 6.10: Prediction result for Participant 49. Comparison of ARIMA and LSTM predictions for foot placement values with a trend. ARIMA predicts only the mean of the time-series, whereas LSTM is able to predict the trend.

the individuals and the type of impairment.

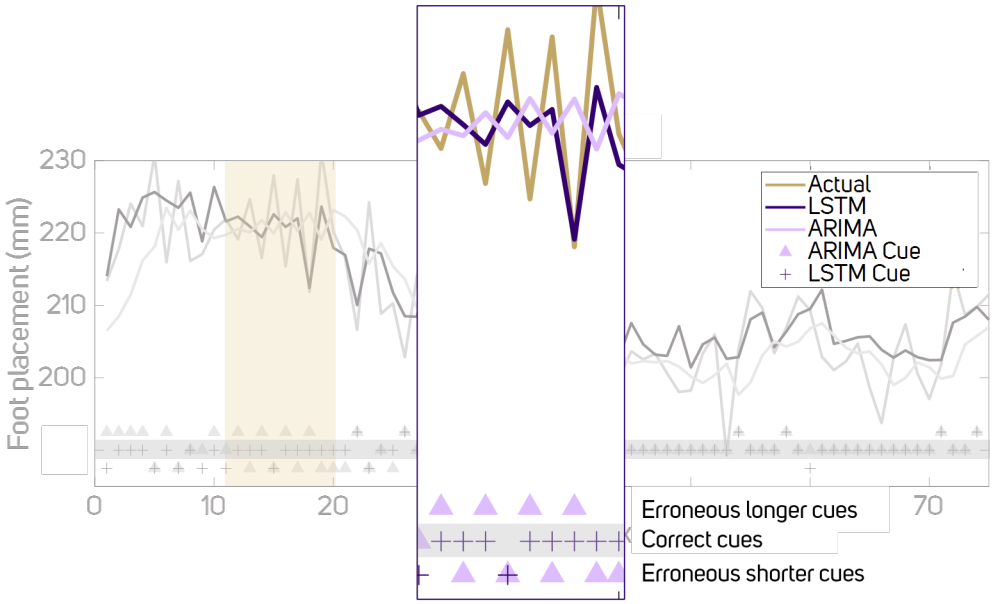


Figure 6.11: Prediction result for Participant 4. Comparison of ARIMA and LSTM predictions for rapid up and down trends for consecutive time steps. ARIMA predicts the trend with a 1 time step lag, while LSTM is able to follow the trend without time lag.

### *6.5.3 Robustness across anthropomorphic variations*

We can see that the LSTM algorithm is capable of predicting foot placement values of unseen individuals. This suggests that the algorithm is generalizable for inter-subject variations, and that our training dataset captures the variability among subjects in the population. This being said, the addition of more data from more individuals can potentially further improve the prediction accuracy. While the algorithm is robust across anthropomorphic variations, all unseen individuals are unimpaired adults with a similar age range. It is important to further test the algorithm in individuals with different anthropomorphic and gait characteristics. For example, we would expect that in individuals in different age groups (children, elderly population), as well as impaired individuals including prosthesis users, the robustness of the algorithm could be altered.

### *6.5.4 Robustness across environmental variations*

We tested and showed that the LSTM algorithm is robust across three different staircase geometries. However, all the staircases tested are nicely and evenly constructed indoor staircases with minimal irregularities or obstacles. We would expect that the presence of irregularities in staircases, such as step edges that were worn off, uneven staircase runs, or even the presence of obstacle such as in crowded subway staircases, or dirty staircases, would affect the prediction capabilities of the LSTM algorithm.

## ***6.6 Limitations and future work***

The results of this study demonstrated the capability of predicting future foot placement for unimpaired adults. Our target population is slightly different than our desired use case of mobility assistance for PWA. The algorithm developed in this study might not be directly translatable for this population, which exhibits different demographics and gait behaviors. Experiments and tests have to be done with PWA in order to assess robustness of this algorithm. Future work could include data collection for PWA and further algorithm training and tuning on top of the algorithm proposed in this study. Furthermore, user research has to be conducted to determine the appropriate threshold for translation of foot placement predictions to step shorter and step longer cues.

Future implementation of this algorithm will also require further work to automatize its activity. For instance, the detection of stair descent should be automatic, such that assistance may be delivered without user input. The algorithm should also be robust to pausing and other behaviors that may occur on a staircase. The use of lower limb sensors, embedded within the prosthesis and on the user's residual limb, may also offer new opportunities to

develop similar gait-predicting algorithms for flat-ground gait, and may be paired with vision-based sensors for obstacle navigation. This predictive information may be used to predict control parameters for a prosthesis, or specific events like falls. Additional algorithms, like variational autoencoders, or attention-based models like transformers, may be employed to enhance the result presented here.

## *6.7 Conclusion*

*This aim successfully developed an algorithm that can predict foot placement at 4 steps ahead during stair descent, down to the accuracy of 5mm. This is the key capability required to make Smart Step, smart. This allows us to answer what the appropriate cue is to give to the users. This cue will be delivered to the users in accordance with the timing requirements found in Aim 2 (Chapter 4) such that users can adjust their foot placement, allowing them to step optimally and hence use the overhanging toe strategy for an easier stair descent.*

# Chapter 7

# CONCLUSION

The goal of my research is to build a smart system that can assist people with mobility impairment on their foot placement intuitively, with the focus on a stair descent task for people with lower limb prostheses.

In Aim 1 (Chapter 3), I evaluated the feasibility of using haptic feedback as a proxy for sensation underneath the foot (sensory substitution). The results of my experiments showed that users can distinguish different vibration locations on the thigh and use this information to distinguish different locations of step edge without visual cues. A challenge with this strategy is that it introduces cognitive burden that could interfere with usability in cases when participants are in motion.

These findings motivated me to shift the cognitive load from the human to the device. I proposed using haptic feedback to deliver useful cues (instructional, instead of sensory substitution). On top of that, I want to deliver an instruction prior to an event, such that users can modify their gait to correct for an error. Predicting or relaying information about the future is not conveyed in sensory substitution. To achieve this, I proposed *Smart Step*, which consists of Aims 2 (Chapter 4) and 3 (Chapters 5 and 6).

To achieve *Smart Step*, I need to know two key pieces of information: knowledge of when the haptic cue should be delivered, and knowledge of the future error.

The first key piece of information is addressed in Aim 2 (Chapter 4). I investigated the requirements for time-to-cue during walking that allow users to adjust their stride lengths (foot placements) in time. The cue is in the form of vibrotactile haptic cues delivered on two sites of the wrist, notifying users to take a shorter or a longer step based on the site of the perceived cue. Findings from this investigation showed that in a mobile task (level-ground walking), such cues have to be delivered at the latest during mid-swing of the prior step. This is the first study to investigate detailed interaction between users and timing of delivery of haptic cues for gait modification.

The second key information is addressed in Aim 3 (Chapters 5 and 6). The goal of Aim 3 is to predict where users are going to place their feet at the next step when descending a flight of staircases. This Aim is two-fold: 1) Aim 3a: understanding where users typically place their feet during stair descent (Chapter 5), and 2) Aim 3b: using this data to build an

algorithm that predicts where the users are going to place their feet in the following steps (Chapter 6).

In Aim 3a (Chapter 5), I built a biomechanics gait dataset of kinematics and kinetics information during stair descent from 101 adults. The participants descended a 13-step real world staircase wearing wearable sensors, resulting in a total of 27,785 steps. The primary finding from this dataset that is directly related to Smart Step is foot placement information at each step, along with the kinematics and kinetics information that result in that particular foot placement. Additionally, this dataset is the first to report gait information in a real-world staircase with the most number of participants and steps. I am making this dataset publicly available to encourage further research in the domain of real-world gait and stair ambulation.

I am using the dataset from Aim 3a (Chapter 5) to build an algorithm that predicts the foot placement of the following steps during stair descent. I am implementing a Long-Short Term (LSTM) neural network algorithm for predicting the location of staircase edge underneath the foot at the 4th step in the future down to 5mm accuracy. This algorithm is capable of predicting foot placement with an improved accuracy of 20% higher than a baseline Auto Regressive Integrated Moving Average (ARIMA) algorithm, with an error bound of ±20mm. For future implementation, this prediction result will be compared to the expert-recommended optimal foot placement. The difference will be translated into a vibrotactile cue on the wrist, either instructing the user to take a shorter step, or a longer step, to achieve optimal foot placement. The cue will be delivered before the mid-swing of prior step, allowing users to make timely adjustments based on findings from Aim 2 (Chapter 4).

Combining results from Aims 2 (Chapter 4) and 3 (Chapters 5 and 6), we will have a prototype of a real-time foot placement cueing device to be used while descending stairs. This last part is a practical engineering implementation to allow a product to be usable in real life, which is beyond the scope of this dissertation, but made possible from findings I discovered throughout my PhD laid out in this dissertation.

The results and findings from Aims 1, 2, and 3 enable the creation of *Smart Step*, a smart, low-cost wearable system that senses the users' movements, uses machine learning to predict a future mobility error, and then sends a haptic cue to the users to prevent the error. *Smart Step* can be used by any individual without further customization, and can provide intuitive cues that minimize cognitive burden, hence require minimal to no training. In this dissertation, *Smart Step* is investigated for the specific use case of stair descent for PWA. Moving forward, *Smart Step* can be expanded for other use cases such as trip and fall prevention for the elderly population, or gait assistance for people with Parkinsons' or cerebral palsy.

# BIBLIOGRAPHY

[1] A. Wilska, "On the Vibrational Sensitivity in Different Regions of the Body Surface," *Acta Physiol. Scand.*, vol. 31, pp. 285–289, feb 1954.

[2] I. Karuei, K. E. Maclean, Z. Foley-Fisher, R. Mackenzie, S. Koch, and M. El-Zohairy, *Detecting Vibrations Across the Body in Mobile Contexts*. 2011.

[3] PhaseSpace, "PhaseSpace Motion Capture — Products — Impulse X2 Motion Capture Solution."

[4] Xsens, "Xsens 3D motion tracking."

[5] Moticon ReGo AG, "Moticon—Sensing Foot Dynamics."

[6] L. Atzori, A. Iera, and G. Morabito, "The Internet of Things: A survey," *Comput. Networks*, vol. 54, pp. 2787–2805, oct 2010.

[7] J. Gubbi, R. Buyya, S. Marusic, and M. Palaniswami, "Internet of Things (IoT): A vision, architectural elements, and future directions," *Futur. Gener. Comput. Syst.*, vol. 29, pp. 1645–1660, sep 2013.

[8] T. Starner, J. Auxier, D. Ashbrook, and M. Gandy, "The gesture pendant: a self-illuminating, wearable, infrared computer vision system for home automation control and medical monitoring," in *Dig. Pap. Fourth Int. Symp. Wearable Comput.*, pp. 87–94, IEEE Comput. Soc, 2000.

[9] S. Majumder, T. Mondal, M. Deen, S. Majumder, T. Mondal, and M. J. Deen, "Wearable Sensors for Remote Health Monitoring," *Sensors*, vol. 17, p. 130, jan 2017.

[10] P. Ross, "Managing care through the air [remote health monitoring]," *IEEE Spectr.*, vol. 41, pp. 26–31, dec 2004.

[11] L. Kraus, E. Lauer, R. Coleman, and A. Houtenville, "2017 Disability Statistics Annual Report," tech. rep., University of New Hampshire, Durham, NH, 2018.

[12] CDC/National Center for Health Statistics, "Disability and Functioning (Noninstitutionalized Adults Aged 18 and Over)," 2017.

[13] D. E.Rosenberg, C. H.Bombardier, S. Artherholt, M. P.Jensen, and R. W.Motl, "Self-Reported Depression and Physical Activity in Adults With Mobility Impairments," *Arch. Phys. Med. Rehabil.*, vol. 94, pp. 731–736, apr 2013.

[14] A. Bergland, L. Jørgensen, N. Emaus, and B. H. Strand, "Mobility as a predictor of all-cause mortality in older men and women: 11.8year follow-up in the Tromsø study," *BMC Health Serv. Res.*, vol. 17, p. 22, dec 2017.

[15] Advanced Amputee Solutions, "Amputee Statistics You Ought to Know."

[16] S. Patel, H. Park, P. Bonato, L. Chan, and M. Rodgers, "A review of wearable sensors and systems with application in rehabilitation," 2012.

[17] L. Piwek, D. A. Ellis, S. Andrews, and A. Joinson, "The Rise of Consumer Health Wearables: Promises and Barriers," *PLoS Med.*, vol. 13, feb 2016.

[18] N. D. Schüll, "Data for life: Wearable technology and the design of self-care," *Biosocieties*, vol. 11, pp. 317–333, dec 2016.

[19] K. Hänsel, N. Wilde, H. Haddadi, and A. Alomainy, "Challenges with current wearable technology in monitoring health data and providing positive behavioural support," in *MOBIHEALTH 2015 - 5th EAI Int. Conf. Wirel. Mob. Commun. Healthc. - Transform. Healthc. through Innov. Mob. Wirel. Technol.*, ICST, dec 2015.

[20] T. Pels, C. Kao, and S. Goel, "FatBelt: Motivating behavior change through isomorphic feedback," in *UIST 2014 - Adjun. Publ. 27th Annu. ACM Symp. User Interface Softw. Technol.*, pp. 123–124, Association for Computing Machinery, Inc, oct 2014.

[21] J. Kangas, J. Rantala, and R. Raisamo, "Gaze Cueing with a Vibrotactile Headband for a Visual Search Task," *Augment. Hum. Res.*, vol. 2, dec 2017.

[22] J. Rantala, J. Kangas, and R. Raisamo, "Directional cueing of Gaze with a vibrotactile headband," in *ACM Int. Conf. Proceeding Ser.*, Association for Computing Machinery, mar 2017.

[23] R. E. Cowan, B. J. Fregly, M. L. Boninger, L. Chan, M. M. Rodgers, and D. J. Reinkensmeyer, "Recent trends in assistive technology for mobility," *J. Neuroeng. Rehabil.*, vol. 9, no. 1, 2012.

[24] S. E. Costa, J. J. Rodrigues, B. M. Silva, J. N. Isento, and J. M. Corchado, "Integration of Wearable Solutions in AAL Environments with Mobility Support," *J. Med. Syst.*, vol. 39, dec 2015.

[25] A. Nieuwboer, "Cueing for freezing of gait in patients with Parkinson's disease: A rehabilitation perspective," 2008.

[26] M. Bächlin, M. Plotnik, D. Roggen, I. Maidan, J. M. Hausdorff, N. Giladi, and G. Tröster, "Wearable assistant for Parkinsons disease patients with the freezing of gait symptom," *IEEE Trans. Inf. Technol. Biomed.*, vol. 14, pp. 436–446, mar 2010.

[27] S. Mazilu, U. Blanke, M. Hardegger, G. Tröster, E. Gazit, and J. M. Hausdorff, "GaitAssist: A daily-life support and training system for Parkinson's disease patients with freezing of gait," in *Conf. Hum. Factors Comput. Syst. - Proc.*, pp. 2531–2540, Association for Computing Machinery, 2014.

[28] B. Najafi, D. G. Armstrong, and J. Mohler, "Novel wearable technology for assessing spontaneous daily physical activity and risk of falling in older adults with diabetes," in *J. Diabetes Sci. Technol.*, vol. 7, pp. 1147–1160, SAGE Publications Inc., 2013.

[29] M. J. S. Benini, M. Bruinink, A. D. Pekel, W. A. Talbott, A. Visser, and P. Markopoulos, "Restoring balance: Replacing the vestibular sense with wearable vibrotactile feedback," in *Smart Healthc. Appl. Serv. Dev. Pract.*, pp. 283–301, IGI Global, 2010.

[30] B. Najafi, D. Horn, S. Marclay, R. T. Crews, S. Wu, and J. S. Wrobel, "Assessing postural control and postural control strategy in diabetes patients using innovative and wearable technology," in *J. Diabetes Sci. Technol.*, vol. 4, pp. 780–791, SAGE Publications Inc., 2010.

[31] J. Xu, T. Bao, U. H. Lee, C. Kinnaird, W. Carender, Y. Huang, K. H. Sienko, and P. B. Shull, "Configurable, wearable sensing and vibrotactile feedback system for real-time postural balance and gait training: Proof-of-concept," *J. Neuroeng. Rehabil.*, vol. 14, oct 2017.

[32] S. Bosman, B. Groenendaal, J. W. Findlater, T. Visser, M. de Graaf, and P. Markopoulos, "GentleGuide: An Exploration of Haptic Output for Indoors Pedestrian Guidance," pp. 358–362, 2003.

[33] S. Paneels, M. Anastassova, S. Strachan, S. P. Van, S. Sivacoumarane, and C. Bolzmacher, "What's around me Multi-actuator haptic feedback on the wrist," in *2013 World Haptics Conf. WHC 2013*, pp. 407–412, 2013.

[34] K. Tsukada and M. Yasumura, "ActiveBelt: Belt-Type Wearable Tactile Display for Directional Navigation," pp. 384–399, 2004.

[35] D. Dakopoulos and N. G. Bourbakis, "Wearable obstacle avoidance electronic travel aids for blind: A survey," *IEEE Trans. Syst. Man Cybern. Part C Appl. Rev.*, vol. 40, no. 1, pp. 25–35, 2010.

[36] R. Velazquez, "Wearable assistive devices for the blind. In Wearable and autonomous biomedical devices and systems for smart environment," *Wearable Auton. Biomed. Devices Syst. Smart Environ. Issues Charact.*, pp. 331–349, nov 2010.

[37] L. R. Timsina, J. L. Willetts, M. J. Brennan, H. Marucci-Wellman, D. A. Lombardi, T. K. Courtney, and S. K. Verma, "Circumstances of fall-related injuries by age and gender among community-dwelling adults in the United States," *PLoS One*, vol. 12, may 2017.

[38] C. S. Florence, G. Bergen, A. Atherly, E. Burns, J. Stevens, and C. Drake, "Medical Costs of Fatal and Nonfatal Falls in Older Adults," *J. Am. Geriatr. Soc.*, vol. 66, pp. 693–698, apr 2018.

[39] D. A. Ross, "Implementing Assistive Technology on Wearable Computers," *IEEE Intell. Syst.*, vol. 16, no. 3, pp. 47–53, 2001.

[40] R. K. Begg and W. A. Sparrow, "Gait Characteristics of Young and Older Individuals Negotiating a Raised Surface: Implications for the Prevention of Falls," *Journals Gerontol. Ser. A Biol. Sci. Med. Sci.*, vol. 55, pp. M147–M154, mar 2000.

[41] J. R. Rebula, L. V. Ojeda, P. G. Adamczyk, and A. D. Kuo, "Measurement of foot placement and its variability with inertial sensors," *Gait Posture*, vol. 38, pp. 974–980, sep 2013.

[42] J. K. Startzell, D. A. Owens, L. M. Mulfinger, P. R. Cavanagh, D. Alfred Owens, L. M. Mulfinger, and P. R. Cavanagh, "Stair Negotiation in Older People: A Review," *J. Am. Geriatr. Soc.*, vol. 48, pp. 567–580, may 2000.

[43] I. C. Narang, B. P. Mathur, P. Singh, and V. S. Jape, "Functional capabilities of lower limb amputees," *Prosrhetics Orthot. Internarional*, vol. 8, pp. 43–51, 1984.

[44] M. J. Highsmith, J. T. Kahle, A. L. Lewandowski, S. H. Kim, and L. J. Mengelkoch, "A Method for Training Step-Over-Step Stair Descent Gait With Stance Yielding Prosthetic Knees," *JPO J. Prosthetics Orthot.*, vol. 24, pp. 10–15, jan 2012.

[45] A. Telonio, S. Blanchet, C. Maganaris, V. Baltzopoulos, and B. McFadyen, "The detailed measurement of foot clearance by young adults during stair descent," *J. Biomech.*, vol. 46, pp. 1400–1402, apr 2013.

[46] J. Muhaidat, A. Kerr, D. Rafferty, D. A. Skelton, and J. J. Evans, "Measuring foot placement and clearance during stair descent," *Gait Posture*, vol. 33, pp. 504–506, mar 2011.

[47] N. Ramstrand and K.-Å. Nilsson, "A Comparison of Foot Placement Strategies of Transtibial Amputees and Able-Bodied Subjects During Stair Ambulation," *Prosthet. Orthot. Int.*, vol. 33, pp. 348–355, dec 2009.

[48] A. Sie, J. Realmuto, and E. Rombokas, "A Lower Limb Prosthesis Haptic Feedback System for Stair Descent," in *2017 Des. Med. Devices Conf.*, p. V001T05A004, ASME, apr 2017.

[49] A. Sie, D. Boe, and E. Rombokas, "Design and Evaluation of a Wearable Haptic Feedback System for Lower Limb Prostheses During Stair Descent," in *2018 7th IEEE Int. Conf. Biomed. Robot. Biomechatronics*, pp. 219–224, IEEE, aug 2018.

[50] A. Sie, C. Fisher, M. Karrenbach, E. Case, C. Caraballo, B. C. Muir, and E. Rombokas, "Timing of Haptic Cues for Stride Adjustments in Mobility Task," *Prep.*, 2020.

[51] A. Sie, M. Karrenbach, C. Fisher, S. Fisher, N. Wiek, C. Caraballo, E. Case, D. Boe, B. C. Muir, and E. Rombokas, "Descending 13 Real World Steps: A Dataset and Analysis of Stair Descent," *to be Submitt. to Gait Posture*, 2020.

[52] A. Sie, D. Boe, and E. Rombokas, "Predicting Future Foot Placement in Stair Ambulation using Long-Short Term Memory (LSTM)," *Prep.*, 2020.

[53] H. M. Herr and A. M. Grabowski, "Bionic ankle-foot prosthesis normalizes walking gait for persons with leg amputation.," *Proceedings. Biol. Sci.*, vol. 279, pp. 457–64, feb 2012.

[54] M. F. Eilenberg, H. Geyer, and H. Herr, "Control of a Powered AnkleFoot Prosthesis Based on a Neuromuscular Model," *IEEE Trans. Neural Syst. Rehabil. Eng.*, vol. 18, pp. 164–173, apr 2010.

[55] J. M. Aldridge, J. T. Sturdy, and J. M. Wilken, "Stair ascent kinematics and kinetics with a powered lower leg system following transtibial amputation," *Gait Posture*, vol. 36, pp. 291–295, jun 2012.

[56] C.-Y. Ko, S.-B. Kim, J. K. Kim, Y. Chang, S. Kim, J. Ryu, and M. Mun, "Comparison of ankle angle adaptations of prosthetic feet with and without adaptive ankle angle during level ground, ramp, and stair ambulations of a transtibial amputee: A pilot study," *Int. J. Precis. Eng. Manuf.*, vol. 15, pp. 2689–2693, dec 2014.

[57] M. Alimusaj, L. Fradet, F. Braatz, H. J. Gerner, and S. I. Wolf, "Kinematics and kinetics with an adaptive ankle foot system during stair ambulation of transtibial amputees," *Gait Posture*, vol. 30, pp. 356–363, oct 2009.

[58] K. G. Pearson, "Generating the walking gait: role of sensory feedback," *Prog. Brain Res.*, vol. 143.

[59] I. Saunders and S. Vijayakumar, "The role of feed-forward and feedback processes for closed-loop prosthesis control," *J. Neuroeng. Rehabil.*, vol. 8, no. 1, p. 60, 2011.

[60] A. F. T. Mak, M. Zhang, and D. A. Boone, "State-of-the-art research in lower-limb prosthetic biomechanics- socket interface: A review," *J. Rehabil. Res. Dev.*, vol. 38, no. 2, pp. 161–174.

[61] W. Deng, I. Papavasileiou, Z. Qiao, W. Zhang, K.-Y. Lam, and S. Han, "Advances in Automation Technologies for Lower Extremity Neurorehabilitation: A Review and Future Challenges," *IEEE Rev. Biomed. Eng.*, vol. 11, pp. 289–305, 2018.

[62] R. Fan, M. Culjat, Chih-Hung King, M. Franco, R. Boryk, J. Bisley, E. Dutson, and W. Grundfest, "A Haptic Feedback System for Lower-Limb Prostheses," *IEEE Trans. Neural Syst. Rehabil. Eng.*, vol. 16, pp. 270–277, jun 2008.

[63] L. Yang, P. S. Dyer, R. J. Carson, J. B. Webster, K. B. Foreman, and S. J. M. Bamberg, "Utilization of a lower extremity ambulatory feedback system to reduce gait asymmetry in transtibial amputation gait," 2012.

[64] C. B. Redd and S. J. M. Bamberg, "A Wireless Sensory Feedback Device for Real-Time Gait Feedback and Training," *IEEE/ASME Trans. Mechatronics*, vol. 17, pp. 425–433, jun 2012.

[65] S. Crea, C. Cipriani, M. Donati, M. C. Carrozza, and N. Vitiello, "Providing Time-Discrete Gait Information by Wearable Feedback Apparatus for Lower-Limb Amputees: Usability and Functional Validation," *IEEE Trans. Neural Syst. Rehabil. Eng.*, vol. 23, pp. 250–257, mar 2015.

[66] R. W. Cholewiak and A. A. Collins, "Vibrotactile localization on the arm: Effects of place, space, and age," *Percept. Psychophys.*, vol. 65, pp. 1058–1077, oct 2003.

[67] L. A. Jones and N. B. Sarter, "Tactile Displays: Guidance for Their Design and Application," *Hum. Factors J. Hum. Factors Ergon. Soc.*, vol. 50, pp. 90–111, feb 2008.

[68] R. W. Cholewiak, J. C. Brill, and A. Schwab, "Vibrotactile localization on the abdomen: Effects of place and space," *Percept. Psychophys.*, vol. 66, pp. 970–987, aug 2004.

[69] J. B. van Erp, "Tactile navigation display," pp. 165–173, Springer, Berlin, Heidelberg, 2001.

[70] I. Karuei, K. E. MacLean, Z. Foley-Fisher, R. MacKenzie, S. Koch, and M. El-Zohairy, "Detecting vibrations across the body in mobile contexts," in *Conf. Hum. Factors Comput. Syst. - Proc.*, pp. 3267–3276, 2011.

[71] T. Machida, N. K. Dim, and X. Ren, "Suitable body parts for vibration feedback in walking navigation systems," in *ACM Int. Conf. Proceeding Ser.*, vol. 18-19-Apri, pp. 32–36, Association for Computing Machinery, apr 2015.

[72] N. K. Dim and X. Ren, "Investigation of suitable body parts for wearable vibration feedback in walking navigation," *Int. J. Hum. Comput. Stud.*, vol. 97, pp. 34–44, jan 2017.

[73] D. Tam, K. E. MacLean, J. McGrenere, and K. J. Kuchenbecker, "The design and field observation of a Haptic Notification System for timing awareness during oral presentations," in *Conf. Hum. Factors Comput. Syst. - Proc.*, pp. 1689–1698, 2013.

[74] G. Grindlay, "Haptic guidance benefits musical motor learning," in *Symp. Haptics Interfaces Virtual Environ. Teleoperator Syst. 2008 - Proceedings, Haptics*, pp. 397–404, 2008.

[75] L. Marchal-Crespo, M. Van Raai, G. Rauter, P. Wolf, and R. Riener, "The effect of haptic guidance and visual feedback on learning a complex tennis task," *Exp. Brain Res.*, vol. 231, pp. 277–291, nov 2013.

[76] A. E. Bouchard, H. Corriveau, and M. H. Milot, "Comparison of haptic guidance and error amplification robotic trainings for the learning of a timing-based motor task by healthy seniors," *Front. Syst. Neurosci.*, vol. 9, mar 2015.

[77] F. Danion, E. Varraine, M. Bonnard, and J. Pailhous, "Stride variability in human gait: The effect of stride frequency and stride length," *Gait Posture*, vol. 18, no. 1, pp. 69–77, 2003.

[78] M. Bonnard and J. Pailhous, "Intentionality in Human Gait Control: Modifying the Frequency-to-Amplitude Relationship," *J. Exp. Psychol. Hum. Percept. Perform.*, vol. 19, pp. 429–443, apr 1993.

[79] K. Baker, L. Rochester, and A. Nieuwboer, "The effect of cues on gait variability - Reducing the attentional cost of walking in people with Parkinson's disease," *Park. Relat. Disord.*, vol. 14, pp. 314–320, may 2008.

[80] M. M. Almarwani, *Timing and coordination of gait: Impact of aging, gait speed and rhythmic auditory cueing*. PhD thesis, University of Pittsburgh, 2006.

[81] P. C. Dixon, J. V. Jacobs, J. T. Dennerlein, and J. M. Schiffman, "Late-cueing of gait tasks on an uneven brick surface impacts coordination and center of mass control in older adults," 2018.

[82] I. Karuei and K. E. Maclean, "Susceptibility to periodic vibrotactile guidance of human cadence," in *IEEE Haptics Symp. HAPTICS*, pp. 141–146, IEEE Computer Society, 2014.

[83] T. Lisini Baldi, G. Paolocci, and D. Prattichizzo, "Human Guidance: Suggesting Walking Pace Under Workload," in *Lect. Notes Comput. Sci. (including Subser. Lect. Notes Artif. Intell. Lect. Notes Bioinformatics)*, vol. 10894 LNCS, pp. 416–427, Springer Verlag, 2018.

[84] G. Paolocci, T. Lisini Baldi, and D. Prattichizzo, "Human Rendezvous via Haptic Suggestion," in *Lect. Notes Electr. Eng.*, vol. 535, pp. 262–267, Springer, Singapore, 2019.

[85] Y. Wang and M. Srinivasan, "Stepping in the direction of the fall: The next foot placement can be predicted from current upper body state in steady-state walking," *Biol. Lett.*, vol. 10, sep 2014.

[86] M. Millard, D. Wight, J. Mcphee, E. Kubica, and D. Wang, "Human Foot Placement and Balance in the Sagittal Plane," *J Biomech Eng*, vol. 131, no. 12, p. 121001, 2009.

[87] M. S. Redfern and T. Schumann, "A Model of Foot Placement during Gait," Tech. Rep. 11, 1994.

[88] N. Kitagawa and N. Ogihara, "Estimation of foot trajectory during human walking by a wearable inertial measurement unit mounted to the foot," *Gait Posture*, vol. 45, pp. 110–114, mar 2016.

[89] E. Varraine, M. Bonnard, and J. Pailhous, "Intentional on-line adaptation of stride length in human walking," *Exp. Brain Res.*, vol. 130, no. 2, pp. 248–257, 2000.

[90] J. P. Scholz and J. A. Kelso, "Intentional switching between patterns of bimanual coordination depends on the intrinsic dynamics of the patterns," *J. Mot. Behav.*, vol. 22, no. 1, pp. 98–124, 1990.

[91] J. S. Matthis and B. R. Fajen, "Humans exploit the biomechanics of bipedal gait during visually guided walking over complex terrain," *Proc. R. Soc.*, vol. 280, no. 1762, 2013.

[92] J. S. Matthis and B. R. Fajen, "Visual control of foot placement when walking over complex terrain.," *J. Exp. Psychol. Hum. Percept. Perform.*, vol. 40, pp. 106–115, feb 2014.

[93] J. S. Matthis, S. L. Barton, and B. R. Fajen, "The biomechanics of walking shape the use of visual information during locomotion over complex terrain," *J. Vis.*, vol. 15, no. 3, p. 10, 2015.

[94] J. S. Matthis, S. L. Barton, and B. R. Fajen, "The critical phase for visual control of human walking over complex terrain.," *Proc. Natl. Acad. Sci. U. S. A.*, vol. 114, no. 32, pp. E6720–E6729, 2017.

[95] J. S. Matthis, J. L. Yates, and M. M. Hayhoe Correspondence, "Gaze and the Control of Foot Placement When Walking in Natural Terrain," *Curr. Biol.*, vol. 28, 2018.

[96] D. Lai, R. Begg, and M. Palaniswami, "Computational Intelligence in Gait Research: A Perspective on Current Applications and Future Challenges," *IEEE Trans. Inf. Technol. Biomed.*, vol. 13, pp. 687–702, sep 2009.

[97] S. R. Simon, "Quantification of human motion: gait analysis-benefits and limitations to its application to clinical problems," *J. Biomech.*, vol. 37, pp. 1869–1880, 2004.

[98] K. C. Foucher, L. E. Thorp, D. Orozco, M. Hildebrand, and M. A. Wimmer, "Differences in Preferred Walking Speeds in a Gait Laboratory Compared With the Real World After Total Hip Replacement," *YAPMR*, vol. 91, pp. 1390–1395, 2010.

[99] M. A. D. Brodie, M. J. M. Coppens, S. R. Lord, N. H. Lovell, Y. J. Gschwind, ·. Stephen, J. Redmond, M. Benjamin, D. Rosario, K. Wang, D. L. Sturnieks, M. Persiani, and ·. K. Delbaere, "Wearable pendant device monitoring using new wavelet-based methods shows daily life and laboratory gaits are different," *Med Biol Eng Comput*, vol. 54, pp. 663–674, 2016.

[100] P. Tamburini, F. Storm, C. Buckley, M. C. Bisi, R. Stagni, and C. Mazzà, "Moving from laboratory to real life conditions: Influence on the assessment of variability and stability of gait," *Gait Posture*, vol. 59, pp. 248–252, jan 2018.

[101] L. C. Benson, C. A. Clermont, E. Bošnjak, and R. Ferber, "The use of wearable devices for walking and running gait analysis outside of the lab: A systematic review," 2018.

[102] A. Muro-de-la Herran, B. Garcia-Zapirain, and A. Mendez-Zorrilla, "Gait analysis methods: an overview of wearable and non-wearable systems, highlighting clinical applications.," *Sensors (Basel).*, vol. 14, pp. 3362–94, feb 2014.

[103] W. Tao, T. Liu, R. Zheng, and H. Feng, "Gait analysis using wearable sensors.," *Sensors (Basel).*, vol. 12, no. 2, pp. 2255–83, 2012.

[104] A. H. A. Razak, A. Zayegh, R. K. Begg, and Y. Wahab, "Foot plantar pressure measurement system: a review.," *Sensors (Basel).*, vol. 12, no. 7, pp. 9884–912, 2012.

[105] A. Ahmed and S. Roumeliotis, "A Visual-Inertial Approach to Human Gait Estimation," in *2018 IEEE Int. Conf. Robot. Autom.*, pp. 1–8, IEEE, may 2018.

[106] B. Snahiranayagam, D. T. Lai, W. Sparrow, and R. K. Begg, "A machine learning approach to estimate Minimum Toe Clearance using Inertial Measurement Units," *J. Biomech.*, vol. 48, pp. 4309–4316, dec 2015.

[107] Motion Workshop, "Shadow Motion Capture System."

[108] NaturalPoint Inc., "Optitrack - Motion Capture Systems."

[109] Noitom Ltd., "Perception Neuron motion capture for virtual reality, animation, sports, gaming, and film."

[110] Rokoko Electronics, "Rokoko - Motion Capture System - Smartsuit Pro."

[111] D. Roetenberg, H. Luinge, and P. J. Slycke, "Xsens MVN : Full 6 DOF Human Motion Tracking Using Miniature Inertial Sensors," 2009.

[112] Tec Gihan Co. Ltd, "Technologies of Tec Gihan."

[113] J.-W. Lee and G.-K. Lee, "Gait Angle Prediction for Lower Limb Orthotics and Prostheses Using an EMG Signal and Neural Networks," tech. rep.

[114] M. Ardestani, X. Zhang, L. Wang, Q. Lian, Y. Liu, J. He, D. Li, and Z. Jin, "Human lower extremity joint moment prediction: A wavelet neural network approach," *Expert Syst. Appl.*, vol. 41, pp. 4422–4433, jul 2014.

[115] M. Ardestani, X. Zhang, L. Wang, Q. Lian, Y. Liu, J. He, D. Li, and Z. Jin, "Feed forward artificial neural network to predict contact force at medial knee joint: Application to gait modification," *Neurocomputing*, vol. 139, pp. 114–129, sep 2014.

[116] G. Dominguez, E. Cardiel, S. Arias, and P. Rogeli, "A Digital Goniometer based on encoders for measuring knee-joint position in an orthosis," in *2013 World Congr. Nat. Biol. Inspired Comput.*, pp. 1–4, IEEE, aug 2013.

[117] H. Maki, H. Ogawa, Y. Yonezawa, A. W. Hahn, and W. M. Caldwell, "A new ultrasonic stride length measuring system.," *Biomed. Sci. Instrum.*, vol. 48, pp. 282–7, 2012.

[118] Y. Wahab and N. A. Bakar, "Gait analysis measurement for sport application based on ultrasonic system," in *2011 IEEE 15th Int. Symp. Consum. Electron.*, pp. 20–24, IEEE, jun 2011.

[119] Yongbin Qi, Cheong Boon Soh, E. Gunawan, Kay-Soon Low, and A. Maskooki, "Using wearable UWB radios to measure foot clearance during walking," in *2013 35th Annu. Int. Conf. IEEE Eng. Med. Biol. Soc.*, pp. 5199–5202, IEEE, jul 2013.

[120] S. Bamberg, A. Benbasat, D. Scarborough, D. Krebs, and J. Paradiso, "Gait Analysis Using a Shoe-Integrated Wireless Sensor System," *IEEE Trans. Inf. Technol. Biomed.*, vol. 12, pp. 413–423, jul 2008.

[121] D. Fong, Y.-Y. Chan, Y. Hong, P. Yung, K.-Y. Fung, and K.-M. Chan, "Estimating the complete ground reaction forces with pressure insoles in walking," *J. Biomech.*, vol. 41, pp. 2597–2601, aug 2008.

[122] A. M. Howell, T. Kobayashi, H. A. Hayes, K. B. Foreman, and S. J. M. Bamberg, "Kinetic Gait Analysis Using a Low-Cost Insole," *IEEE Trans. Biomed. Eng.*, vol. 60, pp. 3284–3290, dec 2013.

[123] A. M. Tan, F. K. Fuss, Y. Weizman, Y. Woudstra, and O. Troynikov, "Design of Low Cost Smart Insole for Real Time Measurement of Plantar Pressure," *Procedia Technol.*, vol. 20, pp. 117–122, jan 2015.

[124] F. Lin, A. Wang, Y. Zhuang, M. R. Tomita, and W. Xu, "Smart Insole: A Wearable Sensor Device for Unobtrusive Gait Monitoring in Daily Life," *IEEE Trans. Ind. Informatics*, vol. 12, pp. 2281–2291, dec 2016.

[125] IEE, "Smart Foot Sensor - IEE - a sense for innovation."

[126] Tekscan Inc., "Insole Pressure Sensor — Force Sensitive Insole — Tekscan."

[127] Novel.de, "pedar."

[128] CARV, "Carv Digital Ski Instructor and Skiing Tracker  Carv USA."

[129] G. Faber, I. Kingma, H. M. Schepers, P. H. Veltink, and J. H. van Dieen, "Determination of joint moments with instrumented force shoes in a variety of tasks," *J. Biomech.*, vol. 43, pp. 2848–2854, oct 2010.

[130] J. A. DeLisa and R. W. Soutas-Little, *Gait analysis in the science of rehabilitation.* Diane Pub Co, 1998.

[131] M. Ardestani, Z. Chen, L. Wang, Q. Lian, Y. Liu, J. He, and Z. Jin, "A neural network approach for determining gait modifications to reduce the contact force in knee joint implant," *Med. Eng. Phys.*, vol. 36, pp. 1253–1265, oct 2014.

[132] R. Baker, "Gait analysis methods in rehabilitation.," *J. Neuroeng. Rehabil.*, vol. 3, p. 4, mar 2006.

[133] J. Favre, M. Hayoz, J. Erhart-Hledik, and T. Andriacchi, "A neural network model to predict knee adduction moment during walking based on ground reaction force and anthropometric measurements," *J. Biomech.*, vol. 45, pp. 692–698, feb 2012.

[134] M. M. Ardestani, M. Moazen, Z. Chen, J. Zhang, and Z. Jin, "A real-time topography of maximum contact pressure distribution at medial tibiofemoral knee implant during gait: Application to knee rehabilitation," *Neurocomputing*, vol. 154, pp. 174–188, apr 2015.

[135] J. van den Noort, M. van der Esch, M. Steultjens, J. Dekker, M. Schepers, P. Vetlink, and J. Harllar, "The knee adduction moment measured with an instrumented force shoe in patients with knee osteoarthritis," *J. Biomech.*, vol. 45, pp. 281–288, jan 2012.

[136] J. van den Noort, M. van der Esch, M. Steultjens, J. Dekker, M. Schepers, P. Vetlink, and J. Harllar, "Ambulatory measurement of the knee adduction moment in patients with osteoarthritis of the knee," *J. Biomech.*, vol. 46, pp. 43–49, jan 2013.

[137] S. E. Oh, A. Choi, and J. H. Mun, "Prediction of ground reaction forces during gait based on kinematics and a neural network model," *J. Biomech.*, vol. 46, pp. 2372–2380, sep 2013.

[138] Y. Jung, M. Jung, K. Lee, and S. Koo, "Ground reaction force estimation using an insole-type pressure mat and joint kinematics during walking," *J. Biomech.*, vol. 47, pp. 2693–2699, aug 2014.

[139] T. Kauppinen and G. M. De Espindola, "Linked open science-communicating, sharing and evaluating data, methods and results for executable papers," in *Procedia Comput. Sci.*, vol. 4, pp. 726–731, Elsevier, jan 2011.

[140] C. Allen and D. M. A. Mehler, "Open science challenges, benefits and tips in early career and beyond," *PLOS Biol.*, vol. 17, p. e3000246, may 2019.

[141] "CGA Normative Gait Database."

[142] "Carnegie Mellon University - CMU Graphics Lab - motion capture library."

[143] C. A. Fukuchi, R. K. Fukuchi, and M. Duarte, "A public dataset of overground and treadmill walking kinematics and kinetics in healthy individuals," *PeerJ*, vol. 6, p. e4640, apr 2018.

[144] M. H. Schwartz and A. Rozumalski, "The gait deviation index: A new comprehensive index of gait pathology," *Gait Posture*, vol. 28, pp. 351–357, oct 2008.

[145] T. F. Besier, M. Fredericson, G. E. Gold, G. S. Beaupré, and S. L. Delp, "Knee muscle forces during walking and running in patellofemoral pain patients and pain-free controls," *J. Biomech.*, vol. 42, pp. 898–905, may 2009.

[146] D. Chang, M. Alban-Hidalgo, and K. Hsu, "Diagnosing Parkinson's Disease From Gait," tech. rep.

[147] B. J. Fregly, T. F. Besier, D. G. Lloyd, S. L. Delp, S. A. Banks, M. G. Pandy, and D. D. D'Lima, "Grand challenge competition to predict in vivo knee loads," *J. Orthop. Res.*, vol. 30, pp. 503–513, apr 2012.

[148] S. Sarkar, P. J. Phillips, Z. Liu, I. Robledo, P. Grother, and K. Bowyer, "The Human ID Gait Challenge Problem: Data Sets, Performance, and Analysis," tech. rep., 2003.

[149] H. Iwama, M. Okumura, Y. Makihara, and Y. Yagi, "The OU-ISIR Gait Database Comprising the Large Population Dataset and Performance Evaluation of Gait Recognition," *IEEE Trans. Inf. Forensics Secur.*, vol. 7, pp. 1511–1521, oct 2012.

[150] R. K. Fukuchi, C. A. Fukuchi, and M. Duarte, "A public dataset of running biomechanics and the effects of running speed on lower extremity kinematics and kinetics," *PeerJ*, vol. 5, p. e3298, may 2017.

[151] T. W. Dorn, A. G. Schache, and M. G. Pandy, "Muscular strategy shift in human running: dependence of running speed on hip and ankle muscle performance.," *J. Exp. Biol.*, vol. 215, pp. 1944–56, jun 2012.

[152] R. R. Neptune, I. C. Wright, and A. J. van den Bogert, "Muscle coordination and function during cutting movements.," *Med. Sci. Sports Exerc.*, vol. 31, pp. 294–302, feb 1999.

[153] P. B. Shull, W. Jirattigalachote, M. A. Hunt, M. R. Cutkosky, and S. L. Delp, "Quantified self and human movement: A review on the clinical impact of wearable sensing and feedback for gait analysis and intervention," *Gait Posture*, vol. 40, pp. 11–19, may 2014.

[154] E. Casilari, J. A. Santoyo-Ramón, and J. M. Cano-García, "UMAFall: A Multisensor Dataset for the Research on Automatic Fall Detection," *Procedia Comput. Sci.*, vol. 110, pp. 32–39, jan 2017.

[155] R. Igual, C. Medrano, and I. Plaza, "A comparison of public datasets for acceleration-based fall detection," *Med. Eng. Phys.*, vol. 37, pp. 870–878, sep 2015.

[156] A. Sucerquia, J. López, and J. Vargas-Bonilla, "SisFall: A Fall and Movement Dataset," *Sensors*, vol. 17, p. 198, jan 2017.

[157] A. Y. Yang, P. Kuryloski, and R. Bajcsy, *WARD: A Wearable Action Recognition Database*.

[158] M. Zhang and A. A. Sawchuk, *USC-HAD: A Daily Activity Dataset for Ubiquitous Activity Recognition Using Wearable Sensors*. 2012.

[159] M. A. R. Ahad, J. I. Tan, H. Kim, and S. Ishikawa, "Action dataset A survey," in *SICE Annu. Conf.*, 2011.

[160] E. Casilari, J.-A. Santoyo-Ramón, and J.-M. Cano-García, "Analysis of Public Datasets for Wearable Fall Detection Systems," *Sensors*, vol. 17, p. 1513, jun 2017.

[161] T. M. A. Ackermans, N. C. Francksen, R. V. Casana-Eslava, C. Lees, V. Baltzopoulos, P. J. G. Lisboa, M. A. Hollands, T. D. O'brien, and C. N. Maganaris, "A novel multivariate approach for biomechanical profiling of stair negotiation," 2019.

[162] T. Cluff, D. Gordon, and E. Robertson, "Kinetic analysis of stair descent: Part 1. Forwards step-over-step descent," *Gait Posture*, vol. 33, pp. 423–428, 2011.

[163] W. I. Schöllhorn, "Applications of artificial neural nets in clinical biomechanics," *Clin. Biomech.*, vol. 19, pp. 876–898, nov 2004.

[164] E. Dolatabadi, B. Taati, and A. Mihailidis, "An Automated Classification of Pathological Gait Using Unobtrusive Sensing Technology," *IEEE Trans. Neural Syst. Rehabil. Eng.*, vol. 25, pp. 2336–2346, dec 2017.

[165] K. Leuenberger, R. Gonzenbach, E. Wiedmer, A. Luft, and R. Gassert, "Classification of Stair Ascent and Descent in Stroke Patients," in *2014 11th Int. Conf. Wearable Implant. Body Sens. Networks Work.*, pp. 11–16, IEEE, jun 2014.

[166] H. Chan, M. Yang, H. Wang, H. Zheng, S. McClean, R. Sterritt, and R. E. Mayagoitia, "Assessing Gait Patterns of Healthy Adults Climbing Stairs Employing Machine Learning Techniques," *Int. J. Intell. Syst.*, vol. 28, pp. 257–270, mar 2013.

[167] W. Xiao, Y. Lu, J. Cui, and L. Ji, "Recognition of Human Stair Ascent and Descent Activities Based on Extreme Learning Machine," pp. 253–265, Springer, Cham, 2015.

[168] J. Snoek, J. Hoey, L. Stewart, R. S. Zemel, and A. Mihailidis, "Automated detection of unusual events on stairs," *Image Vis. Comput.*, vol. 27, pp. 153–166, 2009.

[169] G. S. Parra-Dominguez, B. Taati, and A. Mihailidis, "3D Human Motion Analysis to Detect Abnormal Events on Stairs," in *2012 Second Int. Conf. 3D Imaging, Model. Process. Vis. Transm.*, pp. 97–103, IEEE, oct 2012.

[170] G. S. Parra-Dominguez, J. Snoek, B. Taati, and A. Mihailidis, "Lower body motion analysis to detect falls and near falls on stairs," *Biomed. Eng. Lett.*, vol. 5, pp. 98–108, jun 2015.

[171] C. E. Stepp and Y. Matsuoka, "Vibrotactile Sensory Substitution for Object Manipulation: Amplitude Versus Pulse Train Frequency Modulation," *IEEE Trans. Neural Syst. Rehabil. Eng.*, vol. 20, pp. 31–37, jan 2012.

[172] I. Jiang, *Vibrotactile Sensory Feedback for Lower Limb Prostheses*. Phd thesis, University of Washington, 2015.

[173] J. Lindsay, R. J. Adams, and B. Hannaford, "Improving tactile feedback with an impedance adapter," in *2013 World Haptics Conf.*, pp. 713–718, IEEE, apr 2013.

[174] Texas Instruments, "DRV2605 Haptic Driver for ERM and LRA With Built-In Library and Smart-Loop Architecture," tech. rep., 2018.

[175] S. Viteckova, P. Kutilek, Z. Svoboda, R. Krupicka, J. Kauler, and Z. Szabo, "Gait symmetry measures: A review of current and prospective methods," apr 2018.

[176] T. Liikavainio, J. Isolehto, H. J. Helminen, J. Perttunen, V. Lepola, I. Kiviranta, P. A. Arokoski, and P. V. Komi, "Loading and gait symmetry during level and stair walking in asymptomatic subjects with knee osteoarthritis: Importance of quadriceps femoris in reducing impact force during heel strike?," 2007.

[177] A. Protopapadaki, W. I. Drechsler, M. C. Cramp, F. J. Coutts, and O. M. Scott, "Hip, knee, ankle kinematics and kinetics during stair ascent and descent in healthy young individuals," *Clin. Biomech.*, vol. 22, pp. 203–210, feb 2007.

[178] L. A. Livingston, J. M. Stevenson, and S. J. Olney, "Stairclimbing kinematics on stairs of differing dimensions.," *Arch. Phys. Med. Rehabil.*, vol. 72, pp. 398–402, may 1991.

[179] R. Riener, M. Rabuffetti, and C. Frigo, "Stair ascent and descent at different inclinations," tech. rep., 2002.

[180] B. J. McFadyen and D. A. Winter, "An integrated biomechanical analysis of normal stair ascent and descent," *J. Biomech.*, vol. 21, pp. 733–44, jan 1988.

[181] B. C. Muir, J. M. Haddad, M. J. Heijnen, and S. Rietdyk, "Proactive gait strategies to mitigate risk of obstacle contact are more prevalent with advancing age," *Gait Posture*, vol. 41, pp. 233–239, jan 2015.

[182] B. C. Muir, J. M. Haddad, R. E. van Emmerik, and S. Rietdyk, "Changes in the control of obstacle crossing in middle age become evident as gait task difficulty increases," *Gait Posture*, vol. 70, pp. 254–259, may 2019.

[183] G. G. Simoneau, P. R. Cavanagh, J. S. Ulbrecht, H. W. Leibowitz, and R. A. Tyrrell, "The Influence of Visual Factors on Fall-related Kinematic Variables During Stair Descent by Older Women," *J. Gerontol.*, vol. 46, pp. M188–M195, nov 1991.

[184] N. Ramstrand, &. Kjell-A , and K. E. Nilsson, "A comparison of foot placement strategies of transtibial amputees and able-bodied subjects during stair ambulation,"

[185] H. Sadeghi, P. Allard, F. Prince, and H. Labelle, "Symmetry and limb dominance in able-bodied gait: A review," sep 2000.

[186] M. E. Dewar and G. Judge, "Temporal asymmetry as a gait quality indicator," *Med. Biol. Eng. Comput.*, vol. 18, pp. 689–693, sep 1980.

[187] A. Moevus, M. Mignotte, J. A. De Guise, and J. Meunier, "Evaluating perceptual maps of asymmetries for gait symmetry quantification and pathology detection," in *2014 36th Annu. Int. Conf. IEEE Eng. Med. Biol. Soc. EMBC 2014*, pp. 3317–3320, Institute of Electrical and Electronics Engineers Inc., nov 2014.

[188] W. Forczek and R. Staszkiewicz, "Authors submitted their contribution of the article to the editorial board. Accepted for printing in," *J. Hum. Kinet.*, vol. 35, pp. 47–57, 2012.

[189] R. M. Queen, D. E. Attarian, M. P. Bolognesi, and R. J. Butler, "Bilateral symmetry in lower extremity mechanics during stair ascent and descent following a total hip arthroplasty: A one-year longitudinal study ," 2014.

[190] S. Yu, D. Tan, and T. Tan, "A Framework for Evaluating the Effect of View Angle, Clothing and Carrying Condition on Gait Recognition," tech. rep., 2006.

[191] "Center for Biometrics and Security Research."

[192] "Automatic Gait Recognition for Human ID at a Distance."